UNIVERSITY OF CALIFORNIA, SAN DIEGO

# Assessment of Prospective Controllers : Data-based Approaches Tailor-made for Current Knowledge

A dissertation submitted in partial satisfaction of the requirements
for the degree Doctor of Philosophy

in

Engineering Sciences (Mechanical Engineering)

by

Seunggyun Cheong

Committee in charge:

Professor Robert R. Bitmead, Chair
Professor Jorge Cortés
Professor Raymond A. de Callafon
Professor Tara Javidi
Professor Kenneth Kreutz-Delgado

2012

The dissertation of Seunggyun Cheong is approved, and it is acceptable in quality and form for publication on microfilm and electronically:

_____

_____

_____

_____

_____
Chair

University of California, San Diego

2012

*To my wife, our parents, and our exciting future.*

TABLE OF CONTENTS

LIST OF FIGURES

# LIST OF ACRONYMS

| | |
|---|---|
| SISO | Single-input single-output |
| MIMO | Multi-input multi-output |
| LTI | Linear time-invariant |
| AR | Autoregressive |
| ARMA | Autoregressive moving average |
| FRF | Frequency response function |
| SCLI | Stably causally left-invertible |

ACKNOWLEDGEMENTS

I would like to acknowledge Professor Robert Bitmead for his invaluable guidance. He understood my shy and bashful personality and has been a strong supporter, a wise advisor, and a great role model as an engineer. I deeply appreciate that he has always respected my voice.

The faculty in the Center for Control Systems and Dynamics has provided me with exceptional graduate education as well as various perspectives in the field of Control Theory. Specially, I show my appreciation to Professors Jorge Cortés, Raymond A. de Callafon, Tara Javidi, and Kenneth Kreutz-Delgado for their great advice on my thesis and my profession.

I also gratefully acknowledge Carol and Rick Kornfeld and School of Engineering in University of California, San Diego for supporting me with the generous fellowship during my research. They showed me warm and kind hearts towards our university.

I feel fortunate to meet and thank Professor Michael Safonov for introducing me to unfalsified adaptive control and giving me research opportunities. His philosophy has made a great influence on me.

I thank Jisang Park. He has helped me in many ways since my first year in UCSD.

Much of the material in Chapter 2 appears in S. Cheong, "Safe adaptive switching control with no SCLI assumption" as it appears in American Control Conference, 2010. The dissertation author was the primary author of this paper.

Chapter 3 is a reprint of S. Cheong, R. R. Bitmead, "Instability detection of ARMA systems based on AR system identification" as it appears in Systems & Control Letters, 2011. The dissertation author was the primary author of this paper.

Chapter 4 is a reprint of S. Cheong, R. R. Bitmead, "Divination of closed-loop stability and performance via frequency response function estimates" as it appears in Automatica, 2012. The dissertation author was the primary author of this paper.

Chapter 5 has been accepted for publication of S. Cheong, R. R. Bitmead, "Controller improvement via frequency response function estimates" as it will ap-

pear in 16th IFAC Symposium on System Identification. The dissertation author was the primary author of this paper.

## VITA

| | |
|---|---|
| 2002 | B. S. in Electrical Engineering, KAIST (Korea Advanced Institute of Science and Technology) |
| 2004 | M. S. in Electrical Engineering, Seoul National University |
| 2007 | M. S. in Electrical Engineering, University of Southern California |
| 2012 | Teaching Assistant, University of California, San Diego |
| 2012 | Ph. D. in Mechanical Engineering, University of California, San Diego |

## PUBLICATIONS

S. Cheong, R. R. Bitmead, "Controller improvement via frequency response function estimates", *16th IFAC Symposium on System Identification*, Brussels, Belgium, 2012.

S. Cheong, R. R. Bitmead, "Divination of closed-loop stability and performance via frequency response function estimates", *Automatica*, Volume 48, Issue 7, Pages 1405-1414, 2012.

S. Cheong, "Unfalsified adaptive control with weak cost-detectability", *American Control Conference*, San Francisco, CA, 2011.

S. Cheong, R. R. Bitmead, "Instability detection of ARMA systems based on AR system identification", *Systems & Control Letters*, Volume 60, Issue 3, Pages 185-191, 2011.

S. Cheong, "Safe adaptive switching control with no SCLI assumption", *American Control Conference*, Baltimore, MD, 2010.

S. Cheong, R. R. Bitmead, "System identification based instability detection of noisy ARMA systems", *15th IFAC Symposium on System Identification*, Saint-Malo, France, 2009.

C. Manuelli, S. G. Cheong, E. Mosca, M. G. Safonov, "Stability of unfalsified adaptive control with non SCLI controllers and related performance under different prior knowledge", *European Control Conference*, Kos, Greece, 2007.

S. G. Cheong, J. Back, H. Shim, J. H. Seo. Non-smooth feedback stabilizer for strict-feedback nonlinear systems not even linearizable at the origin", *American Control Conference*, Portland, OR, 2005.

ABSTRACT OF THE DISSERTATION

Assessment of Prospective Controllers :
Data-based Approaches Tailor-made for Current Knowledge

by

Seunggyun Cheong

Doctor of Philosophy in Engineering Sciences (Mechanical Engineering)

University of California, San Diego, 2012

Professor Robert R. Bitmead, Chair

This dissertation is focused on assessment of prospective controllers in the sense of their closed-loop stability and performance. We consider a variety of circumstances depending on knowledge of a given plant and propose corresponding strategies for the assessment. The assessment is performed based on the data from experiments and the strategies assess not only the controller in the loop where the experiments are taken but also the other prospective controllers out of the loop.

The first circumstance is challenging such that there is no available knowledge of a plant and a disturbance signal except we can observe the input and the output signals of the plant. Among many prospective controllers, one controller makes a closed-loop system with the plant and the input and the output signals of the plant are observed. Then, the controller in the loop is assessed by a data-based cost function for the closed-loop stability and performance. The other prospective controllers can be assessed by data-based cost functions with computed fictitious reference signals in corresponding fictitious closed-loop systems. The experiment is performed with a switching control scheme, in which we compare online the cost functions of the controllers and switch the one with the smallest cost into the loop. The stability and performance of this switching control system is shown to be guaranteed when at least one of the controllers is feasible.

In the second circumstance, the available knowledge of the plant is that

the plant is known to be a SISO LTI discrete-time system and the disturbance signal is an i.i.d. random process with zero mean, unknown bounded variance, and finite fourth moment. We consider only one controller and determine its ability to yield closed-loop stability by performing an experiment on the closed-loop system with the plant and the controller. The collection of least squares AR estimators of various orders is shown to have the capacity to detect the instability of the closed-loop system. The order of the system is not necessary information but, instead, an upper bound of the number of unstable poles with the maximal magnitude outside the unit circle is assumed to be known.

In the third circumstance, which is the best situation in this dissertation, we know that the plant is a MIMO LTI discrete-time system stabilized by a MIMO LTI controller in a closed-loop and we also know a bound on the impulse response of the closed-loop system and a bound on a disturbance signal which is additive to the output of the plant. With this knowledge, the closed-loop stability and performance of another prospective controller is assessed without constructing this closed-loop. This is performed through nonparametric identification of the frequency response functions of the plant or other transfer functions, based on a limited amount of signal data collected from experiments on the internally stable closed-loop system excited by designed reference signals and corrupted by disturbances. An error analysis is provided and conditions for the reliable assessments of the closed-loop stability and performance are characterized.

Based on the strategy developed for the third circumstance, we search for a MIMO LTI discrete-time controller better than the currently stabilizing controller in the sense of a certain performance measure. This searching procedure is formulated in the form of an optimization problem. FRF estimates for coprime factors of the plant are obtained with known error bounds from the experimental data collected from the closed-loop system with the currently stabilizing controller and the optimization problem is built in terms of these FRF estimates. In order to reduce the numerical difficulty of the optimization problem, we employ a controller parametrization and propose an algorithm that may not produce the optimal controller but has fast computation ability.

# 1 Introduction

## 1.1 Motivation

Given a problem with a limited amount of information, what engineers usually do is to seek the best solution of all possible solutions. With great efforts by engineers, the chosen solution can approach the achievable limit for the problem. Consequently, the choice of solution becomes more and more dependent on the given information. To a control engineer, the necessary information is about a plant to be controlled and any unknown disturbance signal. Based on the given information, a controller is designed for a control objective and is implemented in a closed-loop system as in Figure 1.1.

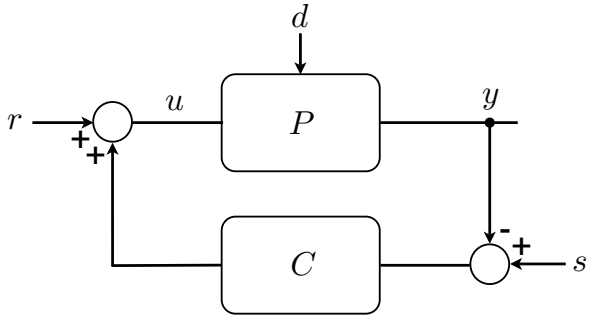


Figure 1.1: A feedback control system.

The more information we have about the plant $P$, the disturbance signal $d$, and the reference signals $r$ and $s$, the better controller we can design. However, in many cases, we make assumptions on the plant and the disturbance in order to design controllers. Thus, we can build controllers with any assumptions on the plant and the disturbance and these controllers are guaranteed to perform successfully under the assumptions but are not guaranteed for the plant and the

disturbance. Naturally, the next thing to do is to assess the controllers for the plant and the disturbance without these assumptions. This dissertation is about assessing pre-designed prospective controllers with various kinds of knowledge of the plant and the disturbance.

## 1.2 Outline of dissertation

In Chapter 2, we pose a challenging controller assessment problem when there is no available knowledge of a plant and a disturbance signal except we can observe the input and the output signals of a plant. Among many prospective controllers, one controller makes a closed-loop system with the plant as in Figure 1.1 and the input and the output signals of the plant are observed. Then, the controller in the loop is assessed by a cost function, e.g. a ratio of the truncated $\mathfrak{L}_2$-norm of the observed signals to the truncated $\mathfrak{L}_2$-norm of the reference signals for the purpose of checking the closed-loop stability. In order to assess the other prospective controllers, we first design fictitious reference signals based on the collected input-output data of the plant and, then, formulate fictitious closed-loop systems with the plant and the prospective controllers. We assign cost functions to the fictitious closed-loop systems for the purpose of the controller assessment. By doing this, we can assess all the prospective controllers at the same time as we collect the data from the current closed-loop system. Since we do not know if the current controller is a stabilizing (or well-performing) controller, we employ a switching control scheme, in which we compare online the cost functions of the prospective controllers and switch the one with the smallest cost into the loop. Then, the stability and performance of this switching control system is guaranteed when one of the prospective controllers is feasibly stabilizing.

The switching algorithm in Chapter 2 does not lead to falsification of the closed-loop stability for each destabilizing prospective controller. Instead, in Chapter 3, we consider only one controller and determine its ability to achieve closed-loop stability by performing an experiment on the closed-loop system with the plant and the controller. If the plant is known to be a SISO LTI discrete-time system and the disturbance signal is an i.i.d. random process with zero mean, unknown variance, and finite fourth moment, then the closed-loop stability of a

SISO LTI discrete-time controller is assessed by investigating the collected data from an experiment on the closed-loop system with the plant and the controller. It is not necessary that the system under test be finite dimensional but necessary that the number of unstable poles of the system be finite. This assessment is carried out in three steps. First, it is shown that unstable poles of the closed-loop system can be detected by a least squares AR estimate with an appropriate order. Second, it is shown that the closed-loop stability of the current controller is indicated by a least squares AR estimate with any order. Last, we develop, combining two results above, a method to assess the closed-loop stability of the current controller using a sequence of least squares AR estimates.

In Chapter 4, the closed-loop stability and performance of a prospective MIMO LTI controller is predicted in three different ways when the knowledge is available that the plant is a MIMO LTI discrete-time system and is stabilized by another MIMO LTI controller, a bound on the impulse response of the closed-loop system is known, and a disturbance signal is additive to the output of the plant with a known bound. The data is collected from experiments on the closed-loop system with the plant and the currently stabilizing controller. We derive three *divination* approaches for the closed-loop stability and performance of a prospective controller and provide data-driven conditions under which these divination approaches are reliable.

Based on the results in Chapter 4, we formulate, in Chapter 5, an optimization problem for the purpose of designing a MIMO LTI discrete-time controller with a better performance than the currently stabilizing MIMO LTI discrete-time controller. FRF estimates for coprime factors of the plant are obtained with known error bounds from the experimental data described in Chapter 4 and the optimization problem is built in terms of the FRF estimates for coprime factors of the plant. Then, due to the numerical difficulty of the optimization problem, we employ a controller parametrization and propose an algorithm that may not produce the optimal controller but has fast computation ability.

## 1.3 Contribution

The main contribution of this dissertation is development of strategies to assess the closed-loop stability and performance of prospective controllers based on collected data. These strategies are suited to three different types of knowledge of a plant and a disturbance signal.

(1) A controller assessment strategy is proposed for the case where there is no available knowledge of the plant and the disturbance signal except we can observe the input and the output signals. (Chapter 2)

- Design of fictitious reference signals based on the collected input-output data of the plant in order to formulate fictitious closed-loop systems with the plant and the prospective controllers.
- Design of cost functions assigned to the fictitious closed-loop systems for the purpose of the controller assessment.
- Application of the cost functions to a switching scheme in order to construct a switching control for the plant and collect the input-output data of the plant from this switching-controlled closed-loop system. The stability and performance of this closed-loop system is only guaranteed when one of the prospective controllers is feasible.

(2) When the plant is known to be a SISO LTI discrete-time system and the disturbance signal is an i.i.d. random process with zero mean, unknown bounded variance, and finite fourth moment, the closed-loop stability of a SISO LTI discrete-time controller is assessed by investigating the collected data from the closed-loop system with the plant and the controller. (Chapter 3)

- Detection of unstable poles of the closed-loop system using a least squares AR estimate with an appropriate order.
- Indication of the closed-loop stability of the current controller using a least squares AR estimate with any order.
- Development of a method to assess the closed-loop stability of the current controller using a series of least squares AR estimates.

(3) The closed-loop stability and performance of a prospective MIMO LTI controller is predicted in three different ways when the knowledge is available that the plant is a MIMO LTI discrete-time system and is stabilized by another known MIMO LTI controller, a bound on the impulse response of the closed-loop system is known, and the disturbance signal is additive to the output of the plant with a known bound. (Chapter 4).

- Derivation of a condition for a reliable estimate for the winding number of a square transfer function.
- Development of three divination approaches for the closed-loop stability and performance of a prospective controller.
- Derivation of conditions under which the divination approaches are reliable.
- Recommendation among the three approaches.

(4) An optimization problem is formulated for the purpose of designing a MIMO LTI discrete-time controller with a better performance than a currently stabilizing MIMO LTI discrete-time controller, when FRF estimates for coprime factors of the plant are available with known bounds. (Chapter 5)

- Development of FRF estimates of the left and the right coprime factors of the plant that satisfy the double Bezout Identity.
- Formulation of an optimization problem in terms of the FRF estimates for coprime factors of the plant.
- Reduction of the numerical difficulty of the optimization problem by employment of a controller parametrization and development of an algorithm.

# 2 Controller Assessment in the Unfalsified Adaptive Control

## 2.1 Introduction

When we first encounter an uncertain system and want to control it, the first thing to do is probably to observe the input and output signals of the system for the purpose of identification. This observation can be performed in an open-loop setting or in a closed-loop setting with any first-choice controller. Since we have to deal with strong uncertainty of the system, unfalsified adaptive control [38, 31] can be a good strategy for the experiments in the early stages of the data collection.

Unfalsified adaptive control has been developed to achieve stabilization of a system under a large class of uncertainty in the plant and disturbance signals. The adaptive switching control scheme exploits the collected data in a real-time experiment rather than employing any assumption on the plant and disturbance signals. Based on the concept of the controller unfalsification [28], unfalsified adaptive control stabilizes a system with an uncertain plant and uncertain disturbance signals using the $\varepsilon$-hysteresis algorithm [19] whenever there exists a stabilizing controller, which is called a feasible controller, in a candidate controller set, provided that a plant-independent cost function of the switching algorithm is cost-detectable.

Due to the lack of knowledge of the plant and disturbance signals, it may be the first idea to place in a candidate controller set as many controllers as possible that have the possibility to stabilize the plant with the disturbance signals. We can place in a candidate controller set all the controllers that would be

used in our trial-and-error strategy. However, there is a restriction on the candidate controllers, which is called the SCLI assumption [38], i.e. each candidate controller has to be causally left invertible and the causal left inverse has to be incrementally stable. Fictitious signals for SCLI candidate controllers are well-defined and make $\mathfrak{L}_{2e}$-gain-related cost functions cost-detectable.

In order to expand the range of controllers that can be placed in a candidate controller set, the matrix fraction description method is employed in [17] and [7]. By factorizing a non-SCLI linear controller in a matrix fraction description form, the controller and a reference signal are reorganized into linear stable factors and a new reference signal. This new controller, composed of the linear stable factors, satisfies the SCLI condition. Then, fictitious reference signals for the new controllers with respect to the new reference signal, together with $\mathfrak{L}_{2e}$-gain-related cost functions, ensure the cost-detectability. In [17], the matrix fraction description method is also applied to nonlinear controllers that can be factorized into incrementally stable nonlinear matrix factors. Consequently, the SCLI assumption still plays a key role in the matrix fraction description method.

In this chapter, another method to generate fictitious signals is proposed. Fictitious signals obtained in this method and some cost functions are proved to be sufficient to directly achieve the cost-detectability without imposing the SCLI assumption on any form of candidate controllers. Since there is virtually no assumption on candidate controllers, the unfalsified adaptive control with this approach can contain virtually any controller in a candidate controller set. Another notable advantage of this approach is that the fictitious signals are generated by mere subtraction between observed signals. A fictitious reference signal for a candidate controller enables us to build a fictitious closed-loop system with the plant and the candidate controller. The cost function for the candidate controller is designed to assess the stability and/or performance of the fictitious system. However, since a finite amount of data are not enough to falsify the stability and/or performance of the fictitious system, we employ a switching algorithm to compare the cost of candidate controllers and switch the one with the smallest cost into the real closed-loop system. We show that a candidate controller whose cost is less than a certain level will remain in the real closed-loop system in the end, provided

that the feasibility assumption is met.

In Section 2.2, an adaptive switching control system is carefully described. In Section 2.3, new fictitious reference signals are introduced and the unfalsified adaptive control is built with these fictitious reference signals. Cost-detectable cost functions using these new fictitious reference signals are introduced in Section 2.4. An example is provided in Section 2.5. Conclusion follows in Section 2.6.

## 2.2 Adaptive control problem formulation

The theory in this chapter is developed for continuous-time systems but can be easily extended for discrete-time systems.

The norm $\|\cdot\|$ is the $\mathfrak{L}_2$-norm and denote by $\mathfrak{L}_2^m$ the $\mathfrak{L}_2$ space of $m$-dimensional functions of time, i.e. $\mathfrak{L}_2^m = \{x : [0,\infty) \mapsto \mathbb{R}^m |\ \|x\| < \infty\}$. Define a truncated version of the $\mathfrak{L}_2$-norm

$$\|x\|_t \triangleq \sqrt{\int_0^t x^T(\tau)x(\tau)d\tau}$$

for any function of time $x$ and denote the extended space of $\mathfrak{L}_2^m$ by $\mathfrak{L}_{2e}^m = \{x : [0,\infty) \mapsto \mathbb{R}^m |\ \|x\|_t < \infty, \forall t \in [0,\infty)\}$.

**Definition 1.** *(Stability) A mapping (or a system) $G : \mathfrak{L}_{2e}^{m_i} \mapsto \mathfrak{L}_{2e}^{m_o}$ is said to be stable if there exist constants $\alpha_s$, $\beta_s \geq 0$ such that for any given input signal $x \in \mathfrak{L}_{2e}^{m_i}$*

$$\|Gx\|_t \leq \alpha_s\|x\|_t + \beta_s \quad \text{for } \forall t \geq 0.$$

*Otherwise, $G$ is said to be unstable.*

An adaptive control system in Figure 2.1 is considered as a mapping from two system-input signals, i.e. a reference signal $w = \begin{bmatrix} r^T & s^T \end{bmatrix}^T \in \mathfrak{L}_{2e}^{(m_u+m_y)}$ and a disturbance signal $d \in \mathfrak{L}_{2e}^{m_d}$, to an observed system-output signal $z = \begin{bmatrix} u^T & y^T \end{bmatrix}^T$ where $u$ is the plant-input signal and $y$ is the measured output signal. The reference signal $w$ is known and the disturbance signal $d$ is unknown. The plant $P : \mathfrak{L}_{2e}^{m_u} \times \mathfrak{L}_{2e}^{m_d} \mapsto \mathfrak{L}_{2e}^{m_y}$ is an uncertain mapping from $u$ and $d$ to $y$, parametrized by unknown initial conditions at time 0, which we suppress in the notation. Then, the input-

output relationship of $P$ can be expressed by

$$\mathbb{Z}_P(d) = \left\{ x_z = \begin{bmatrix} x_u \\ x_y \end{bmatrix} \;\middle|\; x_u \in \mathfrak{L}_{2e}^{m_u}, x_y = P(x_u, d) \right\}$$

whose element is one possible experimental datum over a time interval $[0, \infty)$ for a given $d$.

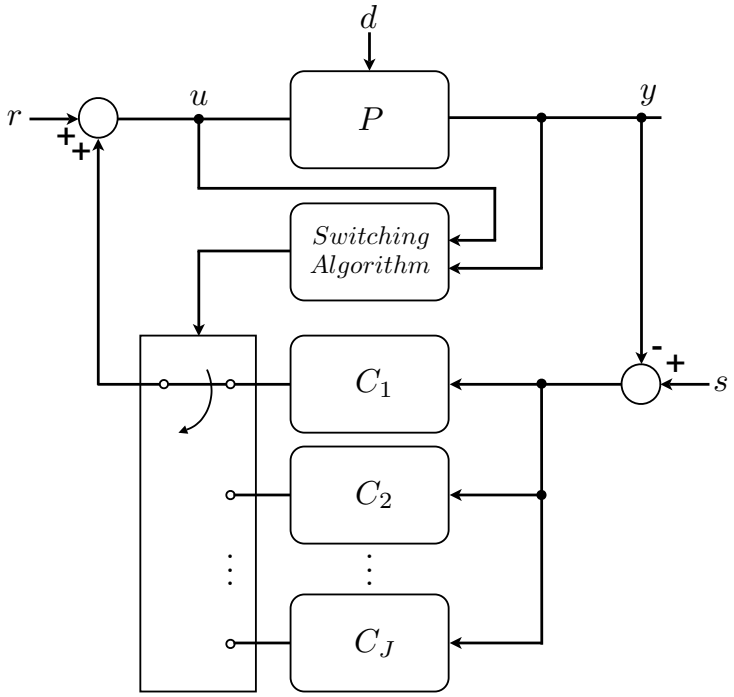


Figure 2.1: An adaptive switching control.

A candidate controller set $\mathbb{C}$ contains $J$ number of candidate controllers. For any given $C \in \mathbb{C}$, the candidate controller $C : \mathfrak{L}_{2e}^{m_y} \mapsto \mathfrak{L}_{2e}^{m_u}$ is a mapping from a controller-input signal, denoted by $y_C \in \mathfrak{L}_{2e}^{m_y}$, to a controller-output signal, denoted by $u_C \in \mathfrak{L}_{2e}^{m_u}$. Further, denote by $z_C = \begin{bmatrix} y_C^T & u_C^T \end{bmatrix}^T$ the input and the output signals of $C$. If $C$ has a state, we choose one initial state. Then, the candidate controller $C$ can be expressed by input-output relationship

$$\mathbb{Z}_C = \left\{ x_{z_C} = \begin{bmatrix} x_{y_C}^T & x_{u_C}^T \end{bmatrix}^T \;\middle|\; x_{y_C} \in \mathfrak{L}_{2e}^{m_y},\ x_{u_C} = C x_{y_C} \right\}.$$

A switching algorithm selects a candidate controller at each selecting time

from the candidate controller set $\mathbb{C}$ and keeps its controller-output signal delivered to the loop of the adaptive control system until the next selecting time. Denote by $\hat{C}$ the sequence of controllers that are chosen and connected in the loop of the adaptive control system by the switching algorithm and let $\hat{C}_t$ denote the candidate controller that is connected in the loop of the adaptive control system at time $t \geq 0$. When a candidate controller $C \in \mathbb{C}$ is selected by the switching algorithm, the input signal $u$ of $P$ is given by the sum of $r$ and the output signal $u_C$ of $C$ as shown in Figure 2.2 (a) until the next selecting time. Thus, the input-output signal of $C$ is obtained by $z_C(t) = \begin{bmatrix} y_C(t)^T & u_C(t)^T \end{bmatrix}^T = \begin{bmatrix} s(t)^T - y(t)^T & u(t)^T - r(t)^T \end{bmatrix}^T$ for any time $t \geq 0$ satisfying $\hat{C}_t = C$.

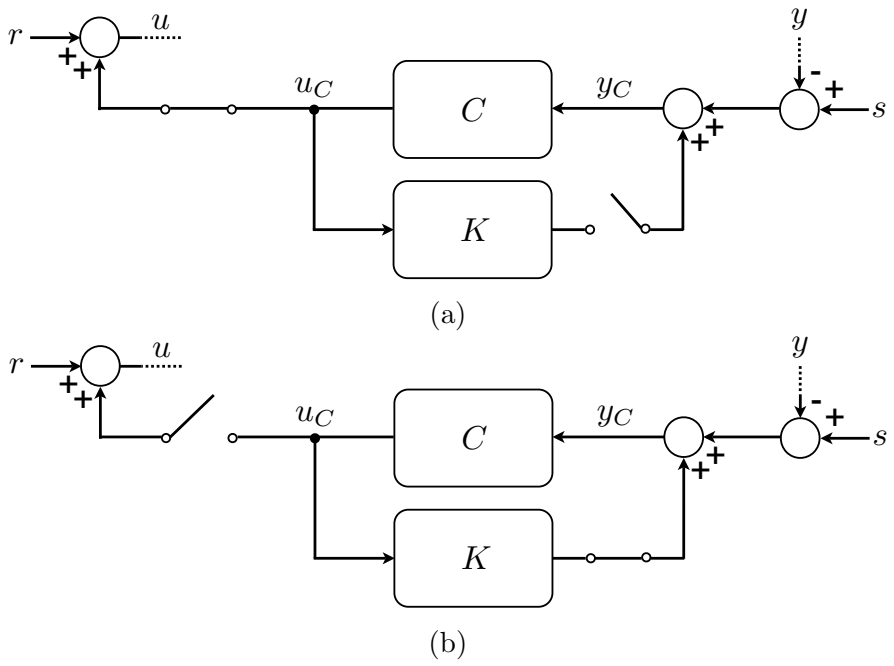


Figure 2.2: A candidate controller and its subcontroller (a) when the candidate controller is selected and connected in the adaptive control system (b) when it is not connected.

When a candidate controller $C \in \mathbb{C}$ is not connected in the loop of the adaptive control system, $C$ makes a closed-loop system with a subcontroller $K$ as shown in Figure 2.2 (b). The subcontroller $K$ is designed to stabilize $C$ in the $(C, K)$ closed loop. Although $K$ in Figure 2.2 is depicted to use only the output signal of $C$, actually $K$ is allowed to use not only the output signal of $C$ but also every information on $C$ with perfect knowledge of $C$. If $C$ is stable itself, $K$ can be given as a zero subcontroller whose output signal is 0 for $\forall t \geq 0$. The role of the

subcontroller is to build a stable mapping, as in Definition 1, from $s-y$ to a signal anywhere in the closed-loop system of $C$ and $K$ while the candidate controller is not in the loop of the adaptive control system. Thus, the output signal and state of $C$ do not become inordinately large while disconnected.

Figure 2.2 shows that, for any given $C \in \mathbb{C}$ and its corresponding subcontroller $K$, we have

$$\begin{aligned} y_C(t) &= s(t) - y(t) \\ u_C(t) &= u(t) - r(t) \end{aligned} \tag{2.1}$$

for any time $t \geq 0$ when $C$ is connected in the loop of the adaptive control system. When $C$ is not connected in the loop of the adaptive control system, the mapping from $s-y$ to $z_C = \begin{bmatrix} u_C & y_C \end{bmatrix}^T$ is stable as in Definition 1. Note that if $C$ is stable itself and, hence, $K$ is a zero subcontroller, then $y_C(t) = s(t) - y(t)$ for $\forall t \geq 0$.

## 2.3 Unfalsified adaptive switching control

**Definition 2.** *(Fictitious reference signal) Given the candidate controller set $\mathbb{C}$ in Section 2.2, fictitious reference signals for a candidate controller $C \in \mathbb{C}$ are defined by*

$$\tilde{w}(x_{z_C}, x_z) \triangleq \begin{bmatrix} \tilde{r}(x_{z_C}, x_z) \\ \tilde{s}(x_{z_C}, x_z) \end{bmatrix} \triangleq \begin{bmatrix} x_u - x_{u_C} \\ x_{y_C} + x_y \end{bmatrix}$$

*for $\forall x_{z_C} \in \mathbb{Z}_C$ and $\forall x_z = \begin{bmatrix} x_u^T & x_y^T \end{bmatrix}^T \in \mathfrak{L}_{2e}^{(m_u+m_y)}$. Denote by $\tilde{w}(x_{z_C}, x_z, t)$ the evaluated value of the signal $\tilde{w}(x_{z_C}, x_z)$ at time $t \geq 0$.*

For any given $C \in \mathbb{C}$, $x_{z_C} \in \mathbb{Z}_C$, and $x_z \in \mathbb{Z}_P(d)$, the fictitious reference signal $\tilde{w}(x_{z_C}, x_z)$ is a hypothetical signal that would have exactly reproduced the input-output signal $x_{z_C} = \begin{bmatrix} x_{y_C}^T & x_{u_C}^T \end{bmatrix}^T$ of $C$ and the input-output signal $x_z = \begin{bmatrix} x_u^T & x_y^T \end{bmatrix}^T$ of $P$ had the fictitious reference signal been injected into a fictitious system in Fig. 2.3, i.e. $\begin{bmatrix} x_r^T & x_s^T \end{bmatrix}^T = \tilde{w}(x_{z_C}, x_z)$.

If a controller $C \in \mathbb{C}$ is stably causally left invertible (SCLI) [38], then there exists $x_{z_C} \in \mathbb{Z}_C$ such that a fictitious reference signal has $\tilde{r}(x_{z_C}, x_z, t) = 0$ for $\forall x_z = \begin{bmatrix} x_u^T & x_y^T \end{bmatrix}^T \in \mathfrak{L}_{2e}^{(m_u+m_y)}$ and $\forall t \geq 0$, which is the unique fictitious reference

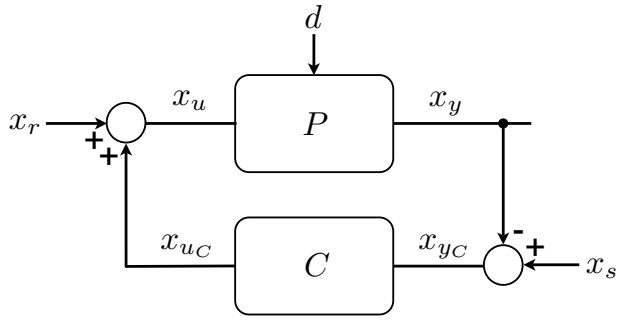


Figure 2.3: A candidate controller and a corresponding fictitious system.

signal in [38]. If a controller $C \in \mathbb{C}$ can be factored into incrementally stable factors, then the fictitious reference signals for $C$ can be represented by one signal, which is the virtual reference signal in [17].

Note that all signals that are needed to generate the fictitious reference signal $\tilde{w}(z_C, z)$ are observed in the adaptive control system and the fictitious reference signal is obtained from mere subtraction between the observed signals. At time $t \geq 0$, if a candidate controller $C$ is connected on the loop of the adaptive control system in Section 2.2, then it is clear from Figure 2.2 that $z_C(t) = \begin{bmatrix} y(t)^T - s(t)^T & u(t)^T - r(t)^T \end{bmatrix}^T$, from which together with the definition of the fictitious reference signal, it follows that

$$\tilde{w}(z_C, z, t) = \begin{bmatrix} r(t)^T & s(t)^T \end{bmatrix}^T = w(t).$$

If $C$ is not connected on the loop of the adaptive control system, then its corresponding subcontroller $K$ makes a closed-loop system with $C$ and stabilizes $C$ so that a mapping from $s - y$ to $z_C$ is stable and, hence, a mapping from $\begin{bmatrix} s^T & z^T \end{bmatrix}^T$ to $\tilde{w}(z_C, z)$ is stable. Therefore, a mapping from $\begin{bmatrix} w^T & z^T \end{bmatrix}^T$ to $\tilde{w}(z_C, z)$ is always stable whether or not the candidate controller is connected in the loop of the adaptive control system.

The observed signals in the adaptive control system in Section 2.2 and the fictitious reference signal for $C \in \mathbb{C}$ can be considered the data from an experiment on the fictitious system $(P, C)$ for $C$ in Figure 2.3 with the fictitious reference signal $\tilde{w}(z_C, z)$ as an external input signal. Based on this data, the fictitious system is assessed by a mapping $V : \mathbb{C} \times \mathfrak{L}_{2e}^{(m_u+m_y)} \times \mathfrak{L}_{2e}^{(m_u+m_y)} \mapsto \mathfrak{L}_{2e}^{1}$, that is called a cost

mapping. In other words, for any given $C \in \mathbb{C}$, $x_{z_C} \in \mathbb{Z}_C$, and $x_z \in \mathbb{Z}_P(d)$, the fictitious system $(P, C)$ in Figure 2.3 is evaluated by $V(C, x_{z_C}, x_z)$. Denote by $V(C, x_{z_C}, x_z, t)$ the evaluated value of $V(C, x_{z_C}, x_z)$ at time $t \geq 0$. The cost mapping $V$ is designed to be causal, which means that $V(C, x_{z_C}, x_z, t)$ depends only on $C$, $x_{z_C}(\tau)$, and $x_z(\tau)$ for $\forall \tau \in [0, t]$. An example of the cost function is

$$V_1(C, x_{z_C}, x_z, t) = \max_{0 \leq \tau \leq t} \frac{\|x_z\|_\tau}{\|\tilde{w}(x_{z_C}, x_z)\|_\tau + \rho} \tag{2.2}$$

for $\forall t \geq 0$ where $\rho$ is a positive constant. This cost function is bounded if, and only if, the fictitious system $(P, C)$ for $C$ in Figure 2.3 is stable (Definition 1). For the stability and the tracking performance, we can employ a cost function

$$V_2(C, x_{z_C}, x_z, t) = \max_{0 \leq \tau \leq t} \frac{\|x_u\|_\tau + \|x_y - x_s\|_\tau}{\|\tilde{w}(x_{z_C}, x_z)\|_\tau + \rho} \tag{2.3}$$

for $\forall t \geq 0$ where $\rho$ is a positive constant.

**Definition 3.** *(Feasibility) Given the plant $P$ and the disturbance signal $d$ in the adaptive control system in Section 2.2, together with a cost mapping $V$, a controller $C$ is said to be a feasible controller if there exist constants $\alpha_f \geq 0$ such that for any given $x_{z_C} \in \mathbb{Z}_C$ and $x_z \in \mathbb{Z}_P(d)$*

$$V(C, x_{z_C}, x_z, t) \leq \alpha_f \quad \text{for } \forall t \geq 0.$$

*The adaptive control problem is said to be feasible if the candidate controller set $\mathbb{C}$ contains at least one feasible controller.*

Given a cost mapping $V$, whether a controller is a feasible controller or not depends on the plant and the disturbance signal in the experiment conducted from time 0 to $\infty$.

In an experiment, the input-output signal $z$ of the plant and the input-output signals $z_C$ for $C \in \mathbb{C}$ in the adaptive control system in Section 2.2 are observed. During the experiment, for each candidate controller $C$, a fictitious reference signal $\tilde{w}(z_C, z, t)$ and a fictitious system is generated, based on which a cost mapping $V(C, z_C, z, t)$ is computed online. With these cost mappings, the $\varepsilon$-Hysteresis Switching Algorithm [19] is employed.

**Algorithm 1.** *(ε-Hysteresis Switching Algorithm)*

$$\hat{C}_t = \arg\min_{C\in\mathbb{C}} \left\{ V(C, z_C, z, t) - \varepsilon\delta_{C\hat{C}_{t^-}} \right\}$$

*where $\varepsilon > 0$ is a constant, $\delta_{ij}$ is the Kronecker's $\delta$, and $\hat{C}_{t^-} = \lim_{\tau\uparrow t} \hat{C}_\tau$.*

The $\varepsilon$-Hysteresis Switching Algorithm compares the candidate controllers and switches into the the closed-loop a controller whose cost function $V(C, x_{z_C}, x_z, t)$ has the smallest value. The controller in the loop is given an advantage of an amount of $\varepsilon$ so that the infinitely fast switching is prevented. Convergence of the switching algorithm in a finite number of switches is stated in the following lemma.

**Lemma 1.** *(Convergence)[38] Consider the adaptive control system in Section 2.2, together with a cost mapping $V$ and Algorithm 1. Suppose that 1) $V(C, x_{z_C}, x_z, t)$ is nondecreasing in time $t$ and 2) the candidate controller set $\mathbb{C}$ contains at least one feasible controller (Definition 3). Then, the number of switches is finite and $V(C_f, z_{C_f}, z, t)$ remains bounded as $t$ increases to infinity where $C_f$ is the final controller in the controller sequence and $z_{C_f}$ is the input-output signal of $C_f$.*

The proof of Lemma 1 also guarantees that if a controller $C$ is in the closed-loop at time $t \geq 0$, then the cost function $V(C, x_{z_C}, x_z, t)$ of $C$ satisfies $V(C, x_{z_C}, x_z, t) \leq \alpha_f + \varepsilon$ where $\alpha_f$ is an upper bound of a feasible controller (Definition 3). Thus, the final controller also satisfies $V(C_f, x_{z_{C_f}}, x_z, t) \leq \alpha_f + \varepsilon$, which means that the performance of $C_f$ measured by the cost function $V(C_f, x_{z_{C_f}}, x_z, t)$ is unfalsified.

On the other hand, the adaptive control system in Section 2.2 is assessed by a mapping $\hat{V} : \mathfrak{L}_{2e}^{(m_u+m_y)} \times \mathfrak{L}_{2e}^{(m_u+m_y)} \mapsto \mathfrak{L}_{2e}^{1}$. Given the signals $w$ and $z$, the adaptive control system in Section 2.2 is evaluated by $\hat{V}(w, z)$. Denote by $\hat{V}(w, z, t)$ the evaluated value of $\hat{V}(w, z)$ at time $t \geq 0$. The cost mapping $\hat{V}$ is designed to be causal, which means that $\hat{V}(w, z, t)$ depends only on $w(\tau)$ and $z(\tau)$ for $\forall\tau \in [0, t]$. An example of the cost function $\hat{V}$ is

$$\hat{V}_1(w, z, t) = \max_{0\leq\tau\leq t} \frac{\|z\|_\tau}{\|w\|_\tau + \rho} \tag{2.4}$$

for $\forall t \geq 0$ where $\rho$ is a positive constant. This cost function is bounded if, and only

if, the stability of the adaptive control system in Section 2.2. Another example of the cost function is

$$\hat{V}_2(w,z,t) = \max_{0\le\tau\le t} \frac{\|u\|_\tau + \|y-s\|_\tau}{\|w\|_\tau + \rho} \tag{2.5}$$

for $\forall t \ge 0$ where $\rho$ is a positive constant. This cost function represents the stability and the tracking performance of the adaptive control system in Section 2.2.

**Definition 4.** *(Cost-detectability) Given the reference signal* $w = \begin{bmatrix} r^T & s^T \end{bmatrix}^T$ *and the candidate controller set* $\mathbb{C}$ *in the adaptive control system in Section 2.2, together with cost mappings* $V$ *and* $\hat{V}$*, the pair* $(V, \hat{V})$ *is said to be cost-detectable if, for every sequence of switched controllers* $\hat{C}$ *with finitely many switches and the accordingly observed system-output signal* $z = \begin{bmatrix} u^T & y^T \end{bmatrix}^T$*, the following statements are equivalent:*

*1) The cost function* $V(C_f, z_{C_f}, z, t)$ *is bounded as* $t$ *increases to infinity where* $C_f$ *is the final controller in the controller sequence* $\hat{C}$ *and* $z_{C_f}$ *is the input-output signal of* $C_f$*.*

*2) The cost function* $\hat{V}(w,z,t)$ *is bounded as* $t$ *increases to infinity.*

Examples of the cost-detectable pairs are $(V_1, \hat{V}_1)$ from (2.2) and (2.4) and $(V_2, \hat{V}_2)$ from (2.3) and (2.5). The details are explained in Section 2.4.

The main result of the unfalsified adaptive control follows.

**Theorem 1.** *Consider the adaptive control system in Section 2.2, together with a cost mapping* $V$ *and Algorithm 1. Suppose that 1)* $V(C, x_{z_C}, x_z, t)$ *is nondecreasing in* $t$*, 2) the adaptive control problem is feasible (Definition 3), and 3) the pair* $(V, \hat{V})$ *is cost-detectable (Definition 4). Then, there exist a constant* $\alpha_u \ge 0$ *such that* $\hat{V}(w,z,t) \le \alpha_u$ *for* $\forall t \ge 0$*.*

**Proof.** By Lemma 1, the number of switches is finite and $V(C_f, z_{C_f}, z, t)$ remains bounded as $t$ increases to infinity. The cost-detectability in Definition 4 completes the proof. □

## 2.4 Cost detectable cost mappings

In this section, cost mappings are introduced that satisfy the first and the third assumptions in Theorem 1.

Using the fictitious reference signals, consider cost mappings $V$ and $\hat{V}$ such that, for any given $x_w \in \mathfrak{L}_{2e}^{(m_u+m_y)}$, $x_z \in \mathfrak{L}_{2e}^{(m_u+m_y)}$, $C \in \mathbb{C}$, and $x_{z_C} \in \mathbb{Z}_C$,

$$\begin{aligned} V(C, x_{z_C}, x_z, t) &= \max_{0\le\tau\le t} \frac{\|x_z\|_\tau}{\|\tilde{w}(x_{z_C}, x_z)\|_\tau + f(\tau)} \\ \hat{V}(w, z, t) &= \max_{0\le\tau\le t} \frac{\|z\|_\tau}{\|w\|_\tau + f(\tau)} \end{aligned} \tag{2.6}$$

for $\forall t \ge 0$ where $f : [0, \infty) \mapsto \mathbb{R}$ is a monotonically increasing function with $f(0) > 0$. Then, cost-detectability as in Definition 4 is proved by the following lemma.

**Proposition 1.** *Given the reference signal* $w = \begin{bmatrix} r^T & s^T \end{bmatrix}^T$*, the candidate controller set* $\mathbb{C}$*, the cost mappings* $V$ *and* $\hat{V}$ *in* (2.6)*, the input-output signal* $z_C = \begin{bmatrix} u_C^T & y_C^T \end{bmatrix}^T$ *of* $C$ *for* $\forall C \in \mathbb{C}$*, and the observed input-output signal* $z = \begin{bmatrix} u^T & y^T \end{bmatrix}^T$ *of the plant in the adaptive control system in Section 2.2, the pair* $(V, \hat{V})$ *is cost-detectable (Definition 4).*

When we choose $f(t) = \rho$ for $\forall t \ge 0$ where $\rho > 0$ is a constant, the bounded property of $\hat{V}$ means stability of the adaptive control system in Section 2.2 considering the disturbance signal a part of the plant. However, in this case, the feasibility assumption becomes very restrictive. To see this, consider a nonvanishing disturbance signal $d \in \mathfrak{L}_{2e}^{m_d} \setminus \mathfrak{L}_2^{m_d}$, i.e. $\|d\| = \infty$, such as a sinusoidal signal, a step signal, or a white noise signal with nonzero variances. In a fictitious system for a controller $C$ in Figure 2.3 with a zero signal $x_w \in \mathfrak{L}_{2e}^{(m_u+m_y)}$, i.e. $\|x_w\| = 0$, substituted for the fictitious reference signal, we observe two signals $x_z \in \mathbb{Z}_P(d)$ and $x_{z_C} = \begin{bmatrix} x_{yC}^T & x_{uC}^T \end{bmatrix}^T \in \mathbb{Z}_C$ and, hence, obtain $\tilde{w}(x_{z_C}, x_z) = x_w = \mathbf{0}_{(m_u+m_y)}$, where $\mathbf{0}_{(m_u+m_y)} \in \mathbb{R}^{(m_u+m_y)\times 1}$ is a zero vector, from Definition 2. Then, from Definition 3, it follows that a necessary condition for the controller $C$ to be a feasible controller is that there exists a finite constant $\alpha_f \ge 0$ such that $\|x_z\|_t \le \alpha_f \rho$ for $\forall t \ge 0$. On the other hand, if $C$ is a stabilizing controller, what is guaranteed is existence of constants $\alpha_s, \beta_s \ge 0$ satisfying $\|x_z\|_t \le \alpha_s \|d\|_t + \beta_s$ for $\forall t \ge 0$. There-

fore, it can be concluded that a controller that stabilizes the plant is required to have an additional ability to attenuate the effect of the nonvanishing disturbance signal on signals observed anywhere in the closed-loop system in order to be a feasible controller, which means that it is highly possible that there does not exist a feasible controller even for a plant that can be easily stabilized.

The bigger the function $f$ is, the larger the number of feasible controllers is according to the definition of a feasible controller in Definition 3, which makes the feasibility assumption in Theorem 1 less restrictive. If $f$ is big enough, any given stabilizing controller as in Definition 1 becomes a feasible controller. The following proposition provides a sufficient condition imposed on $f$ for any stabilizing controller to be a feasible controller.

**Proposition 2.** *Given the unknown disturbance signal $d$, the input-output description of the plant $\mathbb{Z}_P(d)$ in the adaptive control system in Section 2.2 with the cost mappings $V$ and $\hat{V}$ in (2.6), an arbitrarily given stabilizing controller $C$ as in Definition 1 is a feasible controller if there exists a constant $\alpha_d$ such that $\|d\|_t \leq \alpha_d f(t)$ for $\forall t \geq 0$.*

When there is a known monotonically increasing function $f$ such that $f(0) > 0$ and $\|d\|_t \leq \alpha_d f(t)$ for $\forall t \geq 0$ where $\alpha_d$ is an unknown constant, a choice for cost mappings can be $V$ and $\hat{V}$ in (2.6). Then, by Proposition 2 combined with Proposition 1 and Theorem 1, it is guaranteed that there exist constants $\alpha_u, \beta_u \geq 0$ such that

$$\|z\|_t \leq \alpha_u \left(\|w\|_t + f(t)\right) + \beta_u$$

for $\forall t \geq 0$ in the adaptive control system in Section 2.2, provided that the candidate controller set contains at least one stabilizing controller. Clearly, this result is weaker than the stability of the adaptive control system but is still acceptable considering the limited knowledge of the disturbance signal since it is possible that the adaptive control system is stable with $\|d\|_t = \alpha_d f(t)$ for $\forall t \geq 0$. It is also possible that the adaptive control system is unstable, e.g. $\|d\| = 0$ and $f(t) = \sqrt{t+1}$ for $\forall t \geq 0$. Since this possibility of unstable cases comes from discrepancy between $f(t)$ and $\|d\|_t$, a tighter bound on $\|d\|_t$, i.e. a smaller $f$, is preferable to remove more possibility of unstable cases.

In some systems disturbance signals are random signals. A bounding

function $f$ for a random disturbance signal $d$ is obtained in the following. Suppose that the disturbance signal $d$ is given by

$$d(t) = \begin{cases} v[0] & \text{for } 0 \le t < T \\ v[1] & \text{for } T \le t < 2T \\ \vdots & \vdots \end{cases} \tag{2.7}$$

for $\forall t \ge 0$ where $T$ is a positive constant that may represent a sampling period of measurement devices or process of the plant and $\{v[n], n = 0, 1, \cdots\}$ is a random process generated by

$$v[n] = \sum_{k=0}^{\infty} h_n[k] e[n-k]$$

for $n = 0, 1, \cdots$. The random process $\{e[n], n = \cdots, -1, 0, 1, \cdots\}$ is a sequence of independent random vectors whose elements have zero mean values and bounded forth moments and $\{h_n[k], k = 0, 1, \cdots\}$ is impulse response of a discrete-time system $H_n$ for $n = 0, 1, \cdots$, respectively. It is assumed that there exists a function $\bar{h} : \{0, 1, \cdots\} \mapsto \mathbb{R}$ such that absolute values of elements of $h_n[k]$ is less than $\bar{h}[k]$ for $n, k = 0, 1, \cdots$ and $\sum_{k=0}^{\infty} \bar{h}[k] < \infty$.

**Proposition 3.** *Given the random disturbance signal $d$ in (2.7), there, almost surely, exists a constant $\alpha_d$ such that $\frac{\|d\|_t}{\sqrt{t+\rho_d}} \le \alpha_d$ for $\forall t \ge 0$ where $\rho_d$ is a positive constant.*

With a choice of $f(t) = \sqrt{t + \rho_d}$ for $\forall t \ge 0$ where $\rho_d$ is a positive constant, Proposition 3 combined with Proposition 2 confirms that any stabilizing controller is a feasible controller with probability 1. Then, by Proposition 1 and Theorem 1, it is guaranteed that there, almost surely, exist constants $\alpha_u, \beta_u \ge 0$ such that

$$\|z\|_t \le \alpha_u \left( \|w\|_t + \sqrt{t + \rho_d} \right) + \beta_u$$

for $\forall t \ge 0$ in the adaptive control system in Section 2.2 with the disturbance signal $d$ in (2.7), Algorithm 1, and the cost mappings in (2.6), provided that the candidate controller set contains at least one stabilizing controller.

## 2.5 Example

Consider the adaptive switching control system in Figure 2.1 with an uncertain continuous-time plant $P$

$$\dot{x}_p(t) = -x_p(t - 0.5) + u(t) \tag{2.8}$$

whose output signal is $x_p(t)$. The dynamics of this plant $P$ as well as the initial condition $x_p(\tau)$ for $\tau \in [-0.5, 0]$ are unknown. We measure the plant-output signal with a sampling period $T$ and this measurement is corrupted by a noise signal $d$, i.e.

$$y[n] = x_p(nT) + d[n]$$

for $n = 0, 1, \ldots$. The plant-input signal $u$ is given by a zero-order hold method

$$u(t) = u[n] \quad \text{for} \quad nT \leq t < (n + 1)T$$

with the discrete-time signal $u[n]$ produced as an outcome of switching of discrete-time controllers combined with the discrete-time reference signals $r[n]$ and $s[n]$ as well as the measured noisy plant-output signal $y[n]$.

For prospective controllers, we consider two proportional controllers

$$C_1 = -0.9 \quad \text{and} \quad C_2 = -1.1$$

in the candidate controller set $\mathbb{C}$. Then, the input-output signals of those controllers are $z_{C_1} = \begin{bmatrix} s - y & -0.9(s - y) \end{bmatrix}^T$ and $z_{C_2} = \begin{bmatrix} s - y & -1.1(s - y) \end{bmatrix}^T$, respectively, and the fictitious reference signals for those controllers are

$$\tilde{w}(z_{C_1}, z) = \begin{bmatrix} u + 0.9(s - y) \\ s \end{bmatrix} \quad \text{and} \quad \tilde{w}(z_{C_2}, z) = \begin{bmatrix} u + 1.1(s - y) \\ s \end{bmatrix},$$

respectively, with $z = \begin{bmatrix} u & y \end{bmatrix}^T$. For cost-detectable cost functions, we consider

$$V(C_1, z_{C_1}, z, n) = \max_{k\in\{0,\dots,n\}} \frac{\|z\|_k}{\|\tilde{w}(z_{C_1}, z)\|_k + 1}$$
$$V(C_2, z_{C_2}, z, n) = \max_{k\in\{0,\dots,n\}} \frac{\|z\|_k}{\|\tilde{w}(z_{C_2}, z)\|_k + 1}$$
$$\hat{V}(w, z, n) = \max_{k\in\{0,\dots,n\}} \frac{\|z\|_k}{\|w\|_k + 1}$$

where $w = \begin{bmatrix} r & s \end{bmatrix}^T$ and $\|\cdot\|_k$ is a truncated $\ell_2$-norm, e.g. $\|z\|_k \triangleq \sqrt{\sum_{\tau=0}^{k} z^T[\tau] z[\tau]}$. The cost function $\hat{V}(w, z, n)$ represents the stability of the adaptive switching control system.

### 2.5.1 MATLAB simulation

In the MATLAB simulation, the sampling period is set to $T = 1sec$ and the reference signals are given by

$$r[n] = 0 \quad \text{and} \quad s[n] = 1$$

for $n = 0, 1, \dots$. The noise signal $d[n]$ is generated as a realization of an iid random process with a normal distribution. The initial condition is set to $x_p(\tau) = 0$ for $\tau \in [-0.5, 0]$. We set $\varepsilon = 0.2$ for the $\varepsilon$-hysteresis switching algorithm.

The selection of controllers in the $\varepsilon$-hysteresis switching algorithm is shown in Figure 2.4. The initial controller in the $\varepsilon$-hysteresis switching algorithm is $C_1$ and the switching occurs often until $100sec$. After that, the switching stops and $C_1$ stays connected in the adaptive switching control system.

The plant-output signal $y$ is recorded and shown in Figure 2.5. If we run this simulation in infinite time and the input-output signal $z$ of the plant stays bounded, then the cost function $\hat{V}$ stays bounded and, thus, the input-output stability of the adaptive switching control system is unfalsified with the given external signals.

Seemingly, $C_1$ stabilizes the plant and $C_2$ does not. If $C_1$ stays connected as a final controller of the switching in the infinite-duration simulation and the

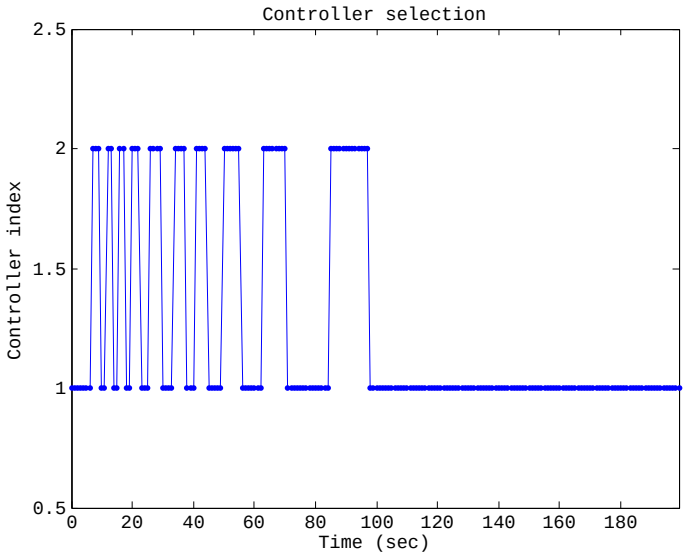


Figure 2.4: The selection of controllers in the switching algorithm.

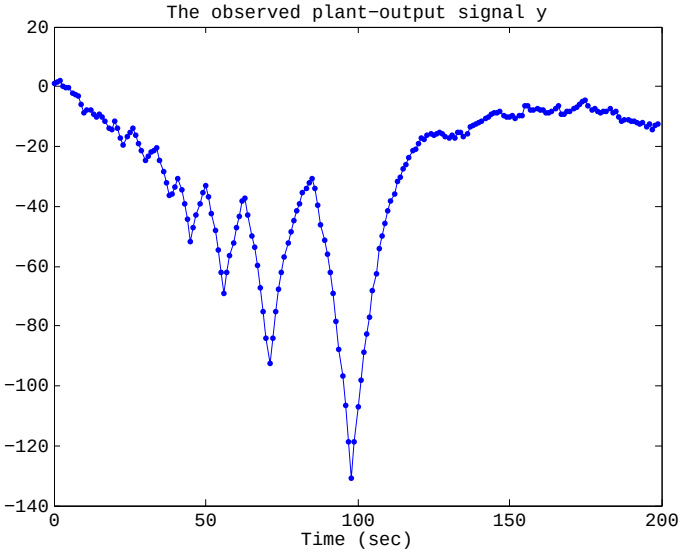


Figure 2.5: The plant-output signal $y$.

input-output signal $z$ of the plant stays bounded, then we may consider $C_1$ a stabilizing controller. But we cannot make any statement about the stabilizing or destabilizing property of $C_2$.

## 2.6 Conclusion

We assessed the stability and/or performance of a closed-loop system with a plant and a candidate controller by assigning a cost function. Since we do not have enough information on the plant and disturbance signals to falsify the stability and/or performance with a finite amount of data, we compare, during an experiment, the cost functions of candidate controllers and try to switch a controller with the lowest cost value. In the end of the experiment, the unfalsified adaptive control guarantees that a controller whose cost value is less than a certain level remains in the closed-loop system, provided the feasibility assumption is met. Future works include development of a method to improve the unfalsified adaptive control based on a limited amount of knowledge of a plant and disturbance signals.

## 2.7 Appendices

### 2.7.1 Proof of Proposition 1

Suppose that there are finite number of switches and denote the final controller and the final switching time by $C_f$ and $t_f < \infty$, respectively.

From Definition 2, it follows that $\tilde{w}(z_{C_f}, z, t) = w(t)$ for $\forall t \geq t_f$ and, hence, it can be obtained that

$$\left\|\tilde{w}(z_{C_f}, z) - w\right\|_t \leq \left\|\tilde{w}(z_{C_f}, z) - w\right\|_{t_f} \triangleq \beta < \infty \tag{2.9}$$

for $\forall t \geq 0$ from the fact that the signals are in $\mathfrak{L}_{2e}$. From the triangle inequality and (2.9), it can be obtained that

$$\left\|\tilde{w}(z_{C_f}, z)\right\|_t \leq \left\|\tilde{w}(z_{C_f}, z) - w\right\|_t + \|w\|_t \leq \|w\|_t + \beta \tag{2.10}$$

for $\forall t \geq 0$ and

$$\|w\|_t \leq \left\|w - \tilde{w}(z_{C_f}, z)\right\|_t + \left\|\tilde{w}(z_{C_f}, z)\right\|_t \leq \left\|\tilde{w}(z_{C_f}, z)\right\|_t + \beta \tag{2.11}$$

for $\forall t \geq 0$.

The two statements in the definition of cost-detectability in Definition 4

is proved to be equivalent by showing 1) the sufficiency part and 2) the necessity part.

1) Suppose that there exists a constant $\alpha_1$ such that

$$V(C_f, z_{C_f}, z, t) = \max_{0\le\tau\le t} \frac{\|z\|_\tau}{\|\tilde{w}(z_C, z)\|_\tau + f(\tau)} \le \alpha_1$$

for $\forall t \ge 0$. Then, it is clear that $\|z\|_t \le \alpha_1 \left(\left\|\tilde{w}(z_{C_f}, z)\right\|_t + f(t)\right)$ for $\forall t \ge 0$, from which, together with (2.6) and (2.10), it follows that

$$\hat{V}(w, z, t) \le \alpha_1 \max_{0\le\tau\le t} \frac{\|w\|_\tau + \beta + f(\tau)}{\|w\|_\tau + f(\tau)} \le \alpha_1 \left(1 + \frac{\beta}{f(0)}\right)$$

for $\forall t \ge 0$.

2) Suppose that there exists a constant $\alpha_2$ such that

$$\hat{V}(w, z, t) = \max_{0\le\tau\le t} \frac{\|z\|_\tau}{\|w\|_\tau + f(\tau)} \le \alpha_2$$

for $\forall t \ge 0$. Then, it is clear that $\|z\|_t \le \alpha_2 \left(\|w\|_t + f(t)\right)$ for $\forall t \ge 0$, from which, together with (2.6) and (2.11), it follows that

$$V(C_f, z_{C_f}, z, t) \le \alpha_2 \max_{0\le\tau\le t} \frac{\left\|\tilde{w}(z_{C_f}, z)\right\|_\tau + \beta + f(\tau)}{\left\|\tilde{w}(z_{C_f}, z)\right\|_\tau + f(\tau)} \le \alpha_2 \left(1 + \frac{\beta}{f(0)}\right)$$

for $\forall t \ge 0$.

Therefore, from 1) and 2), the proof is completed.

### 2.7.2 Proof of Proposition 2

For any given $x_z \in \mathbb{Z}_P(d)$ and $x_{z_C} \in \mathbb{Z}_C$ where $\mathbb{Z}_C$ is the input-output description of $C$, the fictitious reference signal for $C$, $\tilde{w}(x_{z_C}, x_z)$, reproduces $x_{z_C}$ and $x_z$ in a fictitious closed-loop system in Figure 2.3. Suppose that $C$ is a stabilizing controller. Then, the fictitious closed-loop system is stable and, hence, there exist positive constants $\alpha_s, \beta_s \ge 0$ such that

$$\begin{aligned}\|x_z\|_t &\le \alpha_s \left(\|\tilde{w}(x_{z_C}, x_z)\|_t + \|d\|_t\right) + \beta_s \\ &\le \alpha_s \left(\|\tilde{w}(x_{z_C}, x_z)\|_t + \alpha_d f(t)\right) + \beta_s\end{aligned}$$

for $\forall t \geq 0$, from which, together with (2.6), it follows that

$$\begin{aligned} V(C, x_{z_C}, x_z, t) &\leq \max_{0 \leq \tau \leq t} \frac{\alpha_s \left( \|\tilde{w}(x_{z_C}, x_z)\|_\tau + \alpha_d f(\tau) \right) + \beta_s}{\|\tilde{w}(x_{z_C}, x_z)\|_\tau + f(\tau)} \\ &\leq \alpha_s \max\{1, \alpha_d\} + \frac{\beta_s}{f(0)} \end{aligned}$$

for $\forall t \geq 0$. Since the condition in Definition 3 is satisfied, $C$ is a feasible controller.

### 2.7.3 Proof of Proposition 3

From (2.7), it follows that

$$\begin{aligned} \|d\|_t &\leq \left( T \sum_{n=0}^{N-1} v[n]^T v[n] \right)^{1/2} \\ &\leq \sqrt{t+T} \left( \frac{1}{N} \sum_{n=0}^{N-1} v[n]^T v[n] \right)^{1/2} \\ &\leq \alpha_d \sqrt{t+T} \end{aligned}$$

where $N$ is a positive integer satisfying $(N-1)T \leq t < NT$ and

$$\alpha_d \triangleq \sup_{k \in \{1,2,\cdots\}} \left( \frac{1}{k} \sum_{n=0}^{k-1} v[n]^T v[n] \right)^{1/2}$$

and, hence, $\frac{\|d\|_t}{\sqrt{t+\rho_d}} \leq \frac{\alpha_d \sqrt{t+T}}{\sqrt{t+\rho_d}} \leq \alpha_d \max\left\{1, \sqrt{\frac{T}{\rho_d}}\right\}$ for $\forall t \geq 0$.

Since, by Theorem 2.3 in [15], $\frac{1}{k} \sum_{n=0}^{k-1} v[n]^2$ almost surely converges to a finite constant as $k \to \infty$, we have

$$\alpha_d < \infty \tag{2.12}$$

with probability 1.

Much of the material in Chapter 2 appears in S. Cheong, "Safe adaptive switching control with no SCLI assumption" as it appears in American Control Conference, 2010. The dissertation author was the primary author of this paper.

# 3 Instability Detection of ARMA Systems Based on AR System Identification

## 3.1 Introduction

The unfalsified adaptive control, exploited in the previous chapter, can find a controller with the best stabilizing ability among the candidate controllers while the stabilizing ability is measured by a cost function, which is a ratio of the truncated $\mathfrak{L}_2$-norm of the input-output signal of the plant to the truncated $\mathfrak{L}_2$-norm of the external reference signals. But the controller with the best stabilizing ability is not necessarily a stabilizing controller since the stability of the closed-loop system with the plant and the controller is only unfalsified. To see this clearly, let us consider the unfalsified adaptive control with only one candidate controller that actually is destabilizing. This controller is the best in the candidate controller set and no switching occurs. As time goes by, a ratio of the truncated $\mathfrak{L}_2$-norm of the input-output signal of the plant to the truncated $\mathfrak{L}_2$-norm of the external reference signals increases. In order to be able to show that the stability of the closed-loop system is falsified, we need to show that the ratio has no limit. Although the ratio increases with no limit, it is not clear if we can declare the falsification of the stability of the closed-loop system even with sufficiently large amount of collected data. However, when we have some information on the plant and the controller, we can falsify stability of the closed-loop system, which means that we can detect the instability of the system.

In this chapter, we consider the detection of instability in Autoregressive-Moving Average (ARMA) linear systems driven by noise. We develop an approach using techniques from System Identification and Time Series Analysis to determine asymptotically the stability of the system. The methodology uses parameter estimation with reduced-order Auto-Regressive(AR)-only models and relies on the consistent estimation of a subset of AR parameters in the unstable or *explosive* case to provide detection of the instability of the underlying ARMA system. For data from stable ARMA systems, the estimators asymptotically produce only stable AR estimates. There is no requirement to have the correctly characterized system type or order.

Time series parameter estimation in the unstable case has a long history ([16], [25], [1], [35], and [14]). However, its use in instability detection and with deliberately incorrect model type – AR instead of ARMA – and model orders below that of the original system has been studied only by Tiao and Tsay [35], and here only in the case where the unstable poles of the ARMA system lie on the unit circle and with the correct model order assumed for this marginally stable part in the AR model. They establish in-probability consistency of the associated Least Squares AR estimator applied to data from the ARMA system. The work of Lai and Wei [14] establishes almost sure consistency of the full-order Least Squares AR estimator when applied to data from a truly AR system, no matter where the poles of the system lie. Our objective is to merge and extend the results from Tiao and Tsay in the direction of (and using tools derived from) Lai and Wei, and to extend the approach to deliberate undermodeling. That is, we establish that Least Squares $n$th-order AR modeling using data from an unstable ARMA system will almost surely consistently estimate an $n$th-order unstable factor of the AR polynomial of the ARMA system, if that system has $n$ poles of magnitude greater than one and strictly greater than all the remaining system poles, stable or otherwise. Thus for example, for an ARMA system with an isolated maximal-magnitude unstable pole, an AR(1) estimator will consistently estimate that pole and hence determine the ARMA system instability, regardless of the presence of other stable, unstable or marginally stable poles.

We commence by considering the asymptotic behavior of AR parameter

estimators of various orders when applied to fixed stable and unstable ARMA linear systems. The techniques that we apply are largely based on the historical AR analysis, suitably extended to accommodate ARMA systems. The main result of this paper is to show that for an ARMA system with precisely $n$ poles lying outside of a circle of radius $\rho > 1$, an $n$th-order Least Squares AR estimator will almost surely yield consistent estimates of these poles. Accordingly, a collection of $n$ AR estimators of all orders up to $n$ will detect the instability in at least one of the estimators. Likewise, if the ARMA system is stable, then all the AR estimators will asymptotically almost surely return stable estimates. In this way, the AR estimator can be used to detect ARMA instability using only knowledge of an upper bound on the number of unstable roots having the same maximal modulus.

The novelty of this chapter lies in its recognition that the known AR consistency results of Lai and Wei [14] may be combined with their application in reduced order to ARMA systems. Consistently identifying subsets of the unstable AR part and of establishing almost sure consistency for AR modeling of ARMA systems is new, as is the development of a sequence of estimators to test for instability. A limitation of our approach is that it is inconclusive when the most unstable poles are on the unit circle, when we must appeal to Tiao and Tsay as providing the current best result of in-probability consistency provided the correct order is chosen for the unstable part, since all unstable poles share the same magnitude.

From the statistical literature, if the model structure coincides with that of the system, not only is the stability of the system clearly revealed but also the exact parameters of the system are asymptotically detected. The consistency of the least squares autoregressive estimator is proven under various assumptions. A brief summary of the consistency results is provided below with two newly-defined terms. An autoregressive moving average system is said to be *strictly stable* if its poles are strictly inside the unit circle and is said to be *strictly unstable* if at least one pole lies strictly outside the unit circle.

- H. B. Mann and A. Wald [16] showed that the least squares AR estimator converges in probability to the true parameters of a strictly stable AR system

when the AR model of the estimator has the same order as the system.

- Theorem III and Remarks on Theorem III in [25] showed that the least squares AR estimator converges in probability to the true parameters of a strictly unstable AR system when exactly one pole of the system is strictly unstable, the other poles are strictly stable and the model of the estimator has the same order as the system.

- J. Bellach [1] reports that T. J. Muench [20] proved that the least squares AR estimator converges in probability to the true parameters of an AR system when the system has no pole on the unit circle and the model of the estimator has the same order as the system.

- G. C. Tiao and R. S. Tsay [35] studied the case where AR modeling is applied to data from an ARMA system with $d$ poles on the unit circle and all other poles stable. They showed that the $d$th-order Least Squares AR estimator is consistent in probability for the coefficients of the polynomial comprised of the unit circle factors. They also show that higher-order AR estimators yield asymptotically biased estimates of the ARMA denominator polynomial if the ARMA system also has zeros and/or stable poles.

- When the model order is correct, T. L. Lai and C. Z. Wei [14] proved that the least squares AR estimator is almost surely consistent. This is the strongest available result; strongest in terms of mode of convergence and in terms of fewest restrictions on the stability of the true system. It is limited, however, to AR models of AR systems.

These results generally require knowledge of the order of the AR system or at least of its unstable part, with the least squares AR estimator having the same order. To our knowledge, M. M. Rao [25] and G. C. Tiao and R. S. Tsay [35] were the first to deal with AR modeling of less than full order being applied to unstable systems. These avenues are pursued further in this paper using the analytical techniques of [14] but with an emphasis on instability detection rather than on asymptotic consistency and augmentation to the AR modeling of ARMA data which, although technically straightforward, is an important and necessary extension.

The AR-modeling of an ARMA process normally leads to bias in the estimation of the denominator polynomial. A consistency property is established for certain low-order least squares AR estimators applied to a strictly unstable ARMA system, whereby the estimator is able to identify consistently a subset of the strictly unstable part of the system. Also, the least squares AR estimates of various orders indicate that the system is strictly stable when they fit to data from a strictly stable AR system. These two properties are combined to develop an instability detection method for an ARMA system. An advantage of the instability detection method is that the necessary a priori information is not an upper bound on the order of the system but an upper bound on the possible number of the most unstable poles of the system. Thus, this method can be applied to a system of the infinite order with finite number of unstable poles and an example is provided to show this.

This chapter is organized as follows. In Section 3.2, an ARMA system driven by a random process is described and, for the purpose of estimating the autoregressive part of the ARMA system, the least squares AR estimate is employed. In Section 3.3, the least squares AR estimator is proven to be able to detect the strict instability of a noisy ARMA system and this ability is illustrated in an example in Section 3.4. Conclusions follow in Section 3.5.

## 3.2 Problem formulation

Consider an ARMA linear system described by the linear difference equation

$$y_t = P(q)u_t \tag{3.1}$$

for $t = 0, 1, \cdots$ where $q$ is the forward shift operator and the transfer function of the ARMA system $P$ is described, in the $z$-transform, by

$$P(z) = \frac{\mathcal{B}(z)}{\mathcal{A}(z)} = \frac{b_0 + b_1 z^{-1} + \cdots + b_{n_b} z^{-n_b}}{1 + a_1 z^{-1} + \cdots + a_{n_a} z^{-n_a}}$$

with unknown initial conditions where $n_a$ and $n_b$ are the unknown orders of the denominator and the numerator of the ARMA system $P(z)$, respectively, and the

parameters $a = \begin{bmatrix} a_1 & \cdots & a_{n_a} \end{bmatrix}^T$ and $b = \begin{bmatrix} b_0 & \cdots & b_{n_b} \end{bmatrix}^T$ are also unknown but satisfy $a_{n_a} \neq 0$. The order of the ARMA system $P(z)$ is denoted by $n_P = \max\{n_a, n_b\}$. It is assumed that $\mathcal{A}(z)$ and $\mathcal{B}(z)$ have no common zeros. The driving noise $\{u_t, t = 0, 1, \cdots\}$ is an i.i.d. random process with zero mean, unknown variance $0 < \sigma_u^2 < \infty$, and finite fourth moment. The driving noise $\{u_t, t = 0, 1, \cdots\}$ and the initial condition of $P(z)$ are independent of each other.

Necessary notations are introduced in the following.

- deg : degree of a polynomial, e.g. $\deg \mathcal{A}(z) = n_a$.
- $n_Z$: the number of distinct zeros of $\mathcal{A}(z)$. Thus, $n_Z \leq n_a$.
- $z_i$ for $i = 1, \cdots, n_Z$ : distinct zeros of $\mathcal{A}(z)$.
- $m_i$ for $i = 1, \cdots, n_Z$ : multiplicity of $z_i$ in $\mathcal{A}(z)$ for $i = 1, \cdots, n_Z$, respectively.

For a vector $g \in \mathbb{R}^m$ and a square matrix $G \in \mathbb{R}^{m \times m}$, the norm of $g$, $\|g\|$, is the Euclidean norm and the norm of $G$, $\|G\|$, is the corresponding induced norm $\|G\| = \sup_{\|g\|=1} \|Gg\|$. Denote the $i \times i$ identity matrix by $I_i$. Also denote the $i \times j$ zero matrix by $\mathbf{0}_{i \times j}$. $E[\cdot]$ denotes expectation.

**Definition 5.** *An ARMA system is said to be strictly stable if all poles of the system have magnitudes less than* 1 *and is said to be strictly unstable if at least one pole of the system has magnitude greater than* 1.

Since we do not consider the case where the largest magnitude of poles of an ARMA system is 1, Definition 5 does not contain this case.

The stability of the ARMA system in (3.1) is investigated by fitting an AR model to the measured output signal $\{y_t, t = 0, 1, \cdots\}$ using the well-known least squares AR estimator. Suppose that $N$ output data $\{y_t, t = 0, \cdots, N-1\}$ are collected from the ARMA system in (3.1). Then, the least squares AR estimator of order $n \in \{1, 2, \cdots, N-1\}$ is defined by

$$\hat{a}(n, N) = -R(n, N)^{-1} r(n, N) \tag{3.2}$$

where

$$\begin{aligned} R(n,N) &= \sum_{t=n-1}^{N-2} \phi_y(n,t)\phi_y(n,t)^T \\ r(n,N) &= \sum_{t=n-1}^{N-2} \phi_y(n,t)y_{t+1} \end{aligned} \tag{3.3}$$

where $\phi_y(n,t) = \begin{bmatrix} y_t & y_{t-1} & \cdots & y_{t-n+1} \end{bmatrix}^T$ for $t = n-1, n, \cdots$. We note that if $\{u_t, t = 0, 1, \cdots\}$ has a continuous distribution, then $R(n,N)$ will be almost surely positive definite for $N \geq 2n$.

## 3.3 Instability detection

### 3.3.1 Pole detection of purely unstable ARMA systems

Consider the ARMA system $P(z)$ in (3.1). T. L. Lai and C. Z. Wei [14] prove that, when $P(z)$ is AR, the $n_a$-th order least squares AR estimate has strong consistency to the parameter $a$, regardless of pole location of $P(z)$. In this section, the proof in [14] is extended to show that when $P(z)$ is ARMA and the denominator polynomial of $P(z)$, $\mathcal{A}(z)$, has all zeros outside the unit circle, the strong consistency of the $n_a$-th order least squares AR estimate to the parameters of $\mathcal{A}(z)$, $a$, is preserved, i.e. the $n_a$-th order least squares AR estimate almost surely converges to the parameters of the autoregressive part of $P(z)$.

**Theorem 2.** *Suppose that all the zeros of the denominator polynomial $\mathcal{A}(z)$ of the ARMA system $P(z)$ in* (3.1) *have magnitudes greater than* 1. *Then, the $n_a$-th order least squares AR estimate almost surely converges to the parameters of the autoregressive part of $P(z)$, i.e.*

$$\lim_{N\to\infty} \hat{a}(n_a, N) = a \quad \text{a.s.}$$

### 3.3.2 Instability detection of strictly unstable ARMA systems

Suppose that the the ARMA system $P(z)$ in (3.1) is strictly unstable. Then, the denominator of $P(z)$, $\mathcal{A}(z)$, can be factored to

$$\mathcal{A}(z) = \mathcal{A}_E(z)\tilde{\mathcal{A}}_E(z)$$

where $\mathcal{A}_E(z)$ contains all poles of $P(z)$ outside the unit circle and $\tilde{\mathcal{A}}_E(z)$ contains all poles of $P(z)$ on or inside the unit circle. Necessary notations are introduced in the following.

- $n_\rho$: the number of distinct magnitudes of (strictly unstable) zeros of $\mathcal{A}_E(z)$.
- $\{\rho_i, i = 1, \cdots, n_\rho\}$ : a sequence of distinct magnitudes of zeros of $\mathcal{A}_E(z)$ in decreasing order, i.e. $\rho_1 > \cdots > \rho_{n_\rho} > 1$.

Since $P(z)$ has at least one pole outside the unit circle, it is clear that $n_\rho \geq 1$.

Further, a sequence of polynomials $\{\mathfrak{A}_i(z), i = 1, \cdots, n_\rho\}$ is defined by

$$\mathfrak{A}_i(z) = \prod_{\substack{j=1 \\ |z_j| \geq \rho_i}}^{n_Z} (z - z_j)^{m_j}, \tag{3.4}$$

which means that for any given $i \in \{1, \cdots, n_\rho\}$ the polynomial $\mathfrak{A}_i(z)$ consists of all the poles of $P(z)$ whose magnitudes are greater than $\rho_i$. Thus, for a given $i \in \{1, \cdots, n_\rho\}$, the $n_i$ zeros of $\mathfrak{A}_i(z)$ are the $n_i$ most unstable poles of $P(z)$. Note that $\mathfrak{A}_{n_\rho}(z) = \mathcal{A}_E(z)$.

In addition, degrees of $\mathfrak{A}_i(z)$ for $i = 1, \cdots, n_\rho$ are denoted by

$$n_i = \deg \mathfrak{A}_i(z) \tag{3.5}$$

for $i = 1, \cdots, n_\rho$. It is clear that $n_{i-1} \leq n_i$ for $i = 2, \cdots, n_\rho$ when $n_\rho \geq 2$.

The definition of $\{\mathfrak{A}_i(z), i = 1, \cdots, n_\rho\}$ may not be clear at a glance so a simple example is provided in the following. If $\mathcal{A}(z) = (z-6)^2(z+5)^2(z-3+j4)(z-3+j4)(z+2)^3(z-1)^3(z-0.5)^3$, we have $\mathcal{A}_E(z) = (z-6)^2(z+5)^2(z-3+j4)(z-3+j4)(z+2)^3$, $\deg \mathfrak{A}_E(z) = 9$, $n_\rho = 3$, and $\rho_1 = 6 > \rho_2 = 5 > \rho_3 = 2$.

The algorithm produces

$$\mathfrak{A}_1(z) = (z-6)^2$$
$$\mathfrak{A}_2(z) = (z-6)^2(z+5)^2(z-3+j4)(z-3+j4)$$
$$\mathfrak{A}_3(z) = (z-6)^2(z+5)^2(z-3+j4)(z-3+j4)(z+2)^3 = \mathcal{A}_E(z)$$

with $n_1 = 2 < n_2 = 6 < n_3 = 9$.

The following theorem shows that the poles of $P(z)$ outside the unit circle can be consistently estimated with probability 1.

**Theorem 3.** *Suppose that the ARMA system $P(z)$ in* (3.1) *is strictly unstable, i.e. one of the poles of $P(z)$ is outside the unit circle. Then, for any given $i \in \{1, \cdots, n_\rho\}$, the $n_i$-th order least squares AR estimate in* (3.2) *almost surely converges to parameters of $\mathfrak{A}_i(z)$ in* (3.4)*. That is, the most unstable $n_i$ poles are consistently estimated with probability* 1*.*

Note that this theorem ensures that only strictly unstable poles in the system (3.1) are detected.

The proof of Theorem 3 provides a notion that as the most unstable pole becomes dominant in the ARMA system output, it emerges in the corresponding low-order least squares AR estimate. If the system transfer function is written as a partial fraction, the signal that is produced by the subsystem which has the most unstable poles, dominates signals from the other subsystems. Our thesis is that the appropriate order AR estimator will detect the system instability through its coefficients well before the locations of the individual poles can be resolved.

### 3.3.3 Stability detection of strictly stable ARMA systems

Suppose that the ARMA system $P(z)$ in (3.1) is strictly stable, i.e. $P(z)$ has all its poles inside the unit circle. Then, regardless of the order of $P(z)$, the least squares AR estimate of any order is proven in the following theorem to converge to a limit that represents a stable system. The theorem is based on the well-known fact that for a stationary process the least squares estimate is asymptotically equivalent to the autocorrelation method of the same order (e.g. [26]) and extends it to a quasi-stationary process. We omit the proof since it is

straightforward.

**Theorem 4.** *Suppose that the ARMA system $P(z)$ in* (3.1) *is strictly stable, i.e. $P(z)$ has all its poles inside the unit circle. Then with probability one, for any given positive integer $n$, the $n$-th order least squares AR estimate in* (3.2) *asymptotically converges to a limit that delivers only stable poles.*

Note that the limit estimate in Theorem 4 is usually different from the parameters of the denominator of $P(z)$ in (3.1). That is, the least squares AR estimator of any order for measured data from the ARMA system in (3.1) is not consistent with the parameters of the denominator of $P(z)$.

### 3.3.4 Instability detection method

In this and the final section, combining the results in Section 3.3, an instability detection method for the ARMA system $P(z)$ in (3.1) is introduced. Again, the order of $P(z)$ is unknown and the measured output signal $\{y_t, t = 0, 1, \cdots\}$ is available from which stability of $P(z)$ is investigated using a collection of least squares AR estimators.

Suppose that a positive integer $n_{\max}$ is known to satisfy

$$n_1 \leq n_{max} \tag{3.6}$$

where $n_1$ is the number of maximal-magnitude unstable poles of $P(z)$, which is given in (3.5) in Section 3.3.2, when $P(z)$ is strictly unstable and is set to 0 when $P(z)$ is strictly stable. Note that $n_1$ is less than or equal to the number of the poles of $P(z)$ outside the unit circle which is less than or equal to $n_a$. Then, the following statement is asserted by Theorem 3 and Theorem 4.

**Theorem 5.** *Suppose we have an upper bound $n_{max}$ satisfying* (3.6) *and consider a sequence of least squares AR estimators of orders from 1 to $n_{max}$ in* (3.2) *for the output signal $\{y_t, t = 0, 1, \cdots\}$ collected from the ARMA system in* (3.1).

1. *If asymptotically the set of all least squares AR estimators delivers only stable polynomial estimates, then the ARMA system $P(z)$ in* (3.1) *is strictly stable or marginally stable.*

2. *If asymptotically any member of set of all least squares AR estimators contains a strictly unstable polynomial estimate, then $P(z)$ is strictly unstable.*

**Remark 1.** *If there is no possibility that the most unstable pole of the ARMA system $P(z)$ in* (3.1) *is on the unit circle, then the instability detection method reduces to the following statement.*

*The ARMA system $P(z)$ in* (3.1) *is strictly stable if, and only if, for every $n \in \{1, \cdots, n_{\max}\}$ the $n$-th order least squares AR estimate asymptotically delivers only strictly stable poles.*

In practice, the instability detection method relies on asymptotic properties, which is a significant weakness. For finite number $N$ of data, in principle one would like to resort to hypothesis testing for the stability of the underlying system. However, there are two impediments here. For strictly stable systems, one might appeal to asymptotic normality results as described in, say, Theorem 9.1 of [15]. These state that, for sufficiently large $N$, the distribution of the least squares parameter estimate, $\hat{a}(n, N)$, is asymptotically normally distributed about its limiting value, which exhibits the instability detection property, with a certain covariance. This result relies on the parameter estimate arriving into the neighborhood of its limit and on being able to characterize the covariance of the error between the best AR prediction and the ARMA system. Both of these issues are difficult and, in the end, would yield a guarantee against strict instability only. For the case of a strictly unstable system, appeal to the usual asymptotic normality results is not valid, since the system is non-stationary. The only available result, to our knowledge, is [39] where the limiting distribution of the first-order least squares AR estimate is the Cauchy distribution assuming that the underlying system is a first-order AR system. Further, while the appropriately scaled systems used in the proofs of the theorems are asymptotically stationary, the distribution of the estimated parameter is dependent entirely on a few initial signal values, which is the basis for the proofs of convergence. Once again, it is not apparent how this might be transcribed into an hypothesis test for quantifying the probability of detection of instability using finite data. The asymptotic detection of instability is, after all, a relatively simple matter of considering signal norms. The point of the results in this paper is that we have established the guarantee of instability detection even

with model structure mismatch using a new algorithm involving multiple parallel AR estimators.

## 3.4 Example

Consider the uncertain continuous-time plant $P$ in (2.8) in Section 2.5

$$\dot{x}_p(t) = -x_p(t - 0.5) + u(t)$$

whose output signal is $x_p(t)$. This plant is an LTI system with time delay in the state, called internal time delay, and can be described by a transfer function

$$P(s) = \frac{1}{s + e^{-0.5s}}.$$

The dynamics of this plant $P$ as well as the initial condition $x_p(\tau)$ for $\tau \in [-0.5, 0]$ are unknown. However, we know that the plant is LTI.

We measure the plant-output signal with a sampling period $T$ and this measurement is corrupted by a noise signal $d$, i.e.

$$y[n] = x_p(nT) + d[n]$$

for $n = 0, 1, \ldots$. The plant-input signal $u$ is given by a zero-order hold method

$$u(t) = u[n] \quad \text{for} \quad nT \leq t < (n + 1)T$$

with the discrete-time signal $u[n]$ produced as an outcome of switching of discrete-time controllers combined with the discrete-time reference signals $r[n]$ and $s[n]$ as well as the measured noisy plant-output signal $y[n]$.

The zero-order hold, the continuous-time plant $P(s)$, and the measurement block in Figure 3.1 can be considered an equivalent discrete-time system denoted by $P(z)$. However, the order of this discrete-time system is infinite since the continuous-time plant $P(s)$ has internal time delay. To show this, let us con-

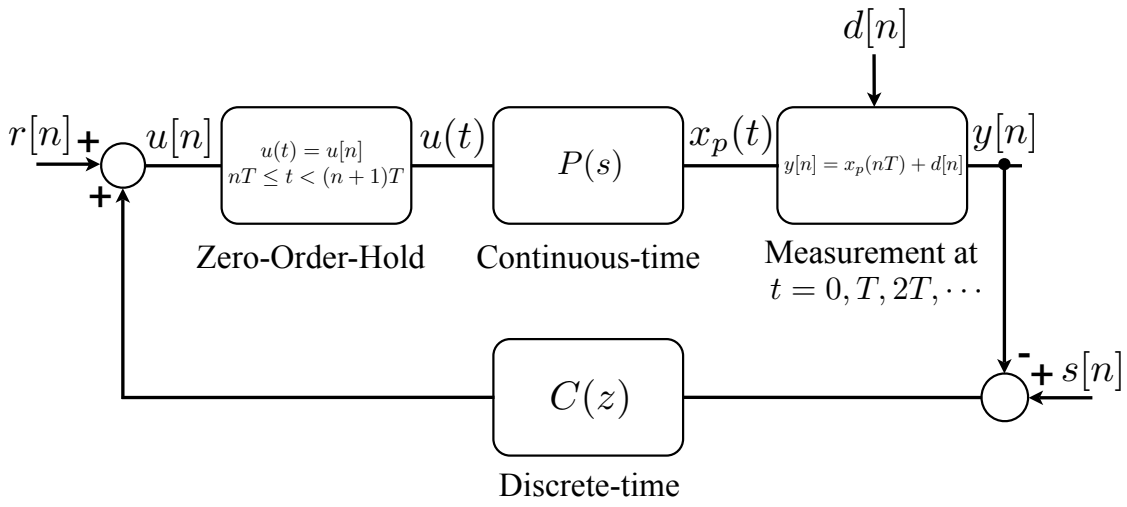


Figure 3.1: A system with a continuous-time plant $P(s)$ and a discrete-time controller $C(z)$

sider the state $x_p(nT)$ of the continuous-time plant $P(s)$. From (2.8), we have

$$\begin{aligned} x_p(nT) &= x_p((n-1)T) + \int_{(n-1)T}^{nT} -x_p(\tau - 0.5)\ d\tau + \int_{(n-1)T}^{nT} u(\tau)\ d\tau \\ &= x_p((n-1)T) + \int_{(n-1)T+0.5}^{nT} -x_p(\tau - 0.5)\ d\tau + u((n-1)T)T \\ &\quad + \int_{(n-1)T}^{(n-1)T+0.5} -x_p(\tau - 0.5)\ d\tau \end{aligned}$$

for any integer $n$ and the fourth term in the right-hand side indicates that, in order to determine $x_p(nT)$, we need to know $x_p(\tau)$ for $\tau \in [(n-1)T - 0.5, (n-1)T]$ in addition to $x_p((n-1)T)$ and $u((n-1)T)$. Similarly, it can be shown that, in order to determine $x_p(\tau)$ for $\tau \in [(n-1)T - 0.5, (n-1)T]$, we need to know $x_p((n-2)T)$, $u((n-2)T)$, and $x_p(\tau)$ for $\tau \in [(n-2)T - 0.5, (n-2)T]$. Then inductively, we can show that $x_p(nT)$ cannot be determined in terms of a finite number of past states, $x((n-1)T)$, $x((n-2)T)$, ..., and past input sequences, $u((n-1)T)$, $u((n-2)T)$, ..., which means that the order of the equivalent discrete-time system $P(z)$ is infinite.

Since the order of $P(z)$ is infinite, it has infinite number of poles and, thus, the number of poles of the closed-loop system $(P, C)$ is also infinite. However, the number of unstable poles is finite and our instability detection methods can

determine the stability of $(P, C)$.

In the example in Section 2.5, the stabilizing property of the controller $C_1$ is unfalsified but we cannot make any statement about the stabilizing or destabilizing property of $C_2$. On the other hand, we investigate this property of $C_2$ in this section by putting it in the closed-loop system in Figure 3.1 with zero reference signals.

If $C_2$ is destabilizing, the measured plant-output signal $y$ will grow unbounded while we collect data for the instability detection method in Section 3.3.4. To prevent this from happening, we employ a simple switching scheme. If the absolute value of $y$ is greater than some pre-decided value, we stop collecting data for the instability detection method and switch $C_1$ into the closed-loop system. This is called the first data segment. If the absolute value of $y$ becomes lower than some pre-decided value with $C_1$ in the loop and stays below that value for pre-determined number of consecutive samples, then we switch $C_2$ back into the loop and start collecting data again. This is the second data segment. We continue collecting the data segments and apply the instability detection method for each data segment. This switching scheme is solely based on our unproved stabilizing property of $C_1$. If $C_1$ turns out to be destabilizing and the signal $y$ does not become lower than the chosen value, then we only use the data segments collected up to that point.

### 3.4.1 MATLAB simulation

In the MATLAB simulation, the sampling period is set to $T = 1sec$ and the reference signals are set to $r[n] = s[n] = 0$ for $n = 0, 1, \ldots$. The noise signal $d[n]$ is generated as a realization of an iid random process with a normal distribution. The initial condition is set to $x_p(\tau) = 0$ for $\tau \in [-0.5, 0]$.

If the absolute value of $y$ becomes greater than 100, we stop collecting data and switch $C_1$ into the closed-loop system. If the absolute value of $y$ becomes lower than 1 with $C_1$ in the loop and stays below 1 for 5 consecutive samples, then we switch $C_2$ back into the loop and start collecting data again. With this switching scheme, we collect seven data segments in this MATLAB simulation.

The seventh data segment of $y$ is shown in the upper part of Figure 3.2.

In this data segment, as we collect data, we accumulate those data and use them

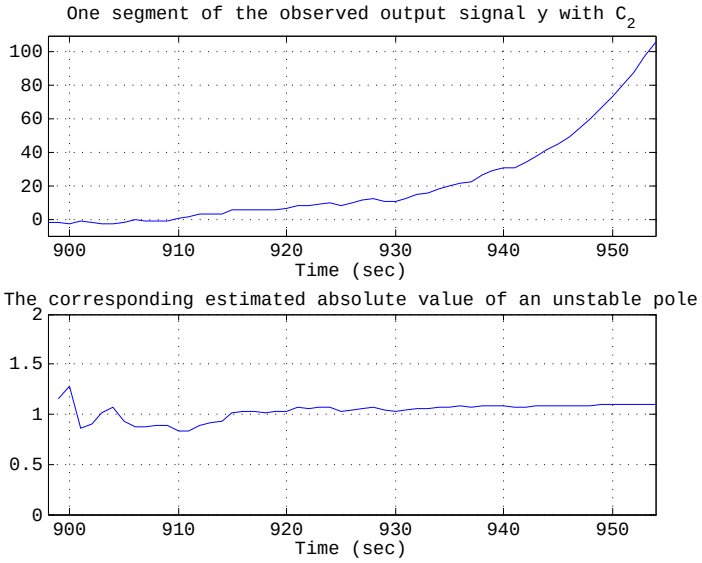


Figure 3.2: The seventh data segment of $y$ and the corresponding sequence of the first order AR least-squares estimates.

to compute the first order AR least-squares estimate. For example, we compute the first order AR least-squares estimate at $940sec$ using the data of $y$ collected from $898sec$ to $940sec$. Similarly, we compute the estimate at each sampling time point. The sequence of the estimates is shown in the lower part of Figure 3.2. The last value of the first order AR least-squares estimate corresponding to each data segment is shown in Figure 3.3. For example, the circle at the seventh segment in Figure 3.3 comes from the estimated value computed at time $954sec$, which is the last estimated value in the seventh data segment.

As the measured signal $y$ gets larger in the upper part of Figure 3.2, we get more confident that $C_2$ is destabilizing. However, the first order AR least-squares estimates in the lower part of Figure 3.2 makes us suspect this instability even at around $25sec$, which means 25 measured samples in this example, before the signal $y$ gets very large. In Figure 3.3, the sequence of the last values of the estimates for the seven data segments indicates that the closed-loop system $(P, C_2)$ has a pole slightly outside the unit circle.

Later in Section 4.9, it is confirmed that $C_2$ destabilizes $P$ and the closed-loop system $(P, C_2)$ has a single unstable pole. This shows that the instability

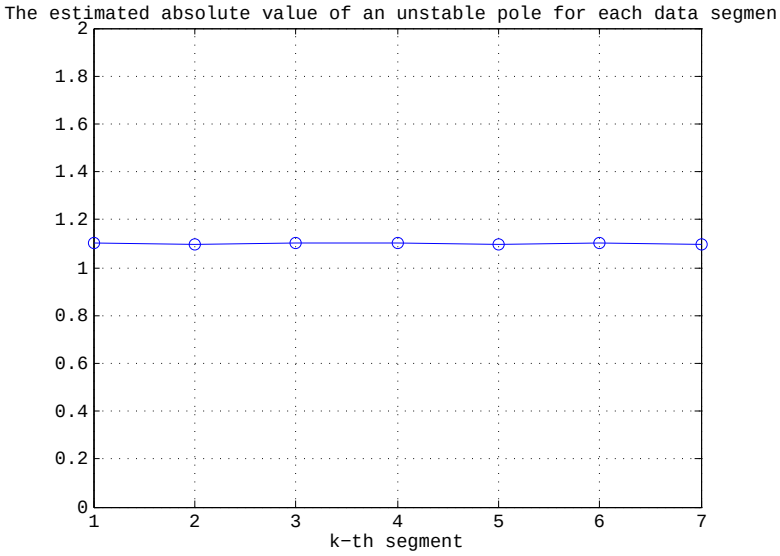


Figure 3.3: The last value of the estimates from the each data segment.

detection method in Section 3.3.4 performs correctly for $(P, C_2)$ with the first order AR least-squares estimate.

## 3.5 Conclusion

We investigated the performance of the least squares AR estimators in identifying the strictly unstable parts of ARMA systems as well as indicating stability of strictly stable ARMA systems. We also provide the development of a new approach to the successive determination of instability using a suite of the least squares AR estimators. Our motivating problem is the detection of instability from operating data, for which we have broached some early questions focused on asymptotic consistency. It remains to use these ideas in the development and quantification of statistical methods for the detection of instability with finite data sets.

## 3.6 Appendices

### 3.6.1 Proof of Theorem 2

The proof of Theorem 2 follows, in principle, [14] and makes use of auxiliary lemmas stated in 3.6.3.

The ARMA system $P(z)$ in (3.1) can be rewritten as

$$y_t = -\phi_y(n_a, t-1)^T a + b^T \phi_u(n_b, t) \tag{3.7}$$

for $t = n_P, n_P+1, \cdots$ where $\phi_u(n,t) = \begin{bmatrix} u_t & u_{t-1} & \cdots & u_{t-n} \end{bmatrix}^T$ for $n = 1, 2, \cdots$, $t = n, n+1, \cdots$, from which, together with (3.3), it follows that

$$\begin{aligned}
r(n_a, N) &= \sum_{t=n_a-1}^{n_P-2} \phi_y(n_a,t) y_{t+1} + \sum_{t=n_P-1}^{N-2} \phi_y(n_a,t) y_{t+1} \\
&= \sum_{t=n_a-1}^{n_P-2} \phi_y(n_a,t) y_{t+1} - \sum_{t=n_P-1}^{N-2} \phi_y(n_a,t)\phi_y(n_a,t)^T a + \sum_{t=n_P-1}^{N-2} \phi_y(n_a,t) b^T \phi_u(n_b, t+1) \\
&= -R(n_a,N)a + \sum_{t=n_a-1}^{n_P-2} \phi_y(n_a,t) \left( y_{t+1} + \phi_y(n_a,t)^T a \right) + \sum_{t=n_P-1}^{N-2} \phi_y(n_a,t) b^T \phi_u(n_b, t+1).
\end{aligned}$$

Thus, it follows, using (3.2), that

$$\begin{aligned}
\hat{a}(n_a,N) - a = -R(n_a,N)^{-1} &\left( \sum_{t=n_a-1}^{n_P-2} \phi_y(n_a,t) \left( y_{t+1} + \phi_y(n_a,t)^T a \right) \right. \\
&\left. + \sum_{t=n_P-1}^{N-2} \phi_y(n_a,t) b^T \phi_u(n_b, t+1) \right) \\
= -N^{\frac{1}{2}} \left(A^{-N}\right)^T &\left\{ A^{-N} R(n_a,N) \left(A^{-N}\right)^T \right\}^{-1} \\
&\left( N^{-\frac{1}{2}} A^{-N} \sum_{t=n_a-1}^{n_P-2} \phi_y(n_a,t) \left( y_{t+1} + \phi_y(n_a,t)^T a \right) \right. \\
&\left. + N^{-\frac{1}{2}} A^{-N} \sum_{t=n_P-1}^{N-2} \phi_y(n_a,t) b^T \phi_u(n_b, t+1) \right)
\end{aligned}$$

where

$$A = \begin{bmatrix} -a_1 & \cdots & -a_{n_a-1} & -a_{n_a} \\ & I_{n_a-1} & & \mathbf{0}_{(n_a-1)\times 1} \end{bmatrix}. \tag{3.8}$$

Clearly, eigenvalues of $A$ are zeros, $z_i$, of $\mathcal{A}(z)$ in (3.1) and, hence, have magnitudes greater than 1. Choose any constant $\zeta_1$ satisfying $|z_i|^{-1} < \zeta_1 < 1$ for $\forall i \in \{1, \cdots, n_Z\}$. Then, Theorem 2.9 in [33] shows that there exists a finite constant $c_1 > 0$ such that

$$\left\|A^{-t}\right\| \leq c_1 \zeta_1^{-t} \tag{3.9}$$

for $t = 0, 1, \cdots$.

From (3.9), it follows that $\lim_{N\to\infty} \left\| N^{\frac{1}{2}} \left(A^{-N}\right)^T \right\| \leq \lim_{N\to\infty} c_1 N^{\frac{1}{2}} \zeta_1^{-N} = 0$ which implies that

$$\lim_{N\to\infty} N^{\frac{1}{2}} \left(A^{-N}\right)^T = \mathbf{0}_{n_a \times n_a}. \tag{3.10}$$

Lemmas 3 and 4 in 3.6.3 show that the matrix

$$\lim_{N\to\infty} A^{-N} R(n_a, N) \left(A^{-N}\right)^T \tag{3.11}$$

is positive definite with probability 1 and, therefore, has almost surely finite inverse.

Lemma 5 shows that

$$\lim_{N\to\infty} N^{-\frac{1}{2}} A^{-N} \sum_{t=n_P-1}^{N-2} \phi_y(n_a, t) b^T \phi_u(n_b, t+1) = \mathbf{0}_{n_a \times 1} \quad \text{a.s.} \tag{3.12}$$

Since it is clear, from (3.9), that

$$\lim_{N\to\infty} N^{-\frac{1}{2}} A^{-N} \sum_{t=n_a-1}^{n_P-2} \phi_y(n_a, t) \left(y_{t+1} + \phi_y(n_a, t)^T a\right) = \mathbf{0}_{n_a \times 1} \quad \text{a.s.},$$

it follows from (3.10), (3.11), and (3.12), that $\lim_{N\to\infty} \hat{a}(n_a, N) - a = \mathbf{0}_{n_a \times 1}$ a.s.

### 3.6.2 Proof of Theorem 3

Since the plant $P(z)$ has at least one pole outside the unit circle, it follows that $n_\rho \geq 1$ and $\rho_1 > \cdots > \rho_{n_\rho} > 1$.

Choose any constant $i \in \{1, \cdots, n_\rho\}$. The denominator of $P(z)$, $\mathcal{A}(z)$,

can be factored to $\mathcal{A}(z) = \mathfrak{A}_i(z)\tilde{\mathfrak{A}}_i(z)$ where $\tilde{\mathfrak{A}}_i(z)$ is comprised of all the poles of $P(z)$ whose magnitudes are less than $\rho_i$. By the partial fraction description, the output signal of the ARMA system in (3.1) can be described by

$$y_t = s_t + \tilde{s}_t, \tag{3.13}$$

for $t = 0, 1, \cdots$ where

$$\begin{aligned} s_t &= \frac{\mathfrak{B}_i(q)}{\mathfrak{A}_i(q)} u_t \\ \tilde{s}_t &= \frac{\tilde{\mathfrak{B}}_i(q)}{\tilde{\mathfrak{A}}_i(q)} u_t \end{aligned} \tag{3.14}$$

for $t = 0, 1, \cdots$ with appropriate $\mathfrak{B}_i(z)$, $\tilde{\mathfrak{B}}_i(z)$, and initial conditions.

Since $\frac{\tilde{s}_t}{\rho_i^t} \xrightarrow[t\to\infty]{\text{a.s.}} 0$ by Lemma 6 in 3.6.4, it follows from (3.13) that

$$\frac{y_t}{\rho_i^t} - \frac{s_t}{\rho_i^t} \xrightarrow[t\to\infty]{\text{a.s.}} 0.$$

and, hence,

$$\frac{1}{\rho_i^{2N}} \sum_{t=n_i-1}^{N-2} y_t^2 - \frac{1}{\rho_i^{2N}} \sum_{t=n_i-1}^{N-2} s_t^2 = \sum_{t=n_i-1}^{N-2} \frac{1}{\rho_i^{2(N-t)}} \left(\frac{y_t}{\rho_i^t}\right)^2 - \sum_{t=n_i-1}^{N-2} \frac{1}{\rho_i^{2(N-t)}} \left(\frac{s_t}{\rho_i^t}\right)^2 \xrightarrow[N\to\infty]{\text{a.s.}} 0.$$

Similarly, it can be shown that all elements of a matrix $\frac{1}{\rho_i^{2N}} R_y(n_i, N) - \frac{1}{\rho_i^{2N}} R_s(n_i, N)$ and a vector $\frac{1}{\rho_i^{2N}} r_y(n_i, N) - \frac{1}{\rho_i^{2N}} r_s(n_i, N)$ almost surely converge to zero, where $R_y(n_i, N)$ and $r_y(n_i, N)$ are defined in (3.3) and

$$\begin{aligned} R_s(n_i, N) &= \sum_{t=n_i-1}^{N-2} \phi_s(n_i, t)\phi_s(n_i, t)^T \\ r_s(n_i, N) &= \sum_{t=n_i-1}^{N-2} \phi_s(n_i, t) s_{t+1} \end{aligned}$$

where $\phi_s(n_i, t) = \begin{bmatrix} s_t & s_{t-1} & \cdots & s_{t-n_i+1} \end{bmatrix}^T$ for $t = n_i - 1, n_i, \cdots$. Therefore, con-

vergence of the $n_i$-th order least squares AR estimate is obtained as

$$\hat{a}(n_i, N) + R_s(n_i, N)^{-1} r_s(n_i, N) = -R_y(n_i, N)^{-1} r_y(n_i, N) + R_s(n_i, N)^{-1} r_s(n_i, N)$$
$$\underset{N \longrightarrow \infty}{\longrightarrow} 0 \quad \text{a.s.}$$

Finally, from (3.14), Theorem 2 guarantees that the $n_i$-th order least squares AR estimate for $\{s_t, t = 0, 1, \cdots\}$, $\hat{a}_s(n_i, N) \triangleq -R_s(n_i, N)^{-1} r_s(n_i, N)$, converges to the parameters of $\mathfrak{A}_i(z)$ with probability 1.

### 3.6.3 Auxiliary lemmas for Theorem 2

The lemmas that are needed to prove Theorem 2, are stated and proved in this section.

From (3.7) and (3.8), it is clear that

$$\phi_y(n_a, t) = A\phi_y(n_a, t-1) + b^T \phi_u(n_b, t) e_1$$

for $t = n_P, n_P + 1, \cdots$ where $n_P = \max\{n_a, n_b\}$ and $e_1 = \begin{bmatrix} 1 & 0 & \cdots & 0 \end{bmatrix}^T \in \mathbb{R}^{n_a}$, from which it follows that

$$\phi_y(n_a, t) = A^{t-n_P+1} \phi_y(n_a, n_P - 1) + \sum_{i=n_P}^{t} A^{t-i} b^T \phi_u(n_b, i) e_1$$

for $t = n_P, n_P + 1, \cdots$.

Define $\xi_{n_P-1} \triangleq A^{-(n_P-1)} \phi_y(n_a, n_P - 1)$ and

$$\begin{aligned} \xi_t &\triangleq A^{-t} \phi_y(n_a, t) \\ &= \xi_{n_P-1} + \sum_{i=n_P}^{t} A^{-i} b^T \phi_u(n_b, i) e_1 \end{aligned} \tag{3.15}$$

for $t = n_P, n_P + 1, \cdots$.

**Lemma 2.** *The sequence of random vectors $\{\xi_t, t = n_P - 1, n_P, \cdots\}$ defined in (3.15) almost surely converges to a random vector denoted by $\bar{\xi}$. Moreover, for any $f \in \mathbb{R}^{n_a} \setminus \{\mathbf{0}_{n_a \times 1}\}$, $f^T \bar{\xi}$ has a continuous distribution.*

**Proof.** From (3.15), it is clear that

$$\xi_t = \xi_{n_P-1} + \sum_{j=0}^{n_b} b_j \sum_{i=n_P}^{t} u_{i-j} A^{-i} e_1$$

for $t = n_P, n_P+1, \cdots$. By (3.9) and Kolmogorov's convergence theorem [27], it can be shown that for any given $j \in \{0, \cdots, n_b\}$ there exists a random vector $\eta_j$ such that $\sum_{i=n_P}^{t} u_{i-j} A^{-i} e_1 \xrightarrow{\text{a.s.}} \eta_j$ and it follows that

$$\xi_t \xrightarrow[t\longrightarrow\infty]{\text{a.s}} \xi_{n_P-1} + \sum_{j=0}^{n_b} b_j \eta_j \triangleq \bar{\xi}. \tag{3.16}$$

For any given $f \in \mathbb{R}^{n_a} \setminus \{\mathbf{0}_{n_a \times 1}\}$ it can be shown using (3.9) that

$$\sum_{i=n_P}^{\infty} \left(f^T A^{-i} e_1\right)^2 < \infty. \tag{3.17}$$

The matrix $\begin{bmatrix} e_1 & Ae_1 & \cdots & A^{n_a-1}e_1 \end{bmatrix}$ is upper triangular with diagonal elements all equal to 1 and is, thus, nonsingular. Since $A$ is nonsingular, it follows that for every $i = 0, 1, \cdots$, the vectors $A^{-i}e_1$, $A^{-i}Ae_1$, $\cdots$, $A^{-i}A^{n_a-1}e_1$ are linearly independent. Hence, there exists $k \in \{0, \cdots, n_a - 1\}$ such that $f^T A^{-i} A^k e_1 \neq 0$ for every $i = 0, 1, \cdots$ and it follows that

$$f^T A^{-i} e_1 \neq 0 \quad \text{for infinitely many } i \tag{3.18}$$

The fact that $\{u_t, t = 0, 1, \cdots\}$ is an iid random process with zero mean, unknown variance $0 < \sigma_u^2 < \infty$, and finite fourth moment, together with (3.17) and (3.18), satisfies the assumptions in Lemma 1 in [14], which leads us to conclude that $f^T\eta_j$ has a continuous distribution for $\forall j \in \{0, \cdots, n_b\}$. It follows that $f^T\bar{\xi} = f^T\xi_{n_P-1} + \sum_{j=0}^{n_b} b_j f^T \eta_j$ has a continuous distribution. □

**Lemma 3.** *The sequence of random matrices*

$$\left\{ \sum_{t=n_a-1}^{N-2} A^{-N} \phi_y(n_a, t) \phi_y(n_a, t)^T \left(A^{-N}\right)^T, N = n_a + 1, n_a + 2, \cdots \right\}$$

*which appears in* (3.11)*, almost surely converges to a random matrix*

$$F \triangleq \sum_{t=2}^{\infty} A^{-t}\bar{\xi}\bar{\xi}^T \left(A^{-t}\right)^T$$

*where the random vector* $\bar{\xi}$ *is obtained in Lemma 2.*

**Proof.** From (3.15), we have

$$\begin{aligned}
&\sum_{t=n_a-1}^{N-2} A^{-N}\phi_y(n_a,t)\phi_y(n_a,t)^T \left(A^{-N}\right)^T \\
&= \sum_{t=n_a-1}^{n_P-2} A^{-N}\phi_y(n_a,t)\phi_y(n_a,t)^T \left(A^{-N}\right)^T + \sum_{t=n_P-1}^{N-2} A^{-(N-t)}\xi_t\xi_t^T \left(A^{-(N-t)}\right)^T .
\end{aligned} \tag{3.19}$$

It follows from (3.9) and (3.19) that

$$\left\| \sum_{t=n_a-1}^{n_P-2} A^{-N}\phi_y(n_a,t)\phi_y(n_a,t)^T \left(A^{-N}\right)^T \right\| \xrightarrow[N\longrightarrow\infty]{\text{a.s}} 0$$

and

$$\begin{aligned}
&\left\| \sum_{t=n_P-1}^{N-2} A^{-(N-t)}\xi_t\xi_t^T \left(A^{-(N-t)}\right)^T - F \right\| = \left\| \sum_{t=2}^{N-n_P+1} A^{-t}\xi_{N-t}\xi_{N-t}^T \left(A^{-t}\right)^T - F \right\| \\
&\leq c_1^2 \sum_{t=2}^{N-n_P+1} \zeta_1^{-2t} \left\|\xi_{N-t}\xi_{N-t}^T - \bar{\xi}\bar{\xi}^T\right\| + c_1^2\zeta_1^{-2N} \left\|\bar{\xi}\bar{\xi}^T\right\| \sum_{t=-n_P+2}^{\infty} \zeta_1^{-2t} \\
&\xrightarrow[N\longrightarrow\infty]{\text{a.s}} 0.
\end{aligned}$$

□

**Lemma 4.** *The random matrix* $F = \sum_{t=2}^{\infty} A^{-t}\bar{\xi}\bar{\xi}^T \left(A^{-t}\right)^T$ *in Lemma 3, where the random vector* $\bar{\xi}$ *is obtained in Lemma 2, is positive definite with probability* 1*.*

**Proof.** $F$ satisfies the following discrete Lyapunov equation

$$F - A^{-1}F\left(A^{-1}\right)^T = \left\{Z^T\left(A^{-1}\right)^T\right\}^T \left\{Z^T\left(A^{-1}\right)^T\right\}.$$

Since all eigenvalues of $\left(A^{-1}\right)^T$ have magnitudes less than 1, if $\left(\left(A^{-1}\right)^T, \bar{\xi}^T\left(A^{-1}\right)^T\right)$ is observable, i.e. $\left(A^{-1}, A^{-1}\bar{\xi}\right)$ is controllable, then the Lyapunov equation has a

unique, symmetric, and positive definite solution by Theorem 5.D5 in [4]. Further, Theorem 6.1 in [4] shows that $\left(A^{-1}, A^{-1}\bar{\xi}\right)$ is controllable if, and only if, $n_a \times (n_a+1)$ matrix $\left[A^{-1} - \lambda I_{n_a} \quad A^{-1}\bar{\xi}\right]$ has full row rank $n_a$ for every eigenvalue, $\lambda$, of $A^{-1}$, i.e. there exists no nonzero vector $f$ satisfying $f^T \left[A^{-1} - \lambda I_{n_a} \quad A^{-1}\bar{\xi}\right] = \mathbf{0}_{1\times(n_a+1)}$.

For any given nonzero vector $f$ such that $f^T\left(A^{-1} - \lambda I_{n_a}\right) = \mathbf{0}_{1\times n_a}$, we have $P\left[f^T A^{-1}\bar{\xi} = 0\right] = 0$ by Lemma 2. Hence, $\left(A^{-1}, A^{-1}\bar{\xi}\right)$ is controllable with probability 1. Therefore, $F$ is almost surely positive definite. □

**Lemma 5.** *The sequence of random vectors*

$$\left\{ N^{-\frac{1}{2}} A^{-N} \sum_{t=n_P-1}^{N-2} \phi_y(n_a, t) b^T \phi_u(n_b, t+1), N = n_P + 1, \cdots \right\}$$

*which appears in* (3.12) *almost surely converges to a zero vector.*

**Proof.** From (3.9) and (3.15), we have

$$\begin{aligned} \sum_{t=n_P-1}^{N-2} \left\| A^{-N} \phi_y(n_a, t) \right\| &= \sum_{t=n_P-1}^{N-2} \left\| A^{-(N-t)} \xi_t \right\| \leq \sum_{t=n_P-1}^{N-2} \left\| A^{-(N-t)} \right\| \|\xi_t\| \\ &\leq c_1 \sum_{t=n_P-1}^{N-2} \zeta_1^{-(N-t)} \|\xi_t\| \end{aligned}$$

and, hence, it can be obtained, using Lemma 2, that

$$\lim_{N\to\infty} \sum_{t=n_P-1}^{N-2} \left\| A^{-N} \phi_y(n_a, t) \right\| < \infty \quad \text{a.s.} \tag{3.20}$$

Since $\{u_t, t = 0, 1, \cdots\}$ has a finite variance, it is clear that

$$\lim_{N\to\infty} N^{-\frac{1}{2}} \left| b^T \phi_u(n_b, t+1) \right| = 0 \quad \text{a.s.} \tag{3.21}$$

for any $t \in \{n_b - 1, n_b, \cdots\}$.

Therefore, from (3.20) and (3.21), it follows that

$$\begin{aligned}
&\left\| N^{-\frac{1}{2}} A^{-N} \sum_{t=n_P-1}^{N-2} \phi_y(n_a,t) b^T \phi_u(n_b,t+1) \right\| \\
&\quad \leq \left( N^{-\frac{1}{2}} \max_{n_P-1 \leq i \leq N-2} \left| b^T \phi_u(n_b,t+1) \right| \right) \sum_{t=n_P-1}^{N-2} \left\| A^{-N} \phi_y(n_a,t) \right\| \\
&\xrightarrow[N \longrightarrow \infty]{\text{a.s}} 0
\end{aligned}$$

which completes the proof. □

### 3.6.4 An auxiliary lemma for Theorem 3

The lemma that is needed to prove Theorem 3, is stated and proved in this section.

**Lemma 6.** *Consider an ARMA system*

$$\tilde{y}_t = \tilde{P}(q) u_t \tag{3.22}$$

*where* $\{u_t, t = 0, 1, \cdots\}$ *is an i.i.d. random process with zero mean, unknown variance* $0 < \sigma_u^2 < \infty$*, and finite fourth moment. For any given integer* $\rho > 1$ *such that magnitudes of poles of* $\tilde{P}(z)$ *are less than* $\rho$*. Then,* $\frac{\tilde{y}_t}{\rho^t}$ *almost surely converges to zero, i.e.*

$$\frac{\tilde{y}_t}{\rho^t} \xrightarrow[t \to \infty]{\text{a.s.}} 0$$

**Proof.** Denote an irreducible realization of the LTI discrete-time system in (3.22) by

$$\begin{aligned}
\tilde{x}_{t+1} &= A_{\tilde{y}} \tilde{x}_t + B_{\tilde{y}} u_t \\
\tilde{y}_t &= C_{\tilde{y}} \tilde{x}_t + D_{\tilde{y}} u_t
\end{aligned}$$

for $t = 0, 1, \cdots$ with an unknown initial condition $\tilde{x}_0$ where $A_{\tilde{y}}$, $B_{\tilde{y}}$, $C_{\tilde{y}}$, and $D_{\tilde{y}}$ are constant matrices. Then, the signal $\{\tilde{y}_t, t = 0, 1, \cdots\}$ can be described by

$\tilde{y}_0 = C_{\tilde{y}} x_0 + D_{\tilde{y}} u_0$ and

$$\tilde{y}_t = C_{\tilde{y}} A_{\tilde{y}}^t \tilde{x}_0 + \sum_{j=0}^{t-1} C_{\tilde{y}} A_{\tilde{y}}^{t-j-1} B_{\tilde{y}} u_0 + D_{\tilde{y}} u_t$$

for $t = 1, 2, \cdots$, from which it follows that

$$\begin{aligned} E\left[\left(\rho^{-t}\tilde{y}_t\right)^2\right] &= \rho^{-2t}\left\{ \left(C_{\tilde{y}} A_{\tilde{y}}^t \tilde{x}_0\right)^2 + \sum_{j=0}^{t-1} \left(C_{\tilde{y}} A_{\tilde{y}}^{t-j-1} B_{\tilde{y}}\right)^2 \sigma_u^2 + D_{\tilde{y}}^2 \sigma_u^2 \right\} \\ &\leq \rho^{-2t}\left\{ \|C_{\tilde{y}}\|^2 \left\|A_{\tilde{y}}^t\right\|^2 \|\tilde{x}_0\|^2 + \|C_{\tilde{y}}\|^2 \|B_{\tilde{y}}\|^2 \sigma_u^2 \sum_{j=0}^{t-1} \left\|A_{\tilde{y}}^{t-j-1}\right\|^2 + D_{\tilde{y}}^2 \sigma_u^2 \right\} \end{aligned} \tag{3.23}$$

for $t = 1, 2, \cdots$.

Using the argument leading to (3.8), for any given $\zeta_2$ satisfying $1 < \zeta_2 < \rho$, there exists a finite constant $c_2 > 1$ such that

$$\left\|A_{\tilde{y}}^t\right\| \leq c_2 \zeta_2^t$$

for $t = 0, 1, \cdots$, from which, together with (3.23), it follows that

$$E\left[\left(\rho^{-t}\tilde{y}_t\right)^2\right] \leq c_2^2 \|C_{\tilde{y}}\|^2 \|\tilde{x}_0\|^2 \left(\rho^{-1}\zeta_2\right)^{2t} + c_2^2 \|C_{\tilde{y}}\|^2 \|B_{\tilde{y}}\|^2 \sigma_u^2 \rho^{-2t} \sum_{j=0}^{t-1} \zeta_2^{2j} + \rho^{-2t} D_{\tilde{y}}^2 \sigma_u^2$$

for $t = 1, 2, \cdots$. Therefore, $E\left[\left(\rho^{-t}\tilde{y}_t\right)^2\right] \underset{t\to\infty}{\longrightarrow} 0$, which completes the proof. □

Chapter 3 is a reprint of S. Cheong, R. R. Bitmead, "Instability detection of ARMA systems based on AR system identification" as it appears in Systems & Control Letters, 2011. The dissertation author was the primary author of this paper.

# 4 Divination of Closed-loop Stability and Performance via Frequency Response Function Estimates

## 4.1 Introduction

In Chapter 3, we introduced a method detecting the stability and instability of a system and, using this method, we can determine if a controller stabilizes a plant by building a closed-loop system and measuring the input or the output signal of the plant. In Chapter 2, we introduced a method that can assesses the stability and performance of candidate controllers even when the controllers are not on the closed-loop system. But the limitation is that the closed-loop stability and performance are only unfalsified and never falsified with a finite amount of collected data in an experiment. In this chapter, we will show that, with additional assumptions, we can determine the closed-loop stability and performance of a controller without really building a closed-loop system. This leads us to the word "divine."

> OED : divine, *v.i.*, 9. To conjecture (as to the unknown or obscure); to make an inference by conjecture, insight, intuition, or other means than actual information.

Given an internally stabilizing multiple-input/multiple-output (MIMO), linear time-invariant (LTI) plant-controller pair, $(P, C_1)$, with $P$ uncertain and $C_1$

known, determine the closed-loop stability and performance of the candidate pair $(P, C_2)$, for given, known controller $C_2$, from deliberately designed experimental data obtained from the stable $(P, C_1)$ closed loop with impinging disturbances, as illustrated in Figure 4.1. The starting point for our analysis is the experiment and

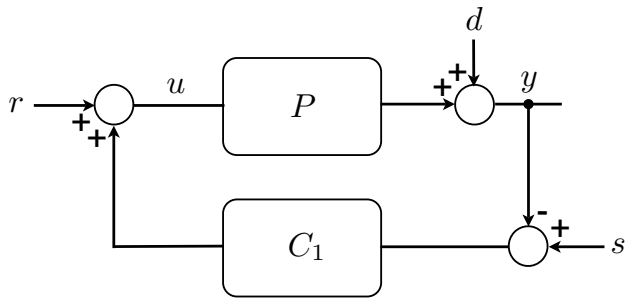


Figure 4.1: An internally stable closed-loop system $(P, C_1)$

resulting data set $\{r, s, u, y\}$ consisting of the measurable physical signals applied to and recorded from the closed loop together with knowledge of the linear controllers $C_1$ and $C_2$. The problem addressed is to design and then use these signals plus knowledge or assumption about the disturbance process $d$ to divine the stability and the performance of the closed-loop system $(P, C_2)$ without constructing this closed loop. Our approach will be via the estimation of certain frequency response functions (FRFs) from the data set. The analysis proceeds using nonparametric identification of the FRFs as opposed to parametric system identification, since this avoids issues of model structure selection, and includes consideration of the choice of external reference signals $r$ and $s$ and the experimental conditions.

The novelty in this chapter is that we provide a unifying view of a number of approaches to the divination of the properties of the $(P, C_2)$ loop and quantify the reliability and viability in terms of the properties required of the experiment and assumed of the plant system and disturbance. These approaches commence from data safely collected from experiments on an internally stable closed-loop system $(P, C_1)$ with additive output disturbances. The data lead us to; identification of an estimate of the FRF of $P$ in the frequency domain, computation of approximate FRFs of the plant right coprime factors, construction of FRFs of transfer functions in $(P, C_2)$, and a fictitious reference signal [31] whose properties reflect those of

the $(P, C_2)$ loop. Cognate approaches of others are situated within the analysis.

The internal stability of $(P, C_2)$ is assessed using the MIMO Nyquist Stability Theorem [37], which applies to FRFs. For the divination of performance, an estimate of the FRF of the generalized sensitivity function [37] of $(P, C_2)$ is obtained from the data set. From the FRF of this sensitivity function, many performance measures can be computed such as the generalized stability margin [37] and the stacked $\mathcal{H}_\infty$ specifications [30].

The divination problem has been considered under a number of guises by different research teams. Part of the contribution in this chapter is to provide a simplification, unification and overview of these techniques and to explore and quantify the methods when the signals necessarily are corrupted by disturbances entering the system. Further, by focusing on experiment design and assumptions, we are able to refine qualitative statements from unpremeditated or adventitious experiments.

This chapter is organized as follows. In Section 4.2, preliminaries and a description of the experiments on $(P, C_1)$ are given. Stability criteria for the divination are presented in Section 4.3 and, then in Section 4.4 the divination methods are stated. In Section 4.5, the general FRF estimation problem for a discrete-time system is studied; first in single-input/single-output (SISO) case with single frequency excitation, and then generalized to multi-frequency MIMO. In Section 4.6, an estimate of the winding number of a transfer function is introduced and a sufficient condition for accurate winding number estimation is provided. Reliability of each divination method is studied in the Section 4.7 and recommendations are provided. Section 4.8 describes the relationship between divination and other methods. An example is provided in Section 4.9. Conclusion follows in Section 4.10.

## 4.2 Preliminaries

Consider an internally stable closed-loop MIMO LTI discrete-time system $(P, C_1)$ in Figure 4.1 with an uncertain $\ell \times m$ plant $P$, a known $m \times \ell$ controller $C_1$, known external input signals $r$ and $s$, measured plant-input and plant-output signals $u$ and $y$, and an unknown disturbance or noise signal $d$.

The closed-loop system $(P, C_1)$ in Figure 4.1 can be described by

$$\begin{bmatrix} y \\ u \end{bmatrix} = \begin{bmatrix} G_{yr} & G_{ys} \\ G_{ur} & G_{us} \end{bmatrix} \begin{bmatrix} r \\ s \end{bmatrix} + \begin{bmatrix} G_{yd} \\ G_{ud} \end{bmatrix} d$$

where

$$T_{P,C_1} \triangleq \begin{bmatrix} G_{yr} & G_{ys} \\ G_{ur} & G_{us} \end{bmatrix} = \begin{bmatrix} P \\ I \end{bmatrix} (I + C_1 P)^{-1} \begin{bmatrix} I & C_1 \end{bmatrix} \tag{4.1}$$

and $\begin{bmatrix} G_{yd} \\ G_{ud} \end{bmatrix} = \begin{bmatrix} -G_{ys} + I \\ -G_{us} \end{bmatrix}$. From experiments on this $(P, C_1)$ loop, we collect data, i.e. the external input signals $r$ and $s$ and the observed signals $u$ and $y$.

Stable transfer functions $\tilde{M}_{C_1}$, $\tilde{N}_{C_1}$, $\tilde{M}_{C_2}$, and $\tilde{N}_{C_2}$ are left coprime factors of $C_1$ and $C_2$, i.e. $C_1 = \tilde{M}_{C_1}^{-1} \tilde{N}_{C_1}$ and $C_2 = \tilde{M}_{C_2}^{-1} \tilde{N}_{C_2}$. These are used to generate an intermediate signal,

$$v \triangleq \tilde{M}_{C_1} r + \tilde{N}_{C_1} s, \tag{4.2}$$

$$= \tilde{M}_{C_1} u + \tilde{N}_{C_1} y. \tag{4.3}$$

The experimental closed-loop $(P, C_1)$ of Figure 4.1 may then be redrawn as in Figure 4.2 and can be described by

$$\begin{bmatrix} y \\ u \end{bmatrix} = \begin{bmatrix} G_{yv} \\ G_{uv} \end{bmatrix} v + \begin{bmatrix} G_{yd} \\ G_{ud} \end{bmatrix} d \tag{4.4}$$

where $\begin{bmatrix} G_{yv} \\ G_{uv} \end{bmatrix} = \begin{bmatrix} P \\ I \end{bmatrix} (I + C_1 P)^{-1} \tilde{M}_{C_1}^{-1}$ and $\begin{bmatrix} G_{yd} \\ G_{ud} \end{bmatrix} = \begin{bmatrix} -G_{yv} \tilde{N}_{C_1} + I \\ -G_{uv} \tilde{N}_{C_1} \end{bmatrix}$.

An additional new signal $\tilde{v}$ is generated as

$$\tilde{v} \triangleq \tilde{N}_{C_2} y + \tilde{M}_{C_2} u. \tag{4.5}$$

As depicted in Figure 4.2, $\tilde{v}$ results from a stable filtering of the plant input and output signals $u$ and $y$. We may also write

$$\tilde{v} = G_{\tilde{v}v} v + G_{\tilde{v}d} d \tag{4.6}$$

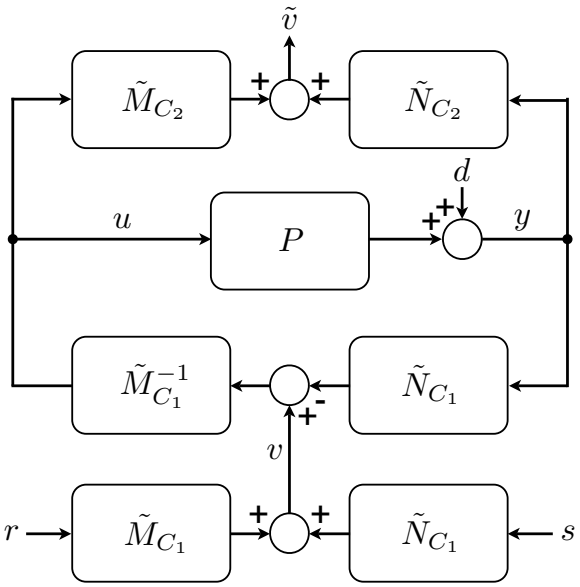


Figure 4.2: An equivalent system $(P, C_1)$ using left coprime factors of the controller $C_1$ and filtering for a signal $\tilde{v}$

where

$$\begin{aligned} G_{\tilde{v}v} &= N_{C_2} G_{yv} + M_{C_2} G_{uv} \\ &= (\tilde{N}_{C_2} N_P + \tilde{M}_{C_2} M_P)(\tilde{N}_{C_1} N_P + \tilde{M}_{C_1} M_P)^{-1} \end{aligned} \tag{4.7}$$

and $G_{\tilde{v}d} = -G_{\tilde{v}v}\tilde{N}_{C_1} + \tilde{N}_{C_2}$ with $M_P$ and $N_P$, right coprime factors of $P$.

The signal $\tilde{v}$ is called a fictitious reference signal for the controller $C_2$ [17], since it would have exactly reproduced the collected plant data $u$ and $y$ had the controller $C_2$ been in the closed-loop system with the plant $P$ as in Figure 4.3 with $P$ possessing the same initial conditions and the same external disturbance signal $d$ as in Figure 4.1. These signals, $v$ and $\tilde{v}$, are also introduced in [9] and [36]. Note that the signal $\tilde{v}$ becomes the same as the signal $v$ in (4.2) if $C_2 = C_1$ from (4.3).

The closed-loop system $(P, C_2)$ in Figure 4.3 can be described by

$$\begin{bmatrix} y \\ u \end{bmatrix} = \begin{bmatrix} G_{y\tilde{v}} \\ G_{u\tilde{v}} \end{bmatrix} \tilde{v} + \begin{bmatrix} G_{y\tilde{d}} \\ G_{u\tilde{d}} \end{bmatrix} d \tag{4.8}$$

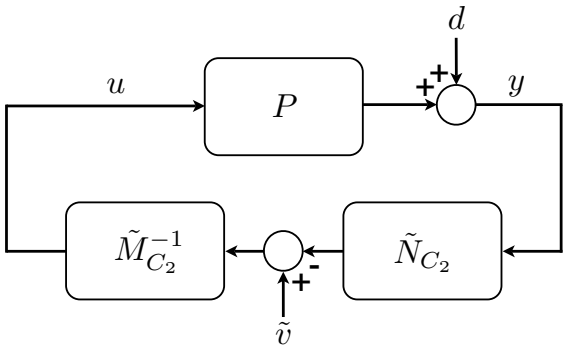


Figure 4.3: The closed-loop system $(P, C_2)$ with the fictitious reference signal $\tilde{v}$

where

$$\begin{bmatrix} G_{y\tilde{v}} \\ G_{u\tilde{v}} \end{bmatrix} = \begin{bmatrix} N_P \\ M_P \end{bmatrix} (\tilde{N}_{C_2} N_P + \tilde{M}_{C_2} M_P)^{-1} \tag{4.9}$$

and $\begin{bmatrix} G_{y\tilde{d}} \\ G_{u\tilde{d}} \end{bmatrix} = \begin{bmatrix} -G_{y\tilde{v}} \tilde{N}_{C_2} + I \\ -G_{u\tilde{v}} \tilde{N}_{C_2} \end{bmatrix}$.

Necessary notations follow. Let $G(z)$ be a transfer function matrix in $z$-transform.

• $G(\omega)$ is short for $G(e^{j\omega})$.

• The winding number, $\operatorname{wno} \det G$, is the number of encirclements around the origin made by $\det G(z)$ as $z$ follows the Nyquist contour with indentations into the exterior of the unit circle around any pole or zero of $\det G(z)$ on the unit circle.

• $\eta\left(G(z)\right)$ is the number of poles of $G(z)$ outside the unit circle.

• $\overline{\sigma}\left(\cdot\right)$ and $\underline{\sigma}\left(\cdot\right)$ are the maximum and minimum singular values, respectively.

## 4.3 Nyquist stability theorem

Divination methods introduced in this paper are based on the following version of the Nyquist Stability Theorem, which consists of discrete-time versions of Theorem 1.10 (ii) and Proposition 1.9 (c) in [37].

**Lemma 7.** *Given a plant $P = N_P M_P^{-1}$ in right coprime factor form and a controller $C = \tilde{M}_C^{-1} \tilde{N}_C$ in left coprime factor form, either of the following is a necessary and sufficient condition for the internal stability of the closed-loop system $(P, C)$.*

*(1)* $T_{P,C} = \begin{bmatrix} P \\ I \end{bmatrix} (I + CP)^{-1} \begin{bmatrix} I & C \end{bmatrix}$ *has no pole on the unit circle and*
$\operatorname{wno} \det (I + CP) + \eta (P) + \eta (C) = 0.$

*(2)* $\det(\tilde{N}_C(\omega)N_P(\omega) + \tilde{M}_C(\omega)M_P(\omega)) \neq 0 \ \forall \omega \in [0, 2\pi)$ *and*
$\operatorname{wno} \det(\tilde{N}_C N_P + \tilde{M}_C M_P) = 0.$

In investigation of internal stability of the closed-loop system $(P, C_2)$, Lemma 7 requires knowledge of either (1) the number of poles of the plant $P$ on or outside the unit circle or (2) $M_P$ and $N_P$, neither of which is available a priori. This requirement can be circumvented using the internally stable closed-loop system $(P, C_1)$ as follows.

**Theorem 6.** *Given; plant $P$, internally-stabilizing controller $C_1 = \tilde{M}_{C_1}^{-1} N_{C_1}$, candidate controller $C_2 = \tilde{M}_{C_2}^{-1} N_{C_2}$, transfer functions $G_{\tilde{v}v}$ in* (4.6) *and $G_{y\tilde{v}}$ and $G_{u\tilde{v}}$ in* (4.9)*, each of the following is a necessary and sufficient condition for internal stability of the closed-loop system $(P, C_2)$.*

*(1) $T_{P,C_2}$ has no pole on the unit circle and*
$\operatorname{wno} \det(I + C_2 P) = \operatorname{wno} \det(I + C_1 P) + \eta(C_1) - \eta(C_2).$

*(2)* $\det G_{\tilde{v}v}(\omega) \neq 0 \ \forall \omega \in [0, 2\pi)$ *and* $\operatorname{wno} \det G_{\tilde{v}v} = 0.$

*(3)* $\det(\tilde{N}_{C_1}(\omega)G_{y\tilde{v}}(\omega) + \tilde{M}_{C_1}(\omega)G_{u\tilde{v}}(\omega))^{-1} \neq 0 \ \forall \omega \in [0, 2\pi)$ *and*
$\operatorname{wno} \det(\tilde{N}_{C_1} G_{y\tilde{v}} + \tilde{M}_{C_1} G_{u\tilde{v}})^{-1} = 0.$

## 4.4 Approaches

We consider three approaches to the stability and performance divination problems on the basis of the data from experiments on the closed-loop system $(P, C_1)$.

**Approach 1.** *Obtain an estimate, $\hat{P}(\omega)$, of the FRF of the plant. Test stability of $(P, C_2)$ using Theorem 6 (1). The FRF of the generalized sensitivity function $T_{P,C_2}$ is estimated by*

$$\hat{T}_{P,C_2}(\omega) = \begin{bmatrix} \hat{P}(\omega) \\ I \end{bmatrix} (I + C_2(\omega)\hat{P}(\omega))^{-1} \begin{bmatrix} I & C_2(\omega) \end{bmatrix}.$$

**Approach 2.** *Obtain estimates, $\hat{G}_{yv}(\omega)$ and $\hat{G}_{uv}(\omega)$, of the FRFs of $G_{uv}$ and $G_{yv}$, right coprime factors of $P$, and compute $\hat{G}_{\tilde{v}v}(\omega)$ from (4.7). Test stability of $(P, C_2)$ using Theorem 6 (2). The FRF of the generalized sensitivity function $T_{P,C_2}$ is estimated by*

$$\hat{T}_{P,C_2}(\omega) = \begin{bmatrix} \hat{G}_{yv}(\omega) \\ \hat{G}_{uv}(\omega) \end{bmatrix} \hat{G}_{\tilde{v}v}(\omega)^{-1} \begin{bmatrix} \tilde{M}_{C_2}(\omega) & \tilde{N}_{C_2}(\omega) \end{bmatrix}.$$

**Approach 3.** *Obtain estimates, $\hat{G}_{y\tilde{v}}(\omega)$ and $\hat{G}_{u\tilde{v}}(\omega)$, of the FRFs of $G_{u\tilde{v}}$ and $G_{y\tilde{v}}$. Test stability of $(P, C_2)$ using Theorem 6 (3). The FRF of the generalized sensitivity function $T_{P,C_2}$ is estimated by*

$$\hat{T}_{P,C_2}(\omega) = \begin{bmatrix} \hat{G}_{y\tilde{v}}(\omega) \\ \hat{G}_{u\tilde{v}}(\omega) \end{bmatrix} \begin{bmatrix} \tilde{M}_{C_2}(\omega) & \tilde{N}_{C_2}(\omega) \end{bmatrix}.$$

**Remark 2.** *The stability test in Approach 2 gives the same result in discrete-time systems as Theorem 6 in [8] in continuous-time systems. Approach 2 estimates the FRFs of right coprime factors of $P$, while Theorem 6 in [8] does not explicitly identify $P$ in any form.*

## 4.5 Frequency response function estimation

In this section, we consider the general FRF estimation problem for a discrete-time system. The material of this section relies strongly on the material contained in the treatise [23], to which we refer the reader for further detail and analysis.

Consider a system

$$z = Gq + Hd \tag{4.10}$$

where $G$ and $H$ are $\beta \times \alpha$ and $\beta \times \beta$ MIMO systems, $q$ is an input signal, $z$ is an output signal, and $d$ is an unknown disturbance signal. Consider an $N$-periodic scalar signal $e$. Conduct $\alpha$ distinct experiments with

$$q_j(t) = \lambda_j e(t) \tag{4.11}$$

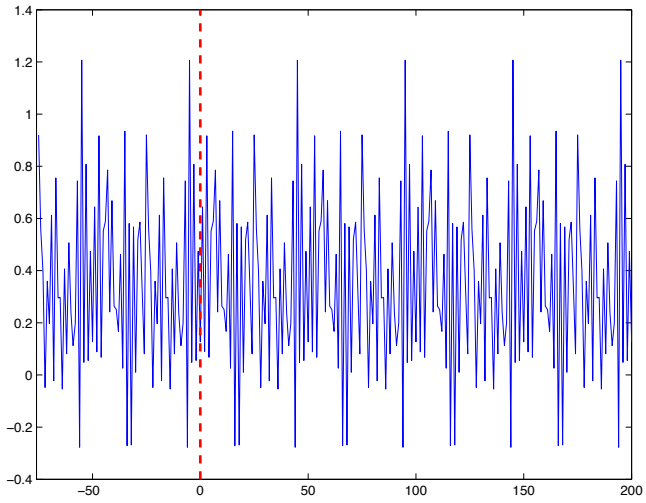


Figure 4.4: Broadband scalar experimental excitation signal $e(t)$ with; pre-experiment length $N_p = 75$, period $N = 50$, repetition $L = 4$. Two hundred experimental data are retained from time $t = 0$.

for $j = 1, \cdots, \alpha$ and $t = -N_p, \cdots, -1, 0, 1, \cdots, LN - 1$ where $\lambda_j$s are column vectors of a nonsingular matrix $\Lambda = \begin{bmatrix} \lambda_1 & \cdots & \lambda_\alpha \end{bmatrix} \in \mathbb{R}^{\alpha \times \alpha}$ and $N_p$ and $L$ are nonnegative integers representing the pre-experiment length and the repetition number of the experiment. The data set for FRF estimation is $\{(q_j(t), z_j(t)), t = 0, \cdots, LN - 1, j = 1, \cdots, \alpha\}$. The *pre-experiment* data [10] for $t = -N_p, \cdots, -1$ is ignored. This is illustrated in Figure 4.4.

The importance of the $N$-periodic property of the signal $q_j$ is that one avoids the Fourier analysis problem known as *leakage*. This is well developed in [23]. Since leakage is avoided by this strategy, the usual approaches, such as windowing, to minimizing its deleterious effects are obviated.

**Assumption 1.** *The systems $G$ and $H$ are LTI systems and can be described by transfer functions, $G(z) = \sum_{\tau=0}^{\infty} g(\tau) z^{-\tau}$ and $H(z) = \sum_{\tau=0}^{\infty} h(\tau) z^{-\tau}$, with impulse response matrices $g(\tau)$ of $G$ and $h(\tau)$ of $H$, which satisfy, respectively,*

$$\bar{\sigma}(g(\tau)) \leq K_g \tau^{\mu-1} \rho^\tau \quad \text{and} \quad \bar{\sigma}(h(\tau)) \leq K_h \tau^{\mu-1} \rho^\tau$$

*for $\tau = 0, 1, \cdots$ with known constants $K_g, K_h \in [0, \infty)$, $\mu \in \{1, 2, \cdots\}$, and $\rho \in [0, 1)$.*

Assumption 1 yields a further but lesser-known property that the FRF of $G$ possesses a level of smoothness.

**Lemma 8.** *If $G$ satisfies Assumption 1, then the FRF of $G$ satisfies the following smoothness condition.*

$$\bar{\sigma}\left(\frac{d}{d\omega}G(\omega)\right) \leq K_g S_\mu(\rho)$$

*for $\forall\omega \in [0, 2\pi)$ where the function $S$ is given in Proposition 6 in Appendix 4.11.*

**Assumption 2.** *The pre-experiment length, $N_p$, is chosen sufficiently large so that $\frac{1}{NL}\sum_{\tau=0}^{NL-1}\|x(\tau)\|_2 \leq K_x(L)$ where the signal $x_j$ is the non-period-$N$ response in $Gq_j$ and $K_x(L)$ is a known decreasing function of $L$.*

Without such an assumption and the preceding stability assumption, there is no realistic manner to estimate the FRF of $G$ reliably from experimental data.

**Assumption 3.** *A function $K_f(L)$ is known such that $\left\|\frac{1}{L}\sum_{\tau=0}^{L-1} f(t+\tau N)\right\|_2 \leq K_f(L)$ for $t = 0, 1, \cdots, N-1$ where $f = Hd$.*

This assumption captures a bound on the disturbance signal and also attempts to accommodate possible reduction of this bound when the disturbance is averaged over $L$ repetitions.

### 4.5.1 Single-frequency SISO cases

Suppose that the system $G$ in (4.10) is scalar, $\Lambda = 1$, and $e(t) = A\cos(\omega_1 t + \phi)$ for $t = -N_p, \cdots, -1, 0, 1, \cdots, LN-1$ with $\omega_1 = \frac{2\pi k_1}{N}$ for some integer $k_1$ in $0 \leq k_1 < \frac{N}{2}$. The phase is set at $\phi = \frac{\pi}{3}$ when $\omega_1 = 0$, otherwise arbitrarily chosen. Then the output signal $z$ is comprised of three components;

$$z(t) = B\cos(\omega_1 t + \phi + \psi) + x(t) + f(t)$$

for $t = -N_p, \cdots, -1, 0, 1, \cdots, LN-1$, where the three constituent parts are the sinusoidal steady-state response, the transient response $x(t) = \sum_{\tau=t+N_p+1}^{\infty} g(\tau)q(t-\tau)$ due to the initial state value, and the additive disturbance signal $f(t) = \sum_{\tau=0}^{\infty} h(\tau)d(t-\tau)$ which is not necessarily periodic. Here $B/A = |G(\omega_1)|$ and $\psi = \angle G(\omega_1)$.

The FRF estimate may be computed by

$$\hat{G}(\omega_1) = \frac{2}{ALN} \sum_{t=0}^{LN-1} z(t) e^{-j\omega_1 t}. \tag{4.12}$$

This is called the empirical transfer function estimation (ETFE) [15] and leads to

$$\hat{G}(\omega_1) = G(\omega_1) + \frac{2}{ALN} \sum_{t=0}^{LN-1} x(t) e^{-j\omega_1 t} + \frac{2}{ALN} \sum_{t=0}^{LN-1} f(t) e^{-j\omega_1 t}.$$

An upper bound on the magnitude of the error for the FRF estimates is obtained in the following proposition.

**Proposition 4.** *Suppose that Assumptions 1-3 hold. Then, the FRF estimate in* (4.12) *satisfies*

$$|\hat{G}(\omega_1) - G(\omega_1)| \leq \frac{2(K_x + K_f)}{A\underline{\sigma}(\Lambda)}.$$

### 4.5.2 Multiple-frequency SISO cases

Suppose that the system $G$ in (4.10) is scalar, $\Lambda = 1$, and

$$e(t) = \sum_{i=1}^{M} A_i \cos(\omega_i t + \phi_i) \tag{4.13}$$

for $t = -N_p, \cdots, -1, 0, 1, \cdots, LN-1$ with $\omega_i = \frac{2\pi k_i}{N}$ for some integers $0 \leq k_1 < \cdots < k_M < \frac{N}{2}$. The phases $\phi_i$s are set at $\phi_i = \frac{\pi}{3}$ when $\omega_i = 0$, otherwise arbitrarily chosen. Then the output signal $z$ is comprised of three components.

$$z(t) = \sum_{i=1}^{M} B_i \cos(\omega_i t + \phi_i + \psi_i) + x(t) + f(t).$$

The FRF of $G$ at each frequency may be computed by

$$\hat{G}(\omega_i) = \frac{2}{A_i LN} \sum_{t=0}^{LN-1} z(t) e^{-j\omega_i t}$$

and this FRF estimate satisfies

$$\hat{G}(\omega_i) = G(\omega_i) + \frac{2}{A_i LN} \sum_{t=0}^{LN-1} x(t) e^{-j\omega_i t} + \frac{2}{A_i LN} \sum_{t=0}^{LN-1} f(t) e^{-j\omega_i t}.$$

If Assumptions 1-3 are satisfied, the linearity of $G$ allows us to independently analyze the FRF estimate at each frequency and Proposition 4 provides the error analysis for the FRF estimate at each frequency.

### 4.5.3 MIMO Cases

If the signal $e$ is given by (4.13), then the output signals, $z_j$ for $j = 1, \cdots, \alpha$, are described by

$$z_j(t) = \sum_{i=1}^{M} \begin{bmatrix} B_{ij1} \cos(\omega_i t + \phi_i + \psi_{ij1}) \\ \vdots \\ B_{ij\beta} \cos(\omega_i t + \phi_i + \psi_{ij\beta}) \end{bmatrix} + x_j(t) + f_j(t)$$

for $j = 1, \cdots, \alpha$ where $B_{ijk}$s and $\psi_{ijk}$s are scalar and $x_j(t)$ and $f_j(t)$ are $\beta \times 1$ vectors.

The FRF of $G$ at each frequency may be computed by

$$\hat{G}(\omega_i) = \frac{2}{A_i LN} \sum_{t=0}^{LN-1} Z(t) e^{-j\omega_i t} \Lambda^{-1} \tag{4.14}$$

where $Z(t) = \begin{bmatrix} z_1(t) & \cdots & z_\alpha(t) \end{bmatrix}$ and this FRF estimate statisfies

$$\hat{G}(\omega_i) = G(\omega_i) + \frac{2}{A_i LN} \sum_{t=0}^{LN-1} X(t) e^{-j\omega_i t} \Lambda^{-1} + \frac{2}{A_i LN} \sum_{t=0}^{LN-1} F(t) e^{-j\omega_i t} \Lambda^{-1}$$

where $X(t) = \begin{bmatrix} x_1(t) & \cdots & x_\alpha(t) \end{bmatrix}$ and $F(t) = \begin{bmatrix} f_1(t) & \cdots & f_\alpha(t) \end{bmatrix}$.

**Proposition 5.** *Suppose that Assumptions 1-3 hold. Then, the FRF estimate in* (4.14) *satisfies*

$$\bar{\sigma}(\hat{G}(\omega_i) - G(\omega_i)) \leq \frac{2\sqrt{\alpha}(K_x + K_f)}{A_i \underline{\sigma}(\Lambda)}$$

*for* $i = 1, \cdots, M$.

We note that the calculations of $\hat{G}(\omega_i)$ in (4.14) are traditionally conducted using the discrete/fast Fourier transforms (DFT/FFT) of the signals.

## 4.6 Winding number estimation

Let $W(z)$ be a square transfer function, which is analytic and non-zero on the unit circle. The winding number of the determinant of $W(z)$ can be obtained from the unwrapped phase of the determinant of the frequency response function, unwarg $\det W(\omega)$. See [18] and [32].

We obtained in Section 4.5.3 the $M$ FRF estimates $\hat{W}(\omega_i)$ at select frequencies $\{\omega_i, i = 1, \cdots, M\}$ and will use a linear interpolant to estimate the winding number of $\det W(z)$. Define the complex conjugate frequencies

$$\omega_i = \begin{cases} 2\pi - \omega_{2M+1-i} & \text{for } i = M+1, \cdots, 2M \\ 2\pi + \omega_1 & \text{for } i = 2M+1 \end{cases}$$

and, then, extend the estimate set to the full $2M+1$ points on the unit circle,

$$\hat{W}(\omega_i) = \begin{cases} \overline{\hat{W}(\omega_{2M+1-i})} & \text{for } i = M+1, \cdots, 2M \\ \hat{W}(\omega_1) & \text{for } i = 2M+1. \end{cases}$$

Next a continuous function $\hat{W}(\omega)$ is defined, using linear interpolation, by

$$\hat{W}(\omega) \triangleq (1-\theta)\hat{W}(\omega_i) + \theta\hat{W}(\omega_{i+1}) \tag{4.15}$$

for $\forall \omega \in [\omega_i, \omega_{i+1})$, $i = 1, \cdots, 2M$ where $\theta = \frac{\omega - \omega_i}{\Delta\omega_i}$ with $\Delta\omega_i = \omega_{i+1} - \omega_i$. We have the following.

**Theorem 7.** *Given the $M$ FRF estimates $\{\hat{W}(\omega_i), i = 1, \cdots, M\}$ of $W(\omega)$ and the linear interpolant $\hat{W}(\omega)$ in (4.15), if*

$$\underline{\sigma}(\hat{W}(\omega)) > \max_{j \in \{i, i+1\}} \bar{\sigma}\left(\hat{W}(\omega_j) - W(\omega_j)\right) + \max_{\xi \in [\omega_i, \omega_{i+1}]} \bar{\sigma}\left(\frac{d}{d\omega} W(\omega)\Big|_{\omega=\xi}\right)(\omega_{i+1} - \omega_i) \tag{4.16}$$

*for* $\forall\omega \in [\omega_i, \omega_{i+1})$, $i = 1, \cdots, 2M$, *then* $\det W(\omega) \neq 0$ *for* $\forall\omega \in [0, 2\pi)$ *and*

$$\operatorname{wno} \det W(\omega) = \operatorname{wno} \det \hat{W}(\omega).$$

The following corollary follows directly from Lemma 8.

**Corollary 1.** *If Assumption 1 holds for the system* $W$ *with constant* $K_w$*, then the second term in the right-hand side of* (4.16) *can be replaced by a more conservative term* $K_w S_\mu(\rho)(\omega_{i+1} - \omega_i)$ *where the function* $S$ *is given in Proposition 6 in Appendix 4.11.*

## 4.7 Assessment of divination

### 4.7.1 Quality of divination using Approach 1

Perfect knowledge of $P(\omega)$ would deliver perfect divination. However, this knowledge is unavailable and the reliability of Approach 1 in Section 4.4 is affected by the accuracy of the estimate of the FRF of the plant.

Estimators for $P(\omega)$ can be obtained by the joint input-output approach, which uses FRF estimates $\hat{G}_{yr}(\omega)$, $\hat{G}_{ur}(\omega)$, $\hat{G}_{ys}(\omega)$, $\hat{G}_{us}(\omega)$, $\hat{G}_{yv}(\omega)$, and $\hat{G}_{uv}(\omega)$ for the transfer functions $G_{yr}$, $G_{ur}$, $G_{ys}$, $G_{us}$, $G_{yv}$, and $G_{uv}$ in Section 4.2. The possible choices for an estimator for the FRF of $P$ are

$$\begin{aligned}
\hat{P}_1(\omega) &\triangleq \hat{G}_{yr}(\omega)\hat{G}_{ur}(\omega)^{-1}, \\
\hat{P}_2(\omega) &\triangleq \hat{G}_{ys}(\omega)\hat{G}_{us}(\omega)^{+}, \\
\hat{P}_3(\omega) &\triangleq \begin{bmatrix} \hat{G}_{yr}(\omega) & \hat{G}_{ys}(\omega) \end{bmatrix} \begin{bmatrix} \hat{G}_{ur}(\omega) & \hat{G}_{us}(\omega) \end{bmatrix}^{+}, \\
\hat{P}_4(\omega) &\triangleq \hat{G}_{yv}(\omega)\hat{G}_{uv}(\omega)^{-1},
\end{aligned}$$

where $^+$ means the Moore-Penrose pseudoinverse. The underlying purpose of these FRF estimates is to select that which ultimately yields the most reliable winding number calculation. Of the four plant estimators, $\hat{P}_3(\omega)$ outperforms $\hat{P}_1(\omega)$ and $\hat{P}_2(\omega)$ in noise handling and $\hat{P}_4(\omega)$ is similar to $\hat{P}_3(\omega)$. See [5] for unreliable properties of $\hat{P}_1(\omega)$ and $\hat{P}_2(\omega)$, due to poles and zeros of $C_1$ on the unit circle. For

brevity, we study just the behavior of $\hat{P}_3(\omega)$ and denominate it $\hat{P}(\omega)$, i.e.

$$\begin{aligned}\hat{P}(\omega) &= \begin{bmatrix}\hat{G}_{yr}(\omega) & \hat{G}_{ys}(\omega)\end{bmatrix}\begin{bmatrix}\hat{G}_{ur}(\omega) & \hat{G}_{us}(\omega)\end{bmatrix}^{+} \\ &\triangleq \hat{G}_Y(\omega)\hat{G}_U(\omega)^{+}.\end{aligned} \tag{4.17}$$

To obtain $\hat{G}_Y(\omega)$ and $\hat{G}_U(\omega)$, consider the closed-loop system $(P, C_1)$ in Figure 4.1,

$$y = G_Y\begin{bmatrix}r\\ s\end{bmatrix} + G_{yd}d \quad \text{and} \quad u = G_U\begin{bmatrix}r\\ s\end{bmatrix} + G_{ud}d \tag{4.18}$$

where $G_Y = \begin{bmatrix}G_{yr} & G_{ys}\end{bmatrix}$ and $G_U = \begin{bmatrix}G_{ur} & G_{us}\end{bmatrix}$, each of which corresponds to the system in (4.10) in Section 4.5. Suppose that the input signals $r_j$ and $s_j$ are chosen in the same way as $q_j$ in (4.11) with $e$ in (4.13);

$$\begin{bmatrix}r_j(t)\\ s_j(t)\end{bmatrix} = \lambda_j e(t).$$

The output signals, $y_j$ and $u_j$ for $j = 1, \cdots, m+\ell$, are recorded until $t = LN-1$. Then, the FRF estimates are computed in the same way as in (4.14), i.e.

$$\begin{bmatrix}\hat{G}_Y(w_i)\\ \hat{G}_U(w_i)\end{bmatrix} = \frac{2}{A_i LN}\sum_{t=0}^{LN-1}\begin{bmatrix}Y(t)\\ U(t)\end{bmatrix} e^{-j\omega_i t}\Lambda^{-1}$$

for $i = 1, \cdots, M$ where

$$\begin{aligned}Y(t) &= \begin{bmatrix}y_1(t) & \cdots & y_{m+\ell}(t)\end{bmatrix} \\ U(t) &= \begin{bmatrix}u_1(t) & \cdots & u_{m+\ell}(t)\end{bmatrix}.\end{aligned}$$

The error of these FRF estimates is described by

$$\begin{bmatrix}\Delta G_Y(\omega_i)\\ \Delta G_U(\omega_i)\end{bmatrix} \triangleq \begin{bmatrix}\hat{G}_Y(w_i)\\ \hat{G}_U(\omega_i)\end{bmatrix} - \begin{bmatrix}G_Y(w_i)\\ G_U(w_i)\end{bmatrix} \tag{4.19}$$

for $i = 1, \cdots, M$.

We are interested in estimating the winding numbers of determinants of

$$\Xi_k(\omega) \triangleq I + C_k(\omega)P(\omega)$$

for $k = 1, 2$ and Section 4.6 provides an estimation method for the winding numbers using a finite number of estimated values. According to Section 4.6, given a finite number of estimated values, $\{(\hat{G}_Y(\omega_i), \hat{G}_U(\omega_i)), i = 1, \cdots, M\}$ and $\{\hat{P}(\omega_i) \triangleq \hat{G}_Y(\omega_i)\hat{G}_U(\omega_i)^+, i = 1, \cdots, M\}$, we define continuous functions, $\hat{G}_U(\omega)$, $\hat{\Xi}_1(\omega)$, and $\hat{\Xi}_2(\omega)$, using the linear interpolation method in Section 4.6, by

$$\begin{aligned}\hat{G}_U(\omega) &\triangleq (1-\theta)\hat{G}_U(\omega_i) + \theta\hat{G}_U(\omega_{i+1}) \\ \hat{\Xi}_k(\omega) &\triangleq (1-\theta)(I + C_k(\omega_i)\hat{P}(\omega_i)) + \theta(I + C_k(\omega_{i+1})\hat{P}(\omega_{i+1}))\end{aligned}$$

for $\forall\omega \in [\omega_i, \omega_{i+1})$, $i = 1, \cdots, 2M$, $k = 1, 2$ where $\theta = \frac{\omega-\omega_i}{\Delta\omega_i}$ with $\Delta\omega_i = \omega_{i+1} - \omega_i$, so that the winding number of $\det \Xi(\omega)$ is estimated by the winding number of $\det \hat{\Xi}(\omega)$.

**Theorem 8.** *Suppose that Assumptions 1-3 hold for each system in* (4.18)*. Then provided*

*(1) the controller $C_2$ has no pole on the unit circle and*

*(2) $\hat{G}_U(\omega)$ and $\hat{\Xi}_k(\omega)$ satisfy*

$$\begin{aligned}\underline{\sigma}(\hat{G}_U(\omega)) &> \max_{j\in\{i,i+1\}} \frac{2\sqrt{\alpha}(K_x + K_f)}{A_j\underline{\sigma}(\Lambda)} + \max_{\xi\in[\omega_i,\omega_{i+1}]} \bar{\sigma}\left(\frac{d}{d\omega}G_U(\omega)\Big|_{\omega=\xi}\right)(\omega_{i+1} - \omega_i) \\ \underline{\sigma}(\hat{\Xi}_k(\omega)) &> \max_{j\in\{i,i+1\}} \frac{2\sqrt{\alpha}(K_x + K_f)}{A_j\underline{\sigma}(\Lambda)\underline{\sigma}(\hat{G}_U(\omega_j))}\ \bar{\sigma}(C_k(\omega_j))\big\{1 + \bar{\sigma}(P(\omega_j))\big\} \\ &\quad + \max_{\xi\in[\omega_i,\omega_{i+1}]} \bar{\sigma}\left(\frac{d}{d\omega}\Xi_k(\omega)\Big|_{\omega=\xi}\right)(\omega_{i+1} - \omega_i)\end{aligned}$$

*for $\forall\omega \in [\omega_i, \omega_{i+1})$, $i = 1, \cdots, 2M$, $k = 1, 2$, the controller $C_2$ stabilizes the plant $P$ if, and only if,*

$$\operatorname{wno}\det\hat{\Xi}_2(\omega) = \operatorname{wno}\det\hat{\Xi}_1(\omega) + \eta(C_1) - \eta(C_2). \tag{4.20}$$

Condition (2) in Theorem 8 ensures that $\underline{\sigma}(G_U(\omega)) \neq 0$ and $\underline{\sigma}(\Xi_2(\omega)) \neq 0$ for $\forall\omega \in [0, 2\pi)$. Condition $\underline{\sigma}(G_U(\omega)) \neq 0$ requires that the plant $P$ has no pole

on the unit circle since $G_U = M_P(N_{C_1}N_P + M_{C_1}M_P)^{-1}\begin{bmatrix} M_{C_1} & N_{C_1}\end{bmatrix}$. Condition $\underline{\sigma}(\Xi_2(\omega)) \neq 0$ requires that the transfer function $(I + C_2P)^{-1}$ has no pole on the unit circle. Thus, combined with Condition (1) in Theorem 8, it is guaranteed that $C_2$, $P$, and $(I + C_2P)^{-1}$ have no pole on the unit circle, which implies the first condition in Theorem 6 (1), i.e. $T_{P,C_2}$ has no pole on the unit circle.

Condition (2) ensures that $\operatorname{wno}\det\Xi_1 = \operatorname{wno}\det\hat{\Xi}_1(\omega)$ and $\operatorname{wno}\det\Xi_2 = \operatorname{wno}\det\hat{\Xi}_2(\omega)$, also. Hence, (4.20) becomes equivalent to the second condition in Theorem 6 (1). Note that $C_1$, under these conditions, cannot have a pole on the unit circle. Otherwise, $\max_{\xi\in[0,2\pi)}\bar{\sigma}\left(\frac{d}{d\omega}\Xi_1(\omega)\big|_{\omega=\xi}\right)$ is unbounded and, hence, Condition (2) is violated. Therefore, this approach can, reliably, be applied only when each of $C_1$, $C_2$, and $P$ has no pole on the unit circle.

The right-hand side of the $\hat{G}_U$ inequality above contains a term representing the disturbance-to-reference ratio of $d(t)$ versus $\begin{bmatrix} r(t)^T & s(t)^T\end{bmatrix}^T$ appearing in the signal $u(t)$. Approach 1 fails, even with good signal ratios, when the second inequality requires multiplication by large numbers due to poles on the unit circle.

### 4.7.2 Quality of divination using Approach 2

The reliability of Approach 2 in Section 4.4 is affected by the accuracy of the FRF estimates, $\hat{G}_{yv}(\omega)$ and $\hat{G}_{uv}(\omega)$, of the transfer functions $G_{yv}(z)$ and $G_{uv}(z)$ in Section 4.2.

In order to obtain $\hat{G}_{yv}(\omega)$ and $\hat{G}_{uv}(\omega)$, consider the closed-loop system $(P, C_1)$

$$\begin{bmatrix} y \\ u\end{bmatrix} = \begin{bmatrix} G_{yv} \\ G_{uv}\end{bmatrix} v + \begin{bmatrix} G_{yd} \\ G_{ud}\end{bmatrix} d, \tag{4.21}$$

described in (4.4), which corresponds to the system in (4.10) in Section 4.5. Suppose that the input signals $r_j$ and $s_j$ are chosen such that the $v_j$ is determined in the same way as $q_j$ in (4.11) with $e$ in (4.13). The output signals, $z_j(t) = \begin{bmatrix} y_j(t)^T & u_j(t)^T\end{bmatrix}^T$ for $j = 1, \cdots, m$, are recorded until $t = LN - 1$. Then, the FRF estimates are computed in the same way as in (4.14), i.e.

$$\begin{bmatrix} \hat{G}_{yv}(w_i) \\ \hat{G}_{uv}(w_i)\end{bmatrix} = \frac{2}{A_iLN}\sum_{t=0}^{LN-1} Z(t)e^{-j\omega_i t}\Lambda^{-1} \tag{4.22}$$

for $i = 1, \cdots, M$ where $Z(t) = \begin{bmatrix} z_1(t) & \cdots & z_m(t) \end{bmatrix}$. The error of these FRF estimates is described by

$$\begin{bmatrix} \Delta G_{yv}(\omega_i) \\ \Delta G_{uv}(\omega_i) \end{bmatrix} \triangleq \begin{bmatrix} \hat{G}_{yv}(w_i) \\ \hat{G}_{uv}(\omega_i) \end{bmatrix} - \begin{bmatrix} G_{yv}(w_i) \\ G_{uv}(w_i) \end{bmatrix} \tag{4.23}$$

for $i = 1, \cdots, M$.

We are interested in estimating the winding number of the determinant of the transfer function $G_{\tilde{v}v}$ in (4.7) and Section 4.6 provides an estimation method for the winding numbers using a finite number of estimated values. According to Section 4.6, given a finite number of estimated values

$$\hat{G}_{\tilde{v}v}(\omega_i) = \tilde{N}_{C_2}(\omega_i)\hat{G}_{yv}(\omega_i) + \tilde{M}_{C_2}(\omega_i)\hat{G}_{uv}(\omega_i) \tag{4.24}$$

for $i = 1, \cdots, M$, we define a continuous function $\hat{G}_{\tilde{v}v}(\omega)$, using the linear interpolation method in Section 4.6, by

$$\hat{G}_{\tilde{v}v}(\omega) \triangleq (1-\theta)\hat{G}_{\tilde{v}v}(\omega_i) + \theta\hat{G}_{\tilde{v}v}(\omega_{i+1})$$

for $\forall \omega \in [\omega_i, \omega_{i+1})$, $i = 1, \cdots, 2M$ where $\theta = \frac{\omega - \omega_i}{\Delta\omega_i}$ with $\Delta\omega_i = \omega_{i+1} - \omega_i$, so that the winding number of $\det G_{\tilde{v}v}(\omega)$ is estimated by the winding number of $\det \hat{G}_{\tilde{v}v}(\omega)$.

**Theorem 9.** *Suppose that Assumptions 1-3 hold for the system in* (4.21). *Then provided*

$$\begin{aligned} \underline{\sigma}(\hat{G}_{\tilde{v}v}(\omega)) > & \max_{j \in \{i, i+1\}} \frac{2\sqrt{\alpha}(K_x + K_f)\tilde{W}_2(\omega_j)}{A_j \underline{\sigma}(\Lambda)} \\ & + \max_{\xi \in [\omega_i, \omega_{i+1}]} \bar{\sigma} \left( \frac{d}{d\omega} G_{\tilde{v}v}(\omega) \Big|_{\omega=\xi} \right) (\omega_{i+1} - \omega_i) \end{aligned} \tag{4.25}$$

*for* $\forall \omega \in [\omega_i, \omega_{i+1})$, $i = 1, \cdots, 2M$ *where* $\tilde{W}_2(\omega_j) = \bar{\sigma}\left( \begin{bmatrix} \tilde{N}_{C_2}(\omega_j) & \tilde{M}_{C_2}(\omega_j) \end{bmatrix} \right)$, *the controller* $C_2$ *stabilizes the plant* $P$ *if, and only if,*

$$\operatorname{wno} \det \hat{G}_{\tilde{v}v}(\omega) = 0. \tag{4.26}$$

The first term in the right-hand side of (4.25) contains again a disturbance-

to-reference ratio for the signals $d(t)$ versus $v(t)$ in the signal $\begin{bmatrix} y(t)^T & u(t)^T \end{bmatrix}^T$. The second term can be replaced, using Lemma 8, by a more conservative (but more likely known or assumed) bound $K_\Gamma S_\mu(\rho)(\omega_{i+1} - \omega_i)$ where $K_\Gamma$ corresponds to $K_g$ in Lemma 8 and the function $S$ is given in Proposition 6 in Appendix 4.11.

This approach can, reliably, be applied, regardless of the locations of poles of $C_1$, $C_2$, and $P$, subject to satisfaction of (4.25) and (4.26). The generalized sensitivity function is estimated, using (4.22) and (4.24), by

$$\hat{T}_{P,C_2}(\omega_i) = \begin{bmatrix} \hat{G}_{yv}(\omega_i) \\ \hat{G}_{uv}(\omega_i) \end{bmatrix} \hat{G}_{\tilde{v}v}(\omega_i)^{-1} \begin{bmatrix} \tilde{M}_{C_2}(\omega_i) & \tilde{N}_{C_2}(\omega_i) \end{bmatrix}$$

for $i = 1, \cdots, M$.

If $\underline{\sigma}(\hat{G}_{\tilde{v}v}(\omega))$ passes far enough from the origin to satisfy the condition (4.25), the condition in (4.26) is a precise indicator for the stability or instability of the closed-loop system $(P, C_2)$. Otherwise, Theorem 9 cannot be applied and, thus, the condition in (4.26) becomes an unreliable indicator for internal stability of the $(P, C_2)$ loop. Moreover, if $\underline{\sigma}(\hat{G}_{\tilde{v}v}(\omega))$ passes close to the origin, the $(P, C_2)$ loop is close to instability or unstable.

### 4.7.3 Quality of divination using Approach 3

The quality of Approach 3 is analyzed by showing that Approach 3 and Approach 2 are very similar.

In order to obtain $\hat{G}_{y\tilde{v}}(\omega)$ and $\hat{G}_{u\tilde{v}}(\omega)$, consider the system in (4.21) with the input signal $v_j$ and the recorded output signals $z_j(t) = \begin{bmatrix} y_j(t)^T & u_j(t)^T \end{bmatrix}^T$ and $\tilde{v}_j(t)$ for $j = 1, \cdots, m$, $t = 0, \cdots, LN - 1$ in Section 4.7.2. Also, recall the closed-loop system $(P, C_2)$ in Figure 4.3 described in (4.8);

$$\begin{bmatrix} y \\ u \end{bmatrix} = \begin{bmatrix} G_{y\tilde{v}} \\ G_{u\tilde{v}} \end{bmatrix} \tilde{v} + \begin{bmatrix} G_{y\tilde{d}} \\ G_{u\tilde{d}} \end{bmatrix} d.$$

Then, the FRF estimates are computed by

$$\begin{bmatrix} \hat{G}_{y\tilde{v}}(w_i) \\ \hat{G}_{u\tilde{v}}(w_i) \end{bmatrix} = \frac{1}{\sqrt{LN}} \sum_{t=0}^{LN-1} Z(t) e^{-j\omega_i t} \left( \frac{1}{\sqrt{LN}} \sum_{t=0}^{LN-1} \tilde{V}(t) e^{-j\omega_i t} \right)^{-1} \tag{4.27}$$

for $i = 1, \cdots, M$ where $Z(t) = \begin{bmatrix} z_1(t) & \cdots & z_m(t) \end{bmatrix}$ and $\tilde{V}(t) = \begin{bmatrix} \tilde{v}_1(t) & \cdots & \tilde{v}_m(t) \end{bmatrix}$ and we can calculate $\tilde{N}_{C_1}(\omega_i)\hat{G}_{y\tilde{v}}(w_i) + \tilde{M}_{C_1}(\omega_i)\hat{G}_{u\tilde{v}}(w_i)$ for $i = 1, \cdots, M$.

On the other hand, the FRF of

$$\Gamma^{-1} \triangleq \tilde{N}_{C_1} G_{y\tilde{v}} + \tilde{M}_{C_1} G_{u\tilde{v}}$$

may be directly estimated by

$$\hat{\Gamma}(w_i)^{-1} = \frac{1}{\sqrt{LN}} \sum_{t=0}^{LN-1} V(t) e^{-j\omega_i t} \left( \frac{1}{\sqrt{LN}} \sum_{t=0}^{LN-1} \tilde{V}(t) e^{-j\omega_i t} \right)^{-1} \tag{4.28}$$

for $i = 1, \cdots, M$ where $V(t) = \begin{bmatrix} v_1(t) & \cdots & v_m(t) \end{bmatrix}$, using the filtered signal $v = \begin{bmatrix} \tilde{N}_{C_1} & \tilde{M}_{C_1} \end{bmatrix} \begin{bmatrix} y \\ u \end{bmatrix}$, which comes from (4.3). Then, since

$$\frac{1}{\sqrt{LN}} \sum_{t=0}^{LN-1} V(t) e^{-j\omega_i t} \Lambda^{-1} = \frac{A_i \sqrt{LN}}{2} I$$

for $i = 1, \cdots, M$, we have

$$\hat{\Gamma}(w_i) = \frac{2}{A_i LN} \sum_{t=0}^{LN-1} \tilde{V}(t) e^{-j\omega_i t} \Lambda^{-1}, \tag{4.29}$$

which can be viewed as an estimate of the FRF of $G_{\tilde{v}v}$. This estimate uses the DFT of $\tilde{v} = \tilde{N}_{C_2} y + \tilde{M}_{C_2} u$ while the Approach 2 estimate (4.24) uses the DFT of $\begin{bmatrix} y^T & u^T \end{bmatrix}^T$, which is multiplied by $\begin{bmatrix} \tilde{N}_{C_2}(\omega_i) & \tilde{M}_{C_2}(\omega_i) \end{bmatrix}$. The difference between these estimates is guaranteed, by Theorem 2.1 in [15], to satisfiy $\bar{\sigma}(\hat{\Gamma}(w_i) - \hat{G}_{\tilde{v}v}(\omega_i)) \leq \frac{K_{\tilde{v}}}{A_i LN}$ for $i = 1, \cdots, M$ for some constant $K_{\tilde{v}}$.

Analogously to earlier, we define

$$\hat{\Gamma}(\omega) \triangleq (1 - \theta)\hat{\Gamma}(\omega_i) + \theta\hat{\Gamma}(\omega_{i+1}).$$

Similarly to Theorem 9, we can develop the following theorem.

**Theorem 10.** *Suppose that Assumptions 1-3 hold for the system in* (4.6)*. Then*

*provided*

$$\underline{\sigma}(\hat{\Gamma}(\omega)) > \max_{j\in\{i,i+1\}} \frac{2\sqrt{\alpha}(K_x+K_f)}{A_j\underline{\sigma}(\Lambda)} + \max_{\xi\in[\omega_i,\omega_{i+1}]} \bar{\sigma}\left(\frac{d}{d\omega}G_{\tilde{v}v}(\omega)\bigg|_{\omega=\xi}\right)(\omega_{i+1}-\omega_i)$$

*for* $\forall\omega\in[\omega_i,\omega_{i+1})$, $i=1,\cdots,2M$, *the controller* $C_2$ *stabilizes the plant* $P$ *if, and only if,*

$$\text{wno}\det\hat{\Gamma}(\omega)=0.$$

The generalized sensitivity functions is estimated, using (4.27) and (4.29), by

$$\begin{aligned}\hat{T}_{P,C_2}(\omega_i) &= \begin{bmatrix}\hat{G}_{y\tilde{v}}(\omega_i)\\ \hat{G}_{u\tilde{v}}(\omega_i)\end{bmatrix}\begin{bmatrix}\tilde{M}_{C_2}(\omega_i) & \tilde{N}_{C_2}(\omega_i)\end{bmatrix}\\ &= \begin{bmatrix}\hat{G}_{yv}(\omega_i)\\ \hat{G}_{uv}(\omega_i)\end{bmatrix}\hat{\Gamma}(\omega_i)^{-1}\begin{bmatrix}\tilde{M}_{C_2}(\omega_i) & \tilde{N}_{C_2}(\omega_i)\end{bmatrix}\end{aligned}$$

for $i=1,\cdots,M$, which is the same as the estimate obtained in Approach 2 with replacement of $\hat{G}_{\tilde{v}v}(\omega_i)$ by $\hat{\Gamma}(\omega_i)$.

### 4.7.4 Divination recommendations

Since all three approaches commence with the same experiment and data set, we can test all three divination approaches at the same time and check whether any of them provides a clear solution. However, as mentioned earlier, the conditions in Approach 1 are only satisfied when $C_1$, $C_2$, and $P$ have no pole on the unit circle. Approaches 2 and 3 are similar and work without restriction on pole locations. Each approach has corresponding error terms for the estimate of transfer functions and these error terms should be sufficiently small to satisfy the conditions in their respective theorems. These error terms depend on the initial condition of $(P,C_1)$ loop (ameliorated by the pre-experiment length $N_p$), the disturbance effect, the FRFs of $C_1$, $C_2$, and $P$, and the selected frequency points.

If the data from the experiment do not satisfy the conditions for any approach, one remedy is to increase $N_p$ in order to decrease the initial condition effect, or to increase $L$ in the case of random disturbances which average to zero,

or to increase $N$ to diminish the interpolation errors. With a simple bound on the disturbance, there is no guarantee that this will work without a concomitant effort to increase SNR. As we collect the data from the experiment, we can freely assign $N_p$ and $L$ and continue the experiment until the conditions for any approach are satisfied or the time is exhausted.

When it is possible to perform multiple experiments, the regions of the frequency axis where divination is guaranteed to be reliable, i.e. the closed loop FRF is bounded away from zero, can be augmented by new experiments with different frequency content or SNR at the frequency.

When we have more than one candidate controller, the stability and performance of the candidate controllers can be divined concurrently.

## 4.8 Relationship with other methods

**Controller validation:** as explored by Dehghani *et al.* [6, 8, 9], is the closest in principle approach to our own of direct divination of the stability of $(P, C_2)$ through the analysis of experimentally derived FRFs. Their approach is largely qualitative and concentrates on continuous-time systems, but explores much of the same territory as here without the explicit error analysis or experiment design. Thus, the controller validation problem can be interpreted as two-step validation which is identification of FRFs of coprime factors, $G_{yv}$ and $G_{uv}$, of the plant and then determination of the stability of $(P, C_2)$ using the identified information as in Approach 2. Our work develops the computational discrete-time approach in order to treat the estimation and divination confidence, including the performance analysis side.

**Controller certification:** as treated by [22] deals with the application of the Vinnicombe $\nu$-gap metric, $\delta_\nu(C_1, C_2)$, and the generalized stability margin, $b_{P,C_1}$, to certify from FRFs that new controllers will stabilize the plant $P$. Their approach uses the $(P, C_1)$ FRF as the starting point for the analysis of the certification/divination, which proceeds via the Vinnicombe stability inference, $b_{P,C_2} \geq b_{P,C_1} - \delta_\nu(C_1, C_2)$. While [21] does consider both the experiment design and the ETFE calculation, the error analysis with disturbances

is carried much further here, including the development of approaches less susceptible to corruption by FRF errors.

**Controller unfalsification:** as presented by [3, 28] covers the problem of using input-output, $\{u, y\}$, data from the plant $P$ to falsify the stabilization of $P$ by $C_2$. They introduce the idea of an associated *fictitious* reference signal, $\tilde{v}$, which is also part of Approach 3. There is a required intellectual leap to presume validation of the controller. For our work here, this leap is accomplished via experiment design and explicit assumptions about systems and disturbance to yield a corresponding capacity of the computed FRFs with errors to provide guarantees.

**Model unfalsification:** commencing with the data from an adventitious experiment and a model, model unfalsification [13, 24] proceeds to find a pair – model uncertainty bound and disturbance signal – that could have produced the data from the specific underlying plant model. The approach uses a linear matrix inequality approach based on Toeplitz matrices composed of time-domain signals. In this framework, controller $C_1$ is not explicitly present, nor is the data necessarily derived from a stable closed loop. The estimated trio of model, model uncertainty bound and disturbance signal can invalidate or falsify a candidate trio. The approach does not seek to validate models. By comparison, the approach in this paper is to extract an empirical model FRF, $\hat{P}(\omega)$, from the designed experimental data and to validate its performance in closed loop with $C_1$ and $C_2$. Additional assumptions are used, such as the linearity of the plant, the internal stability of $(P, C_1)$ and knowledge of the controllers. We do not validate this model $\hat{P}$ but only the closed loops.

**Model validation:** as developed by [11, 12] approaches the identification of a parametric model for the plant together with an associated model error description derived from the asymptotic normality properties of prediction error system identification methods. This provides both a nominal parametrized model and an estimation set, which (it is asserted) contains the true plant with a prescribed probability. They consider tuning this full-order model error description to the requirements of the subsequent controller design. In the

context of controller divination, this could proceed via the robust stabilization and performance for the entire set containing the true plant. Our analysis might commence from the same data set, although we require no sense of model order, since our methods use nonparametric FRF descriptions. The techniques are developed for FRFs estimated at a finite number of frequencies with a concomitant stability/smoothness assumption, but without a concept of plant system order.

## 4.9 Example

In this example, we consider the uncertain continuous-time plant $P$ in (2.8) in Section 2.5

$$\dot{x}_p(t) = -x_p(t - 0.5) + u(t)$$

whose output signal is $x_p(t)$. This plant is an LTI system with time delay in the state, called internal time delay, and can be described by a transfer function

$$P(s) = \frac{1}{s + e^{-0.5s}}.$$

The dynamics of this plant $P$ as well as the initial condition $x_p(\tau)$ for $\tau \in [-N_pT - 0.5, -N_pT]$ are unknown. However, in this example, we assume that the plant $P$ is known to be LTI and the controller $C_1$ in Section 2.5 is known to stabilize the plant.

We measure the plant-output signal with a sampling period $T$ and this measurement is corrupted by a noise signal $d$, i.e.

$$y[n] = x_p(nT) + d[n]$$

for $n = 0, 1, \ldots$. The plant-input signal $u$ is given by a zero-order hold method

$$u(t) = u[n] \quad \text{for} \quad nT \leq t < (n + 1)T$$

with the discrete-time signal $u[n]$ produced as an outcome of the discrete-time controller $C_1(z)$ combined with the discrete-time reference signals $r[n]$ and $s[n]$ as well as the measured noisy plant-output signal $y[n]$.

The zero-order hold, the continuous-time plant $P(s)$, and the measurement block in Figure 4.5 can be considered an equivalent discrete-time system denoted by $P(z)$. And, as shown in Section 3.4, the order of this discrete-time sys-

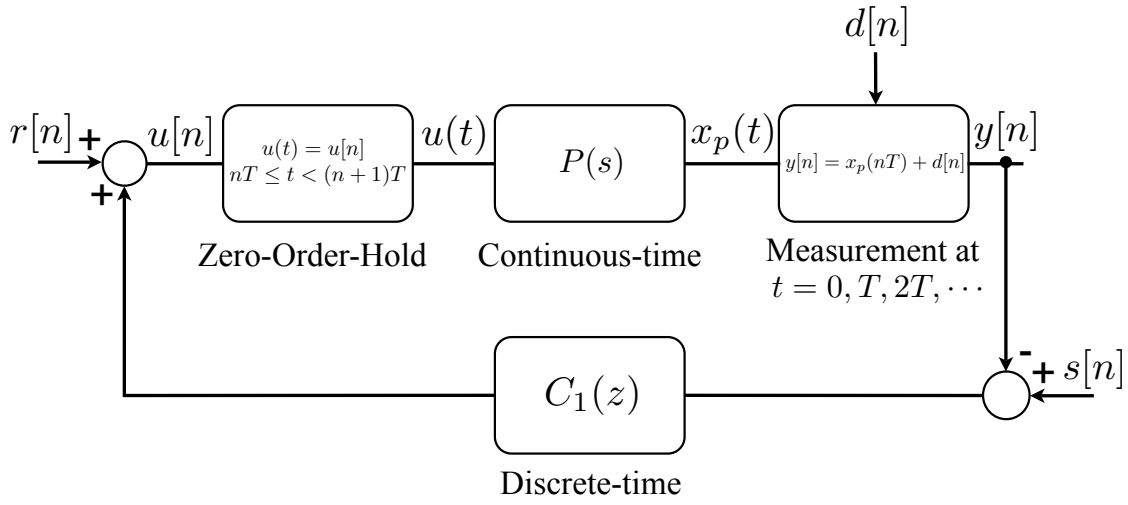


Figure 4.5: A system with a continuous-time plant $P(s)$ and a discrete-time controller $C_1(z)$

tem is infinite since the continuous-time plant $P(s)$ has internal time delay. Since $C_1$ is known to stabilize the plant, we perform experiments on the closed-loop system $(P, C_1)$.

We apply reference signals

$$r[n] = s[n] = \sum_{i=1}^{M} A_i \cos(\omega_i T n + \phi_i)$$

for $n = -N_p, -N_p+1, \cdots, LN-1$ to the closed-loop system $(P, C_1)$. The positive integer $N$ is the period of $r$ and $s$ and the constant $L$ is the repetition number of the period. The positive integer $M < \frac{N}{2}$ is the number of the sinusoidal functions, the constants $A_i$s are the amplitudes of the sinusoidal functions, and the frequencies of the sinusoidal functions are given by $\omega_i = \frac{2\pi k_i}{N}$ with integers $0 \le k_1 < \cdots < k_M < \frac{N}{2}$. The phases $\phi_i$s are set at $\phi_i = \frac{\pi}{3}$ when $\omega_i = 0$, otherwise arbitrarily chosen. Then from the experiment, we collect the data $\{(u[n], y[n]), n = -N_p, -N_p + 1, \cdots, LN-1\}$ from the closed-loop system $(P, C_1)$.

Using a left coprime factorization $C_1(z) = \tilde{M}_{C_1}(z)^{-1}\tilde{N}_{C_1}(z)$ with $\tilde{M}_{C_1}(z) =$

1 and $\tilde{N}_{C_1}(z) = -0.9$, we compute the intermediate signal $v$ in (4.2) as

$$v[n] = r[n] - 0.9s[n] = 0.1 \sum_{i=1}^{M} A_i \cos(\omega_i T n + \phi_i)$$

for $n = -N_p, -N_p + 1, \cdots, LN - 1$.

A controller designer tries to build a new controller based on a plant model

$$\dot{x}_m(t) = -x_m(t) + u(t)$$

whose output signal is $x_m(t)$. This plant is an LTI system with no time delay. Combining this continuous-time model with the zero-order hold and the measurement block in Figure 4.5, the designer develops a discrete-time model

$$\begin{aligned} x_m[n+1] &= 0.3679\ x_m[n] + 0.6321\ u[n] + w[n] \\ y_m[n] &= x_m[n] + d[n] \end{aligned} \tag{4.30}$$

where each of $w$ and $d$ is an iid gaussian random process with variances $\sigma_w^2 = 1$ and $\sigma_d^2 = 1$. Then, an LQG controller is designed as

$$C_3(z) = \frac{0.02005}{z - 0.1427}.$$

Since $C_3$ is stable, two systems $\tilde{N}_{C_3}(z) = C_3(z)$ and $\tilde{M}_{C_3}(z) = 1$ are a pair of left coprime factors.

Using the data from the experiment and this new prospective controller $C_3$ as well as the controller $C_2$ in Section 2.5 and Section 3.4, we obtain the FRF estimates of $G_{\tilde{v}v}$ for $C_2$ and $C_3$.

### 4.9.1 MATLAB simulation

In the MATLAB simulation, the sampling period is set to $T = 1sec$ and the number of samples in one repetition of the reference signals is set to $N = 200$. The frequencies in the reference signals are $\omega_i = \frac{2\pi k_i}{N}$ for $i = 1, \ldots, M$ with $k_i = 2(i-1)$ for $i = 1, \ldots, M$ and $M = 51$, which results in $\omega_1 = \frac{2\pi \times 0}{N}$, $\omega_2 = \frac{2\pi \times 2}{N}$, ..., and $\omega_M = \frac{2\pi \times 100}{N} = \pi$. Set $\phi_1 = \frac{1}{3}$, $\phi_M = \frac{1}{3}$, and select $\{\phi_i, i = 2, \ldots, M-1\}$ as

a realization of a random process which is independent and uniformly distributed over $[0, 2\pi]$. Then, we apply reference signals

$$r[n] = s[n] = \sum_{i=1}^{M} A_i \cos(\omega_i T n + \phi_i)$$

with $A_i = 1$ for $i = 1, \ldots, M$ to the closed-loop system $(P, C_1)$. The number of samples in the pre-experiment is set to $N_p = 75$. As we perform the experiment, the repetition number $L$ increases. We will look at the effect of $L$ later.

The noise signal $d[n]$ is generated as a realization of a random process which is independent and uniformly distributed over $[-1, 1]$. Initial condition of the plant is set to $x_p(\tau) = 0$ for $\tau \in [-N_p T - 0.5, -N_p T]$.

Using a left coprime factorization $C_1(z) = \tilde{M}_{C_1}(z)^{-1}\tilde{N}_{C_1}(z)$ with $\tilde{M}_{C_1}(z) = 1$ and $\tilde{N}_{C_1}(z) = -0.9$, we compute the intermediate signal $v$ in (4.2) as

$$v[n] = r[n] - 0.9s[n] = 0.1 \sum_{i=1}^{M} A_i \cos(\omega_i T n + \phi_i)$$

for $n = -N_p, -N_p + 1, \cdots, LN - 1$.

Using the data from the experiment and the prospective controller $C_2$, we compute the FRF estimate of $G_{\tilde{v}v}$ with $L = 10$, which is shown as blue dots in Figure 4.6. The smooth red line is the true FRF of $G_{\tilde{v}v}$ for $C_2$, which can be obtained in a different simulation with a long pre-experiment and no noise signal. The FRF estimate indicates that $\operatorname{wno} \det \hat{G}_{\tilde{v}v}(\omega) \neq 0$ and, thus, the controller $C_2$ does not stabilize the plant $P$. The lower part in Figure 4.6 is a zoomed-in plot around $(1.1, 0)$. Also, the FRF estimates of $G_{\tilde{v}v}$ for $C_2$ with $L = 50$ and $L = 200$ are shown as blue dots in Figure 4.7 and Figure 4.8, respectively. As $L$ increases, the error of the the FRF estimate diminishes. This is because both $K_x$ in Assumption 2 and $K_f$ in Assumption 3 decrease. For large $L$, the FRF estimate becomes reliable with small error and the diminishing noise influence is shown in the zoomed-in plots around $(1.1, 0)$.

Similarly, we compute the FRF estimate of $G_{\tilde{v}v}$ for the prospective controller $C_3$ with $L = 10$, which is shown as blue dots in Figure 4.9. The smooth red line is the true FRF of $G_{\tilde{v}v}$ for $C_3$. The lower part in Figure 4.9 is a zoomed-in plot

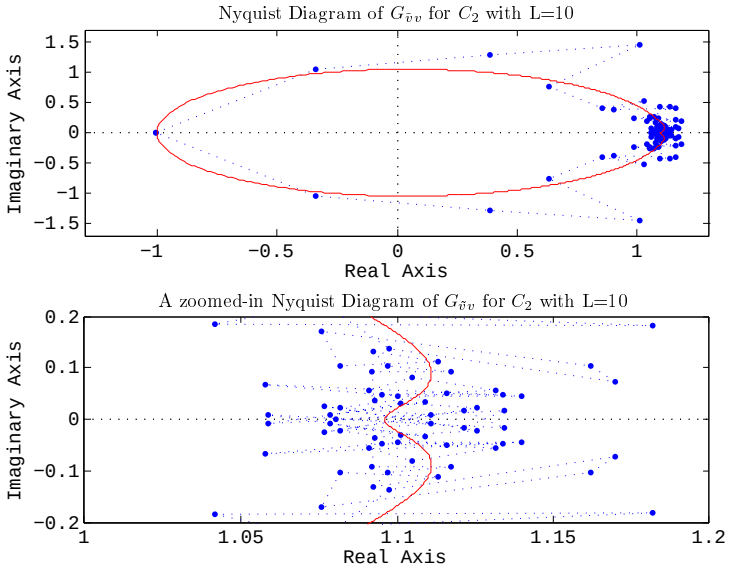


Figure 4.6: The FRF estimate (blue dots) and the true FRF (smooth red line) of $G_{\tilde{v}v}$ for $C_2$ with $L = 10$ and a zoomed-in plot around $(1.1, 0)$

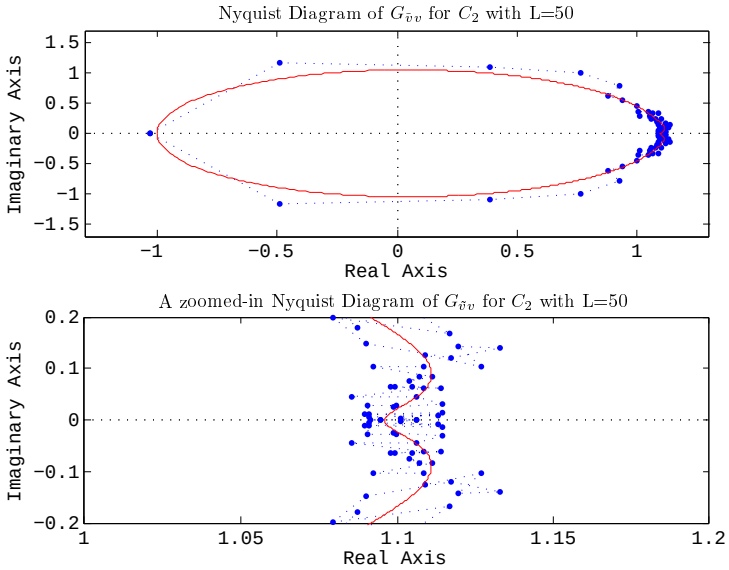


Figure 4.7: The FRF estimate (blue dots) and the true FRF (smooth red line) of $G_{\tilde{v}v}$ for $C_2$ with $L = 50$ and a zoomed-in plot around $(1.1, 0)$

around $(0.5, 0)$. Also, the FRF estimates of $G_{\tilde{v}v}$ for $C_3$ with $L = 50$ and $L = 200$ are shown as blue dots in Figure 4.10 and Figure 4.11, respectively. Again, as $L$ increases, the error of the the FRF estimate diminishes. For large $L$, the FRF estimate becomes reliable and its indication of wno $\det \hat{G}_{\tilde{v}v}(\omega) = 0$ with small error

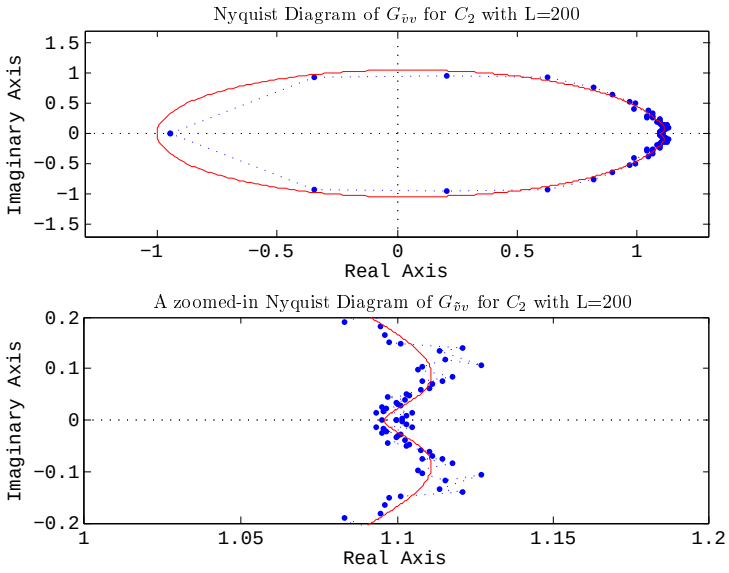


Figure 4.8: The FRF estimate (blue dots) and the true FRF (smooth red line) of $G_{\tilde{v}v}$ for $C_2$ with $L = 200$ and a zoomed-in plot around $(1.1, 0)$

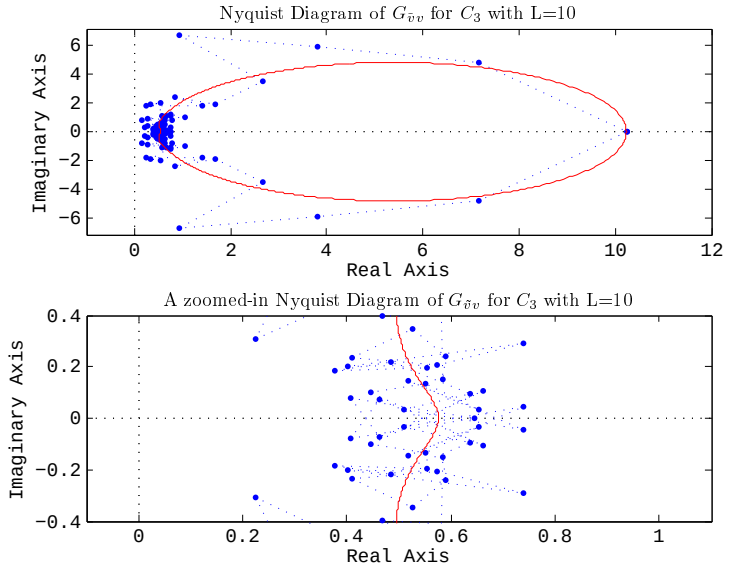


Figure 4.9: The FRF estimate (blue dots) and the true FRF (smooth red line) of $G_{\tilde{v}v}$ for $C_3$ with $L = 10$ and a zoomed-in plot around $(0.5, 0)$

leads to the conclusion that the controller $C_3$ stabilizes the plant $P$.

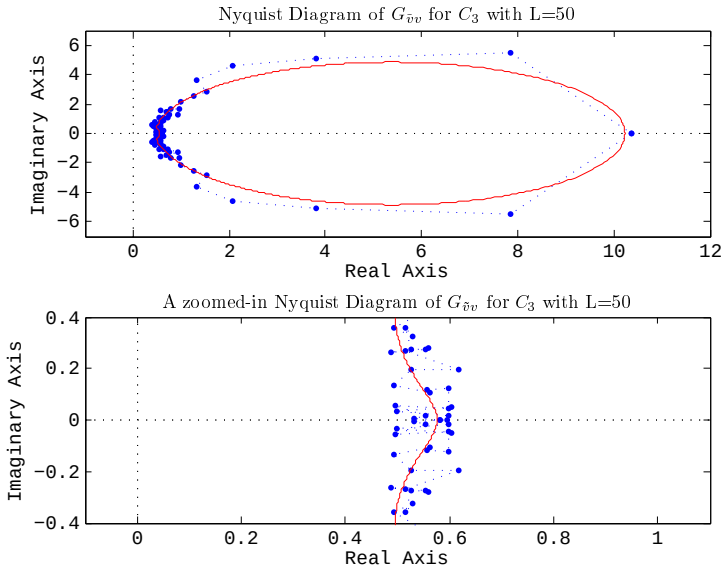


Figure 4.10: The FRF estimate (blue dots) and the true FRF (smooth red line) of $G_{\tilde{v}v}$ for $C_3$ with $L = 50$ and a zoomed-in plot around $(0.5, 0)$

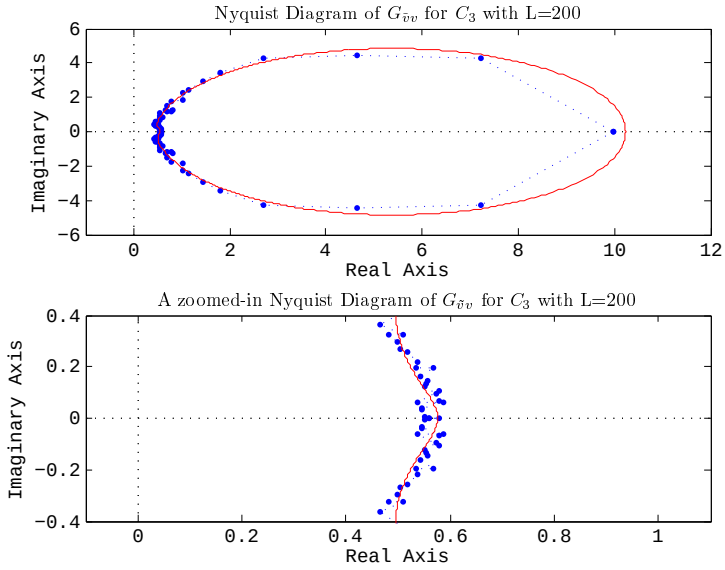


Figure 4.11: The FRF estimate (blue dots) and the true FRF (smooth red line) of $G_{\tilde{v}v}$ for $C_3$ with $L = 200$ and a zoomed-in plot around $(0.5, 0)$

## 4.10 Conclusion

The stability and performance of a closed-loop system $(P, C_2)$ with an uncertain MIMO LTI plant $P$ and a known MIMO LTI candidate controller $C_2$ are divined by three approaches presented in this paper without constructing the

closed loop, provided that $P$ is known to be stabilized by another known MIMO LTI controller $C_1$. These approaches commence with data set $\{r, s, u, y\}$ collected from designed experiments on the internally stable $(P, C_1)$ loop in Figure 4.1. Then, the FRFs of the plant or other transfer functions, depending on the approaches, are estimated using the data set. The divination approaches are performed with the estimates for the FRFs and we provide a thorough comparison with a number of other related methods and focus our attention on the capacity of the data to provide a divination solution reliably. Also, we provide an error analysis for the estimates for the FRFs and link this to (assumptions about) the SNR pertaining at the time when the data set was recorded.

## 4.11 Appendices

**Proof of Theorem 6.** (1) Since the closed-loop system $(P, C_1)$ is internally stable, Lemma 7 (1) guarantees that

$$\eta(P) = -\text{wno}\det(I + C_1P) - \eta(C_1). \tag{4.31}$$

Then, Lemma 7 (1) applied to $(P, C_2)$ with (4.31) completes the proof.

(2) Since the closed-loop system $(P, C_1)$ is internally stable, $G_{yv}$ and $G_{uv}$ are stable. In addition, from (4.4), it follows that $P = G_{yv}G_{uv}^{-1}$ and $\tilde{N}_{C_1}G_{yv} + \tilde{M}_{C_1}G_{uv} = I$. Thus, the transfer functions $G_{yv}$ and $G_{uv}$ are right coprime factors of $P$. Then, Lemma 7 (2) applied to $(P, C_2)$ with $G_{\tilde{v}v}$ in (4.6) completes the proof.

(3) From (4.7) and (4.9), it is clear that

$$(\tilde{N}_{C_1}G_{y\tilde{v}} + \tilde{M}_{C_1}G_{u\tilde{v}})^{-1} = (\tilde{N}_{C_2}N_P + \tilde{M}_{C_2}M_P)(\tilde{N}_{C_1}N_P + \tilde{M}_{C_1}M_P)^{-1} = G_{\tilde{v}v},$$

and, hence, Theorem 6 (2) completes the proof.

**Proposition 6.** *For any given* $\nu \in \{0, 1, \cdots\}$,

$$\sum_{\tau=0}^{\infty} \tau^{\nu}\zeta^{\tau} = S_{\nu}(\zeta)$$

*for* $\forall\zeta \in (-1, 1)$ *where the function* $S$ *is defined, inductively, by* $S_0(\zeta) = \frac{1}{1-\zeta}$,

$S_1(\zeta) = \zeta \frac{d}{d\zeta} S_0(\zeta)$, $S_2(\zeta) = \zeta \frac{d}{d\zeta} S_1(\zeta)$, $\cdots$.

**Proof.** (1) For $\nu = 0$, $\sum_{\tau=0}^{\infty} \zeta^\tau = \frac{1}{1-\zeta} = S_0(\zeta)$ for $\forall \zeta \in (-1, 1)$. (2) For any given $n \in \{0, 1, \cdots\}$, if $\sum_{\tau=0}^{\infty} \tau^n \zeta^\tau = S_n(\zeta)$ for $\forall \zeta \in (-1, 1)$, then we have $\sum_{\tau=0}^{\infty} \tau^{n+1} \zeta^\tau = \zeta \frac{d}{d\zeta} \sum_{\tau=0}^{\infty} \tau^n \zeta^\tau = \zeta \frac{d}{d\zeta} S_n(\zeta) = S_{n+1}(\zeta)$ for $\forall \zeta \in (-1, 1)$. Therefore, the proof is completed by the induction.

**Proof of Lemma 8.** It is clear that, for $\forall \omega \in [0, 2\pi)$,

$$\bar{\sigma}\left(\frac{d}{d\omega} G(\omega)\right) = \bar{\sigma}\left(\sum_{\tau=0}^{\infty} (-j\tau) g(\tau) e^{-j\omega\tau}\right) \leq K_g \sum_{\tau=0}^{\infty} \tau^\mu \rho^\tau = K_g S_\mu(\rho).$$

**Proof of Proposition 4.** This is a special case of Proposition 5.

**Proof of Proposition 5.** Denote by $\|\cdot\|_F$ the Frobenius matrix norm. Then, we have $\bar{\sigma}(X(t)) \leq \|X(t)\|_F = \sqrt{\sum_{j=1}^{\alpha} \|x_j(t)\|_2^2} \leq \sqrt{\alpha} \max_{j \in \{1,\ldots,\alpha\}} \|x_j(t)\|_2$ for $t = 0, \cdots, LN-1$, from which, together with Assumption 2, it follows that $\bar{\sigma}\left(\frac{1}{LN} \sum_{t=0}^{LN-1} X(t) e^{-j\omega_i t} \Lambda^{-1}\right) \leq \frac{1}{LN} \sum_{t=0}^{LN-1} \bar{\sigma}\left(X(t)\right) \bar{\sigma}\left(\Lambda^{-1}\right) \leq \frac{\sqrt{\alpha} K_x}{\underline{\sigma}(\Lambda)}$. Similarly, it follows, from the fact that $\frac{1}{LN} \sum_{t=0}^{LN-1} F(t) e^{-j\omega_i t} = \frac{1}{N} \sum_{t=0}^{N-1} \frac{1}{L} \sum_{\tau=0}^{L-1} F(t+\tau N) e^{-j\omega_i t}$ and Assumption 3, that $\bar{\sigma}\left(\frac{1}{LN} \sum_{t=0}^{LN-1} F(t) e^{-j\omega_i t} \Lambda^{-1}\right) \leq \frac{\sqrt{\alpha} K_f}{\underline{\sigma}(\Lambda)}$.

**Proof of Theorem 7.** Choose any $\omega \in [\omega_1, \omega_{2M+1})$ and define the true system linear interpolant

$$\bar{W}(\omega) \triangleq (1-\theta) W(\omega_i) + \theta W(\omega_{i+1}) \tag{4.32}$$

for $\forall \omega \in [\omega_i, \omega_{i+1})$, $i = 1, \cdots, 2M$ where $\theta = \frac{\omega - \omega_i}{\Delta\omega_i}$ with $\Delta\omega_i = \omega_{i+1} - \omega_i$. Using this and (4.15), we have

$$\begin{aligned} \bar{\sigma}(\hat{W}(\omega) - W(\omega)) &= \bar{\sigma}(\hat{W}(\omega) - \bar{W}(\omega) + \bar{W}(\omega) - W(\omega)) \\ &\leq \bar{\sigma}(\hat{W}(\omega) - \bar{W}(\omega)) + \bar{\sigma}(\bar{W}(\omega) - W(\omega)). \end{aligned} \tag{4.33}$$

An upper bound of the first term in the right-hand side of the inequality in (4.33) can be obtained, using (4.32) and (4.15), by

$$\begin{aligned} \bar{\sigma}(\hat{W}(\omega) - \bar{W}(\omega) &\leq (1-\theta) \bar{\sigma}(\hat{W}(\omega_i) - W(\omega_i)) + \theta \bar{\sigma}(\hat{W}(\omega_{i+1}) - W(\omega_{i+1})) \\ &\leq \max\{\bar{\sigma}(\hat{W}(\omega_i) - W(\omega_i)), \bar{\sigma}(\hat{W}(\omega_{i+1}) - W(\omega_{i+1}))\}. \end{aligned} \tag{4.34}$$

To obtain an upper bound on the second term in the right-hand side of the

inequality in (4.33), two cases are considered. If $\omega_i \le \omega \le \frac{\omega_i+\omega_{i+1}}{2}$, i.e. $0 \le \theta \le \frac{1}{2}$, then we have, using (4.32),

$$\begin{aligned}\bar{\sigma}(\bar{W}(\omega) - W(\omega)) &\le \theta\bar{\sigma}\left(W(\omega_{i+1}) - W(\omega_i)\right) + \bar{\sigma}\left(W(\omega_i) - W(\omega)\right) \\ &\le \frac{1}{2}\max_{\xi\in[\omega_i,\omega_{i+1}]}\bar{\sigma}\left(\frac{d}{d\omega}W(\omega)\Big|_{\omega=\xi}\right)(\omega_{i+1}-\omega_i) \\ &\quad + \max_{\xi\in[\omega_i,\omega_{i+1}]}\bar{\sigma}\left(\frac{d}{d\omega}W(\omega)\Big|_{\omega=\xi}\right)\frac{1}{2}(\omega_{i+1}-\omega_i) \\ &= \max_{\xi\in[\omega_i,\omega_{i+1}]}\bar{\sigma}\left(\frac{d}{d\omega}W(\omega)\Big|_{\omega=\xi}\right)(\omega_{i+1}-\omega_i).\end{aligned} \tag{4.35}$$

Similarly, if $\frac{\omega_i+\omega_{i+1}}{2} < \omega \le \omega_{i+1}$, i.e. $\frac{1}{2} < \theta \le 1$, we have

$$\begin{aligned}\bar{\sigma}(\bar{W}(\omega) - W(\omega)) &\le (1-\theta)\bar{\sigma}\left(W(\omega_i) - W(\omega_{i+1})\right) + \bar{\sigma}\left(W(\omega_{i+1}) - W(\omega)\right) \\ &\le \max_{\xi\in[\omega_i,\omega_{i+1}]}\bar{\sigma}\left(\frac{d}{d\omega}W(\omega)\Big|_{\omega=\xi}\right)(\omega_{i+1}-\omega_i).\end{aligned} \tag{4.36}$$

From (4.35) and (4.36), it follows that

$$\bar{\sigma}(\bar{W}(\omega) - W(\omega)) \le \max_{\xi\in[\omega_i,\omega_{i+1}]}\bar{\sigma}\left(\frac{d}{d\omega}W(\omega)\Big|_{\omega=\xi}\right)\Delta\omega_i,$$

from which, together with (4.33), (4.34), and the fact that $\det\hat{W}(\omega)\ \forall\omega\in[0,2\pi)$, we have

$$\begin{aligned}&\bar{\sigma}\{(W(\omega)-\hat{W}(\omega))\hat{W}(\omega)^{-1}\} \\ &\le \bar{\sigma}(W(\omega)-\hat{W}(\omega))\bar{\sigma}(\hat{W}(\omega)^{-1}) \\ &\le \frac{1}{\underline{\sigma}(\hat{W}(\omega))}\left\{\max_{j\in\{i,i+1\}}\bar{\sigma}\left(\hat{W}(\omega_j)-W(\omega_j)\right) + \max_{\xi\in[\omega_i,\omega_{i+1}]}\bar{\sigma}\left(\frac{d}{d\omega}W(\omega)\Big|_{\omega=\xi}\right)\Delta\omega_i\right\} \\ &< 1.\end{aligned}$$

Since $\omega$ is arbitrarily chosen in $[\omega_1,\omega_{2M+1})$, we have

$$\bar{\sigma}\{(W(\omega)-\hat{W}(\omega))\hat{W}(\omega)^{-1}\} < 1 \tag{4.37}$$

for $\forall \omega \in [\omega_1, \omega_{2M+1})$. Note that $\omega_{2M+1} = \omega_1 + 2\pi$.

It is clear that

$$\begin{aligned} W(\omega) &= \hat{W}(\omega) + (W(\omega) - \hat{W}(\omega)) \\ &= \{I + (W(\omega) - \hat{W}(\omega))\hat{W}(\omega)^{-1}\}\hat{W}(\omega), \end{aligned} \tag{4.38}$$

from which, together with (4.37), it follows that

$$\begin{aligned} \underline{\sigma}(W(\omega)) &\geq [1 - \bar{\sigma}\{(W(\omega) - \hat{W}(\omega))\hat{W}(\omega)^{-1}\}]\underline{\sigma}(\hat{W}(\omega)) \\ &> 0 \end{aligned}$$

and, hence, $\det W(\omega) \neq 0$ for $\forall \omega \in [0, 2\pi)$.

Using Lemma 17.5 in [40], it follows, from (4.37) and (4.38), that

$$\text{wno}\det W(\omega) = \text{wno}\det \hat{W}(\omega).$$

**Proof of Theorem 8.** Proposition 5 guarantees that

$$\bar{\sigma}(\Delta G_Y(\omega_i)), \bar{\sigma}(\Delta G_U(\omega_i)) \leq \frac{2\sqrt{\alpha}(K_x + K_f)}{A_i \underline{\sigma}(\Lambda)} \tag{4.39}$$

for $i = 1, \cdots, M$, from which, together with Condition (1) in Theorem 8, it follows that

$$\begin{aligned} &\underline{\sigma}(\hat{G}_U(\omega)) \\ &> \max_{j \in \{i, i+1\}} \bar{\sigma}\left(\hat{G}_U(\omega_j) - G_U(\omega_j)\right) + \max_{\xi \in [\omega_i, \omega_{i+1}]} \bar{\sigma}\left(\frac{d}{d\omega} G_U(\omega)\Big|_{\omega=\xi}\right)(\omega_{i+1} - \omega_i) \end{aligned}$$

for $\forall \omega \in [\omega_i, \omega_{i+1})$, $i = 1, \cdots, 2M$. With this condition, following the proof of Theorem 7, it can be obtained that $\underline{\sigma}(G_U(\omega)) \neq 0$ for $\forall \omega \in [0, 2\pi)$. This implies that the plant $P$ has no pole on the unit circle. Since $C_2$ also has no pole on the unit circle, there is no pole-zero cancellation on the unit circle between $C_2$ and $P$. Thus, in order to satisfy the first condition in Theorem 6 (1), we need to show that $\Xi_2 = I + C_2 P$ has no zero on the unit circle, which is proved in the following.

From (4.19) and the fact that $G_Y(\omega) = P(\omega)G_U(\omega)$ for $\forall \omega \in [0, 2\pi)$, it

follows that

$$\begin{aligned}\hat{G}_Y(\omega_i) &= P(\omega_i)G_U(\omega_i) + \Delta G_Y(\omega_i) \\ &= P(\omega_i)(\hat{G}_U(\omega_i) - \Delta G_U(\omega_i)) + \Delta G_Y(\omega_i)\end{aligned}$$

$i = 1, \cdots, M$, from which, together with (4.17), it is clear that

$$\begin{aligned}\Delta P(\omega_i) &\triangleq \hat{G}_Y(\omega_i)\hat{G}_U(\omega_i)^+ - P(\omega_i) \\ &= (\Delta G_Y(\omega_i) - P(\omega_i)\Delta G_U(\omega_i))\hat{G}_U(\omega_i)^+\end{aligned} \tag{4.40}$$

$i = 1, \cdots, M$ since $\hat{G}_U(\omega_i)$ has a full row rank. Then, it follows, from (4.40) and (4.39), that

$$\begin{aligned}\bar{\sigma}(\hat{\Xi}_k(\omega_i) - \Xi_k(\omega_i)) &= \bar{\sigma}(C_k(\omega_i)\Delta P(\omega_i)) \\ &\le \frac{\bar{\sigma}(C_k(\omega_i))\{\bar{\sigma}(\Delta G_Y(\omega_i)) + \bar{\sigma}(P(\omega_i))\bar{\sigma}(\Delta G_U(\omega_i))\}}{\underline{\sigma}(\hat{G}_U(\omega_i))} \\ &\le \frac{2\sqrt{\alpha}(K_x + K_f)\bar{\sigma}(C_k(\omega_i))\{1 + \bar{\sigma}(P(\omega_i))\}}{A_i\underline{\sigma}(\Lambda)\underline{\sigma}(\hat{G}_U(\omega_i))}\end{aligned}$$

for $i = 1, \cdots, M$, $k = 1, 2$. This inequality, combined with Condition (2) in Theorem 8, ensures that the condition in Theorem 7 is satisfied and, hence, Theorem 7 guarantees that $\det \Xi_k(\omega) \neq 0$ for $\forall \omega \in [0, 2\pi)$ and

$$\text{wno} \det \Xi_k(\omega) = \text{wno} \det \hat{\Xi}_k(\omega) \tag{4.41}$$

for $k = 1, 2$. Since $\det \Xi_2(\omega)$ does not go through the origin, the system $\Xi_2 = I + C_2P$ has no zero on the unit circle. Therefore, the first condition in Theorem 6 is satisfied.

By Theorem 6 (1) with (4.41), the condition (4.20) becomes a necessary and sufficient condition for the internal stability of the closed-loop system $(P, C_2)$.

**Proof of Theorem 9.** Proposition 5 guarantees that

$$\bar{\sigma}\left(\begin{bmatrix}\Delta G_{yv}(\omega_i) \\ \Delta G_{uv}(\omega_i)\end{bmatrix}\right) \le \frac{2\sqrt{\alpha}(K_x + K_f)}{A_i\underline{\sigma}(\Lambda)}$$

for $i = 1, \cdots, M$, from which it follows that

$$\begin{aligned}\bar{\sigma}(\hat{G}_{\tilde{v}v}(\omega_i) - G_{\tilde{v}v}(\omega_i)) &= \bar{\sigma}\left(\begin{bmatrix}\tilde{N}_{C_2}(\omega_i) & \tilde{M}_{C_2}(\omega_i)\end{bmatrix}\begin{bmatrix}\Delta G_{yv}(\omega_i) \\ \Delta G_{uv}(\omega_i)\end{bmatrix}\right) \\ &\leq \frac{2\sqrt{\alpha}(K_x + K_f)\tilde{W}_2(\omega_i)}{A_i \underline{\sigma}(\Lambda)}\end{aligned} \tag{4.42}$$

for $i = 1, \cdots, M$ where $\tilde{W}_2(\omega_i) = \bar{\sigma}\left(\begin{bmatrix}\tilde{N}_{C_2}(\omega_i) & \tilde{M}_{C_2}(\omega_i)\end{bmatrix}\right)$.

The inequalities in (4.25) and (4.42) ensure that the condition in Theorem 7 is satisfied and, hence, Theorem 7 guarantees that $\det G_{\tilde{v}v}(\omega) \neq 0$ for $\forall \omega \in [0, 2\pi)$ and

$$\text{wno}\det G_{\tilde{v}v}(\omega) = \text{wno}\det \hat{G}_{\tilde{v}v}(\omega). \tag{4.43}$$

Therefore, by Theorem 6 (2), the condition (4.26) becomes a necessary and sufficient condition for the internal stability of the closed-loop system $(P, C_2)$.

Chapter 4 is a reprint of S. Cheong, R. R. Bitmead, "Divination of closed-loop stability and performance via frequency response function estimates" as it appears in Automatica, 2012. The dissertation author was the primary author of this paper.

# 5 Controller Improvement via Frequency Response Function Estimates

## 5.1 Introduction

In the previous chapter, we proposed controller divination methods with which we can, given an LTI prospective controller, investigate the closed-loop stability and performance without building the closed-loop with the controller. In general, one may design prospective controllers in terms of parameters and investigate grid-points in the parameter space of prospective controllers. The number of prospective controllers is large when the resolution of the grid is high. However, as long as the number of prospective controllers is finite, we can perform the controller divination methods using computers.

In this chapter, given an internally stable multiple-input/multiple-output (MIMO), linear time-invariant (LTI) plant-controller pair, $(P, C_1)$, with $P$ uncertain and $C_1$ known, we seek a better controller in the sense of a given cost function from deliberately designed experimental data obtained from the stable $(P, C_1)$ closed loop with impinging disturbances. Our analysis starts with the experiment and collected data consisting of the measurable physical signals applied to and recorded from the closed loop, together with knowledge of the linear controller $C_1$. The problem addressed is to design and then use these applied signals plus knowledge or assumptions about the plant and the disturbance signal to design a controller with better performance, if possible.

We formulate the controller design problem in the form of an optimization based on the estimates of the frequency response functions (FRFs) of coprime factors of the plant. The cost function that we pursue in this optimization problem is the weighted $\mathcal{H}_\infty$-norm of the generalized sensitivity function of the closed-loop system with the plant and a prospective controller. The stabilizing property of a newly-designed controller, which is a necessary condition in our controller design, can be confirmed by controller divination approaches in Chapter 4 without constructing the closed loop. This condition is included in the optimization problem as a constraint and, hence, makes the optimization problem nonconvex. Thus, we propose an algorithm where we solve the optimization problem without imposing the constraint and, then, search over the controllers between the found controller and the currently stabilizing controller. These approaches are via the estimation of certain FRFs from the data set. The analysis proceeds using nonparametric identification of the FRFs as opposed to parametric system identification, since this avoids issues of model structure selection, and includes consideration of the choice of applied signals and the experimental conditions. Thus, the controller design procedure is based on quantitative system identification when the signals necessarily are corrupted by disturbances entering the system.

In Section 5.2, given the collected data in Chapter 4, we introduce FRF estimates of left and right coprime factors of the plant that satisfy the double Bezout Identity. These estimates are employed in an optimal controller design problem in Section 5.3.

## 5.2 Estimation of FRFs of coprime factors of a plant

### 5.2.1 Experiments and data collection

Consider an internally stable closed-loop MIMO LTI discrete-time system $(P, C_1)$ in Figure 4.1. The $\ell \times m$ plant $P$ is uncertain and the $m \times \ell$ controller $C_1$ is known. The signals in the closed-loop system consist of known external input signals $r$ and $s$, measured plant-input and plant-output signals $u$ and $y$, and an unknown disturbance or noise signal $d$.

In total, $m + \ell$ distinct experiments are conducted and, in the $j$-th exper-

iment, we apply $N$-periodic input signal

$$\begin{bmatrix} r_j(t) \\ s_j(t) \end{bmatrix} = \lambda_j \sum_{i=1}^{M} A_i \cos(\omega_i t + \phi_i) \tag{5.1}$$

for $t = -N_{pre}, \cdots, -1, 0, 1, \cdots, LN-1$ where $\lambda_j$ is the $j$-th column vector of some $(m+\ell)\times(m+\ell)$ nonsingular matrix $\Lambda$, an integer $M < \frac{N}{2}$ is the number of frequency components, and the frequencies are chosen as $\omega_i = \frac{2\pi k_i}{N}$ for some integers $0 \le k_1 < \cdots < k_M < N/2$. The phases $\phi_i$s are arbitrarily chosen except $\phi_1 = \pi/3$ if $\omega_1 = 0$. Nonnegative integers $N_{pre}$ and $L$ represent the pre-experiment length and the repetition number of the periods. The data set from the experiments is $\{(r_j(t), s_j(t), u_j(t), y_j(t)), t = 0, \cdots, LN-1, j = 1, \cdots, m+\ell\}$. The *pre-experiment* data (see [10]) for $t = -N_{pre}, \cdots, -1$ is ignored. Then, the DFT of the input signals is given by

$$\mathbb{Q}(\omega) \triangleq \frac{1}{\sqrt{LN}} \sum_{t=0}^{LN-1} \begin{bmatrix} r_1(t) & \cdots & r_{m+\ell}(t) \\ s_1(t) & \cdots & s_{m+\ell}(t) \end{bmatrix} e^{-j\omega t}$$

for $\omega = 0, \frac{2\pi}{N}, \ldots, \frac{2\pi(N-1)}{N}$. From (5.1), It is clear that $\mathbb{Q}(\omega_i) = \frac{A_i\sqrt{LN}}{2} e^{j\phi_i}\Lambda$ for $\omega_i \neq 0$ and $\mathbb{Q}(\omega_i) = \frac{A_i\sqrt{LN}}{2}\Lambda$ for $\omega_i = 0$.

Necessary notations follow. Let $G(z)$ be a transfer function matrix in $z$-transform.

- $G(\omega)$ is short for $G(e^{j\omega})$ for $\forall \omega \in [0, 2\pi)$.
- $\overline{\sigma}(\cdot)$ is the maximum singular values.
- $\|\cdot\|_2$ is the induced 2-norm.
- $\|\cdot\|_\infty$ is the $\mathcal{H}_\infty$-norm.

### 5.2.2 FRF estimates of coprime factors of the plant that satisfy the double Bezout Identity

In this section, given the collected data $r_j(t)$, $s_j(t)$, $u_j(t)$, $y_j(t)$ for $t = 0, \cdots, LN-1, j = 1, \cdots, m+\ell$, we introduce FRF estimates of the left and the right coprime factors of the plant that satisfy the double Bezout Identity.

Consider any prospective controller $C_2$. Stable transfer functions $\tilde{M}_{C_1}$, $\tilde{N}_{C_1}$, $\tilde{M}_{C_2}$, and $\tilde{N}_{C_2}$ are left coprime factors of $C_1$ and $C_2$, i.e. $C_1 = \tilde{M}_{C_1}^{-1}\tilde{N}_{C_1}$ and $C_2 = \tilde{M}_{C_2}^{-1}\tilde{N}_{C_2}$. These are used to generate an intermediate signal in (4.2) and the

fictitious reference signal $\tilde{v}$ in (4.5).

From (4.4), we have

$$G_{yv}G_{uv}^{-1} = \left\{P(I + C_1P)^{-1}\tilde{M}_{C_1}^{-1}\right\}\left\{(I + C_1P)^{-1}\tilde{M}_{C_1}^{-1}\right\}^{-1} = P,$$

from which, together with the fact that $G_{yv}$ and $G_{uv}$ are stable, it follows that $G_{yv}$ and $G_{uv}$ are right coprime factors of the plant. Furthermore, $G_{yv}$ and $G_{uv}$ satisfy

$$\tilde{N}_{C_1}G_{yv} + \tilde{M}_{C_1}G_{uv} = \tilde{M}_{C_1}\left(C_1G_{yv} + G_{uv}\right) = I. \tag{5.2}$$

For any given right coprime factors $M_{C_1}$ and $N_{C_1}$ of $C_1$, i.e. $C_1 = N_{C_1}M_{C_1}^{-1}$, the closed-loop $(P, C_1)$ in Figure 4.1 can be redrawn as in Figure 5.1 and the signal

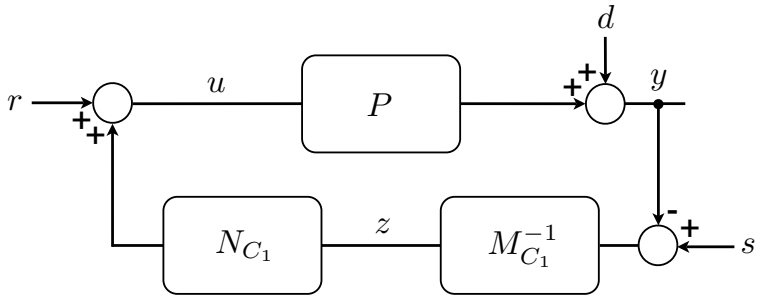


Figure 5.1: A discrete-time closed-loop system equivalent to $(P, C_1)$

$z$ in Figure 5.1 can be described by

$$z = \begin{bmatrix} G_{zr} & G_{zs} \end{bmatrix} \begin{bmatrix} r \\ s \end{bmatrix} + G_{zd}d \tag{5.3}$$

where

$$\begin{aligned} \begin{bmatrix} G_{zr} & G_{zs} \end{bmatrix} &= \begin{bmatrix} -M_{C_1}^{-1}G_{yr} & M_{C_1}^{-1}(I - G_{ys}) \end{bmatrix} \\ &= \begin{bmatrix} -M_{C_1}^{-1}(I + PC_1)^{-1}P & M_{C_1}^{-1}(I + PC_1)^{-1} \end{bmatrix} \end{aligned}$$

and $G_{zd} = -M_{C_1}^{-1}G_{yd}$. From (5.3), we have

$$G_{zs}^{-1}(-G_{zr}) = \left\{M_{C_1}^{-1}(I + PC_1)^{-1}\right\}^{-1}\left\{M_{C_1}^{-1}(I + PC_1)^{-1}P\right\} = P,$$

from which, together with the fact that $G_{zs}$ and $G_{zr}$ are stable, it follows that $G_{zs}$

and $-G_{zr}$ are left coprime factors of the plant. Furthermore, $G_{zs}$ and $-G_{zr}$ satisfy

$$(-G_{zr})N_{C_1} + G_{zs}M_{C_1} = (-G_{zr}C_1 + G_{zs})\,M_{C_1} = I. \tag{5.4}$$

Denote $(N_P, M_P, \tilde{N}_P, \tilde{M}_P) \triangleq (G_{yv}, G_{uv}, -G_{zr}, G_{zs})$. Then, from (5.2) and (5.4), these coprime factors satisfy the double Bezout identity

$$\begin{bmatrix} \tilde{M}_{C_1} & -\tilde{N}_{C_1} \\ \tilde{N}_P & \tilde{M}_P \end{bmatrix} \begin{bmatrix} M_P & N_{C_1} \\ -N_P & M_{C_1} \end{bmatrix} = \begin{bmatrix} M_P & N_{C_1} \\ -N_P & M_{C_1} \end{bmatrix} \begin{bmatrix} \tilde{M}_{C_1} & -\tilde{N}_{C_1} \\ \tilde{N}_P & \tilde{M}_P \end{bmatrix} = I. \tag{5.5}$$

The DFT of the intermediate signals $\{v_j(t), t = 0, \cdots, LN-1, j = 1, \cdots, m+\ell\}$ is $\mathbb{V}(\omega) \triangleq \frac{1}{\sqrt{LN}} \sum_{t=0}^{LN-1} \begin{bmatrix} v_1(t) & \cdots & v_m(t) \end{bmatrix} e^{-j\omega t}$ and satisfies $\mathbb{V}(\omega_i) = \begin{bmatrix} \tilde{M}_{C_1}(\omega_i) & \tilde{N}_{C_1}(\omega_i) \end{bmatrix} \mathbb{Q}_m(\omega_i)$ for $i = 1, \cdots, M$ where $\mathbb{Q}_m(\omega_i)$ is composed of first $m$ columns of $\mathbb{Q}(\omega_i)$, provided that the initial conditions of $C_1$ are appropriately chosen or the effect of the initial conditions is negligible by a sufficiently long pre-experiment.

The signals $\{z_j(t), t = 0, \cdots, LN-1, j = 1, \cdots, m+\ell\}$ are observed in Figure 5.1 or computed from $M_{C_1}^{-1}$ and the input signals of $C_1$. Their DFT is $\mathbb{Z}(\omega) \triangleq \frac{1}{\sqrt{LN}} \sum_{t=0}^{LN-1} \begin{bmatrix} z_1(t) & \cdots & z_{m+\ell}(t) \end{bmatrix} e^{-j\omega t}$.

The observed signal $\begin{bmatrix} u_j^T & y_j^T \end{bmatrix}^T$ in the $j$-th experiment is the sum of (i) the sinusoidal steady-state response, (ii) the transient response, denoted by $x_j$, due to the initial state value, and (iii) the signal due to the disturbance $d_j$.

The FRFs of $G_{yv}$, $G_{uv}$, $G_{zr}$, and $G_{zs}$ are estimated by

$$\begin{aligned} \begin{bmatrix} \hat{G}_{yv}(\omega_i) \\ \hat{G}_{uv}(\omega_i) \end{bmatrix} &\triangleq \begin{bmatrix} \mathbb{Y}_m(\omega_i) \\ \mathbb{U}_m(\omega_i) \end{bmatrix} \mathbb{V}(\omega_i)^{-1} \\ \begin{bmatrix} \hat{G}_{zr}(\omega_i) & \hat{G}_{zs}(\omega_i) \end{bmatrix} &\triangleq \mathbb{Z}(\omega_i)\mathbb{Q}(\omega_i)^{-1} \end{aligned} \tag{5.6}$$

for $i = 1, \cdots, M$ where $\mathbb{Y}(\omega_i)$ and $\mathbb{U}(\omega_i)$ are the DFTs of $\begin{bmatrix} y_1(t) & \cdots & y_{m+\ell}(t) \end{bmatrix}$ and $\begin{bmatrix} u_1(t) & \cdots & u_{m+\ell}(t) \end{bmatrix}$, respectively, and $\mathbb{Y}_m(\omega_i)$ and $\mathbb{U}_m(\omega_i)$ are composed of first $m$ columns of $\mathbb{Y}(\omega_i)$ and $\mathbb{U}(\omega_i)$, respectively.

**Remark 3.** *Since we know the coprime factors satisfy the the double Bezout identity in* (5.5)*, we can employ, as alternative estimates, solutions of optimization*

*problems*

$$\begin{bmatrix}\hat{G}_{yv}(\omega_i)\\ \hat{G}_{uv}(\omega_i)\end{bmatrix} \triangleq \arg\min_{G} \left\| \begin{bmatrix}\mathbb{Y}_m(\omega_i)\\ \mathbb{U}_m(\omega_i)\end{bmatrix} \mathbb{V}(\omega_i)^{-1} - G \right\|_2$$
$$\textit{subject to } \begin{bmatrix}\tilde{N}_{C_1}(\omega_i) & \tilde{M}_{C_1}(\omega_i)\end{bmatrix} G = I$$

*and*

$$\begin{bmatrix}\hat{G}_{zr}(\omega_i) & \hat{G}_{zs}(\omega_i)\end{bmatrix} \triangleq \arg\min_{G} \left\|\mathbb{Z}(\omega_i)\mathbb{Q}(\omega_i)^{-1} - G\right\|_2$$
$$\textit{subject to } G \begin{bmatrix}-N_{C_1}(\omega_i)\\ M_{C_1}(\omega_i)\end{bmatrix} = I.$$

### 5.2.3 Choice of coprime factors of $C_1$ and the FRF estimation error due to the disturbance signal

From (4.4) and $\mathbb{V}(\omega_i) = \begin{bmatrix}\tilde{M}_{C_1}(\omega_i) & \tilde{N}_{C_1}(\omega_i)\end{bmatrix} \mathbb{Q}(\omega_i)$, we have

$$\begin{aligned}\begin{bmatrix}\mathbb{Y}(\omega_i)\\ \mathbb{U}(\omega_i)\end{bmatrix} &= \begin{bmatrix}G_{yv}(\omega_i)\\ G_{uv}(\omega_i)\end{bmatrix} \begin{bmatrix}\tilde{M}_{C_1}(\omega_i) & \tilde{N}_{C_1}(\omega_i)\end{bmatrix} \mathbb{Q}(\omega_i) + \mathbb{X}(\omega_i) + \mathbb{F}(\omega_i)\\ &= \begin{bmatrix}G_{yv}(\omega_i)\\ G_{uv}(\omega_i)\end{bmatrix} \mathbb{V}(\omega_i) + \mathbb{X}(\omega_i) + \mathbb{F}(\omega_i)\end{aligned}$$

where $\mathbb{X}(\omega_i)$ is the DFT of the transient response and $\mathbb{F}(\omega_i)$ is the DFT of the response to the disturbance signal. Since $\begin{bmatrix}\tilde{M}_{C_1}(\omega_i) & \tilde{N}_{C_1}(\omega_i)\end{bmatrix}$ has full row rank, if $\mathbb{Q}(\omega_i)$ has full column rank, then $\mathbb{V}(\omega_i)$ is nonsingular, which means that we do not lose any frequency components in $\mathbb{V}(\omega_i)$.

Meanwhile, we have

$$\begin{aligned}\begin{bmatrix}\hat{G}_{yv}(\omega_i)\\ \hat{G}_{uv}(\omega_i)\end{bmatrix} &= \begin{bmatrix}\mathbb{Y}(\omega_i)\\ \mathbb{U}(\omega_i)\end{bmatrix} \mathbb{V}(\omega_i)^{-1}\\ &= \begin{bmatrix}G_{yv}(\omega_i)\\ G_{uv}(\omega_i)\end{bmatrix} + \mathbb{X}(\omega_i)\mathbb{V}(\omega_i)^{-1} + \mathbb{F}(\omega_i)\mathbb{V}(\omega_i)^{-1}\\ &= \begin{bmatrix}G_{yv}(\omega_i)\\ G_{uv}(\omega_i)\end{bmatrix} + \mathbb{X}(\omega_i)\mathbb{V}(\omega_i)^{-1} + \mathbb{F}(\omega_i) \left( \begin{bmatrix}\tilde{M}_{C_1}(\omega_i) & \tilde{N}_{C_1}(\omega_i)\end{bmatrix} \mathbb{Q}(\omega_i) \right)^{-1}.\end{aligned}$$

If $\begin{bmatrix}\tilde{M}_{C_1}(\omega_i) & \tilde{N}_{C_1}(\omega_i)\end{bmatrix}$ is small, then the disturbance-error term might become large. However, in this case $\begin{bmatrix}G_{yv}(\omega_i)\\ G_{uv}(\omega_i)\end{bmatrix}$ would become large, too, since

$$\begin{bmatrix}\tilde{M}_{C_1}(\omega_i) & \tilde{N}_{C_1}(\omega_i)\end{bmatrix}\begin{bmatrix}G_{yv}(\omega_i)\\ G_{uv}(\omega_i)\end{bmatrix} = I,$$

which means roughly that the choice of coprime factors of $C_1$ has little effect on the signal-to-noise ratio of the FRF estimation of the transfer function. Similarly, this property applies to the estimates $\begin{bmatrix}G_{zr}(\omega_i) & G_{zs}(\omega_i)\end{bmatrix}$.

## 5.3 Optimal controller design problem

Given a weighting function $W(z)$ and a controller $C = N_C M_C^{-1}$, we pursue a performance measure

$$\|WT_{P,C}\|_\infty = \left\| W\begin{bmatrix}N_P\\ M_P\end{bmatrix}\left(\tilde{M}_C M_P + \tilde{N}_C N_P\right)^{-1}\begin{bmatrix}\tilde{M}_C & \tilde{N}_C\end{bmatrix}\right\|_\infty,$$

which is a weighted $\mathcal{H}_\infty$ specification (see [30]). This measure can only be calculated at $\omega_i$, $i = 1, \cdots, M$ using the estimated values $\hat{N}_P(\omega_i)$ and $\hat{M}_P(\omega_i)$ for $i = 1, \cdots, M$. Thus, a new controller is designed as a solution of an optimization problem

$$\min_C \max_{i=1,\cdots,M} \bar{\sigma}\left(W(\omega_i)\begin{bmatrix}\hat{N}_P(\omega_i)\\ \hat{M}_P(\omega_i)\end{bmatrix}\left(\tilde{M}_C(\omega_i)\hat{M}_P(\omega_i) + \tilde{N}_C(\omega_i)\hat{N}_P(\omega_i)\right)^{-1} \times \begin{bmatrix}\tilde{M}_C(\omega_i) & \tilde{N}_C(\omega_i)\end{bmatrix}\right)$$

subject to $(P, C)$ is stable,

where the stability of the closed-loop system $(P, C)$ is investigated by the divination methods in Section 4.4. This optimization problem is hard to solve both

analytically and numerically. Thus, we employ a controller parameterization

$$\begin{bmatrix} M_C & N_C \end{bmatrix} = \begin{bmatrix} M_{C_1} & N_{C_1} \end{bmatrix} + \begin{bmatrix} Q_M & Q_N \end{bmatrix} \tag{5.7}$$

where

$$\begin{bmatrix} Q_M(z) & Q_N(z) \end{bmatrix} = C_Q(zI - A_Q)^{-1}B_Q + D_Q = \begin{bmatrix} C_Q & D_Q \end{bmatrix} \begin{bmatrix} (zI - A_Q)^{-1}B_Q \\ I \end{bmatrix}$$

with some fixed matrices $A_Q$, stable, and $B_Q$. This parameterization is based on the Youla-Kučera parameterization and also addresses the fixed-order controller design problem.

The optimization problem above is harder to solve than the high performance design problem in [34], where a controller is designed based on information on the frequency response functions over the entire frequency region.

The variables $C_Q$ and $D_Q$ are the new parameters determining the controller $C$ and the optimization problem becomes

$$\begin{aligned} \min_{C_Q, D_Q} \max_{i=1,\cdots,M} \bar{\sigma} \Bigg( & W(\omega_i) \begin{bmatrix} \hat{N}_P(\omega_i) \\ \hat{M}_P(\omega_i) \end{bmatrix} \\ & \times \left( \begin{bmatrix} \tilde{M}_{C_1}(\omega_i) + Q_M(\omega_i) & \tilde{N}_{C_1}(\omega_i) + Q_N(\omega_i) \end{bmatrix} \begin{bmatrix} \hat{M}_P(\omega_i) \\ \hat{N}_P(\omega_i) \end{bmatrix} \right)^{-1} \\ & \times \begin{bmatrix} \tilde{M}_{C_1}(\omega_i) + Q_M(\omega_i) & \tilde{N}_{C_1}(\omega_i) + Q_N(\omega_i) \end{bmatrix} \Bigg) \end{aligned}$$

subject to $(P, C)$ is stable.

In order to simplify this optimization problem, define new variables $\Pi_i$ for $i = 1, \cdots, M$ in the optimization problem with additional constraints

$$\left( \begin{bmatrix} \tilde{M}_{C_1}(\omega_i) & \tilde{N}_{C_1}(\omega_i) \end{bmatrix} + \begin{bmatrix} C_Q & D_Q \end{bmatrix} \begin{bmatrix} (e^{j\omega_i}I - A_Q)^{-1} \\ I \end{bmatrix} \right) \left( \begin{bmatrix} \hat{M}_P(\omega_i) \\ \hat{N}_P(\omega_i) \end{bmatrix} \Pi_i - I \right) = 0 \tag{5.8}$$

for $i = 1, \cdots, M$. Then, the optimization problem becomes

$$\min_{C_Q, D_Q, \Pi_1, \cdots, \Pi_M} \max_{i=1,\cdots,M} \bar{\sigma} \left( W(\omega_i) \begin{bmatrix} \hat{N}_P(\omega_i) \\ \hat{M}_P(\omega_i) \end{bmatrix} \Pi_i \right)$$
$$\text{subject to } (P, C) \text{ is stable and (5.8).}$$

Even with the parameterization of $C$ in (5.7) and the introduction of $\Pi_i$, this optimization problem is still hard to solve. Thus, we propose an algorithm in the following.

**Algorithm 2.**

*Step 1. Find a solution,* $\begin{bmatrix} C_Q^{\#} & D_Q^{\#} \end{bmatrix}$*, of the bilinear matrix inequality problem*

$$\min_{C_Q, D_Q, \Pi_1, \cdots, \Pi_M} \max_{i=1,\cdots,M} \bar{\sigma} \left( W(\omega_i) \begin{bmatrix} \hat{N}_P(\omega_i) \\ \hat{M}_P(\omega_i) \end{bmatrix} \Pi_i \right)$$
$$\textit{subject to } (5.8).$$

*Step 2. Find the largest constant* $\varepsilon \in [0, 1]$ *such that the closed-loop system* $(P, C)$ *with* $\begin{bmatrix} C_Q & D_Q \end{bmatrix} = \varepsilon \begin{bmatrix} C_Q^{\#} & D_Q^{\#} \end{bmatrix}$ *is determined to be stable by the divination methods in Section 4.4. The new controller comprises this* $\begin{bmatrix} C_Q & D_Q \end{bmatrix}$*.*

The optimization problem in Step 1 in Algorithm 2 has a bilinear constraint and, to solve this problem, we can apply the XY-centering optimization algorithm in [29] where the cost value of the optimization problem decreases and for each cost value a feasibility problem is solved. Alternatively, this step can be replaced with many optimization methods such as gradient methods in [2].

The controller designed by Algorithm 2 is not guaranteed to be the optimal controller. This is not surprising since the optimal controller design problem with the FRF estimates at a finite number of frequency values is much harder than the design problem with the FRF estimates over the entire frequency range. Specifically, the fixed-order optimal controller design problem involves the bilinear constraint and, hence, it is even harder to find the optimal controller with a given order. To compound matters, the final controller is chosen as one which uses a proper fraction of the minimizing adjustment parameter but which is guaranteed stabilizing. These are the rigors imposed by using solely the specific data sets and

their corresponding FRF estimates.

In general, one may design prospective controllers in terms of parameters and investigate grid-points in the parameter space of prospective controllers. The number of prospective controllers is large when the resolution of the grid is high. However, as long as the number of prospective controllers is finite, we can numerically find a controller better than the current controller using computers. The newly-designed controller may not be the optimal controller but this may be an efficient way to find a controller better than the current controller.

## 5.4 Conclusion

A controller design method is introduced whose outcome is a new controller that stabilizes an uncertain MIMO LTI plant $P$, provided that $P$ is known to be stabilized by a known MIMO LTI controller $C_1$. This design process commences with signal data collected from deliberately designed experiments on the internally stable $(P, C_1)$ system. Based on collected signal data in a closed-loop system, the FRFs of the plant or other transfer functions in $(P, C_1)$ are estimated. The controller design method is formulated as an optimization problem and controller improvement is performed by solving an optimization problem. The cost function of this optimization problem is the $\mathcal{H}_\infty$-norm of a weighted generalized sensitivity function of a closed-loop system with the plant and a prospective controller. In order to confirm that a new controller stabilizes the plant, controller divination methods are employed as a constraint in the optimization problem and this constraint makes the optimization problem nonconvex. To formulate a numerically solvable optimization problem, we introduced an algorithm where we solve the optimization problem without imposing the constraint and, then, search over the controllers between the new controller and the currently stabilizing controller. The final product of this algorithm is not guaranteed to be the optimal controller and this is caused by the limitation of the nonconvex optimization problem.

Chapter 5 has been accepted for publication of S. Cheong, R. R. Bitmead, "Controller improvement via frequency response function estimates" as it will appear in 16th IFAC Symposium on System Identification. The dissertation author was the primary author of this paper.

# 6 Conclusions and Future Research

## 6.1 Conclusions

The main contribution of this dissertation is development of data-based assessment strategies for prospective controllers in the sense of the closed-loop stability and performance. These strategies are tailor-made for our knowledge of a plant and a disturbance signal and three different types of knowledge are considered in this dissertation.

The most challenging circumstance studied in Chapter 2 is that we can only observe the input and output signals of the plant and we have no other knowledge of the plant and the disturbance signal. In this case, we first design fictitious reference signals using the collected input-output data of the plant in order to formulate fictitious closed-loop systems with the plant and the prospective controllers. Then, we assign cost functions to these fictitious closed-loop systems for the purpose of the controller assessment, e.g. a ratio of the truncated $\mathfrak{L}_2$-norm of the observed signals to the truncated $\mathfrak{L}_2$-norm of the fictitious reference signals for the purpose of checking the closed-loop stability. For the input-output data collection from the plant, we design an experiment using the unfalsified adaptive control where we assess all the prospective controllers at the same time as we collect the data from the current closed-loop system. Since we do not know if the current controller is a stabilizing (or well-performing) controller, we employ a switching control scheme, in which we compare online the cost functions of the prospective controllers and switch the one with the smallest cost into the loop. The stability and performance of this closed-loop system is only guaranteed when one of the

prospective controllers is feasible.

A better circumstance is considered in Chapter 3 where the plant is known to be a SISO LTI discrete-time system and the disturbance signal is an i.i.d. random process with zero mean, unknown bounded variance, and finite fourth moment. The closed-loop stability of a SISO LTI discrete-time controller is assessed by performing a closed-loop experiment with the plant and the controller. Based on the collected data, we employ least squares AR estimates with various orders. Then, unstable poles of the closed-loop system, if they exist, are detected by a least squares AR estimate with an appropriate order and, otherwise, the closed-loop stability of the controller is indicated by a least squares AR estimate with any order. Combining those two properties of the least squares AR estimates, we propose an instability detection method to assess the closed-loop stability of the current controller using a series of least squares AR estimates.

The circumstance considered in Chapter 4 is that the plant is a MIMO LTI discrete-time system and is stabilized by a MIMO LTI controller and the disturbance signal is additive to the output of the plant with a known bound. From the internally stable closed-loop system, we collect signal data to obtain FRF estimates of some transfer functions in the loop. Using these estimates, we propose three divination approaches for the closed-loop stability and performance of a prospective controller. These divination approaches are mainly based on the Nyquist stability theorem combined with a reliable counting method for winding numbers of some transfer functions. We also provide conditions under which the divination approaches are reliable and suggest recommendations among the three approaches.

Naturally, the divination ideas in Chapter 4 lead us to seek a new controller with better performance than a currently stabilizing MIMO LTI discrete-time controller, instead of just testing a given prospective controller. In Chapter 5, an optimization problem is formulated for the purpose of designing a MIMO LTI discrete-time controller with the optimal performance. We, first, develop FRF estimates of left and right coprime factors of the plant that satisfy the double Bezout Identity. Then, the optimization problem is formulated in terms of the FRF estimates for the coprime factors of the plant. In order to reduce the numer-

ical difficulty of the optimization problem, we employ a controller parametrization and propose an algorithm, although this algorithm may not produce the optimal controller.

## 6.2 Future research

• Controller assessment approaches for nonlinear plants and/or controllers, e.g. model predictive controllers.

• Application of unfalsified adaptive control to ARMA systems in Chapter 3 with cost functions built based on the least squares AR estimates of various orders.

• Modification of the controller assessment approaches for the cases where the data collection is interrupted or the operation is interspersed with experiments.

• Controller design and assessment at the same time as the data are collected.

# Bibliography


[1] J. Bellach. Consistency of the least-squares-estimators for linear stochastic difference equations. *Statistics*, 10(1):79–106, 1979.

[2] D. P. Bertsekas. *Nonlinear Programming, Second Edition.* Athena Scientific, Belmont, Massachusetts, USA, 1999.

[3] T. F. Brozenec, T. C. Tsao, and M. G. Safonov. Controller validation. *International Journal of Adaptive Control and Signal Processing*, 15(5):431–444, 2001.

[4] C. Chen. *Linear System Theory and Design, Third Edition.* Oxford University Press, Inc., New York, New York, USA, 1999.

[5] B. Codrons, B. D. O. Anderson, and M. Gevers. Closed-loop identification with an unstable or nonminimum phase controller. *Automatica*, 38(12):2127–2137, 2002.

[6] A. Dehghani, B. D. O. Anderson, and S. H. Cha. Verifying closed-loop performance before inserting a new controller. In *Proc. American Control Conf.*, Baltimore, MD, USA, Jun. 2010.

[7] A. Dehghani, B. D. O. Anderson, and A. Lanzon. Unfalsified adaptive control: a new controller implementation and some remarks. In *Proc. European Control Conf.*, Kos, Greece, Jul. 2007.

[8] A. Dehghani, B. D. O. Anderson, A. Lanzon, and A. Lecchini-Visintini. Verifying stability controllers via closed-loop noisy data : Mimo case. In *Proc. Conf. on Decision and Control*, New Orleans, LA, USA, Dec. 2007.

[9] A. Dehghani, A. Lecchini-Visintini, A. Lanzon, and B. D. O. Anderson. Validating controllers for internal stability utilizing closed-loop data. *IEEE Transaction on Automatic Control*, 54(11):2719–2725, 2009.

[10] D. K. de Vries. *Identification of Model Uncertainty for Control Design.* PhD thesis, Delft University of Technology, 1994.

[11] M. Gevers, X. Bombois, B. Codrons, G. Scorletti, and B. D. O. Anderson. Model validation for control and controller validation in a prediction error identification framework—part i: theory. *Automatica*, 39(3):403–415, 2003.

[12] M. Gevers, X. Bombois, B. Codrons, G. Scorletti, and B. D. O. Anderson. Model validation for control and controller validation in a prediction error identification framework—part ii: illustrations. *Automatica*, 39(3):417–427, 2003.

[13] R. L. Kosut. Uncertainty model unfalsification : A system identification paradigm compatible with robust control design. In *Proc. Conf. on Decision and Control*, New Orleans, LA, USA, Dec. 1995.

[14] T. L. Lai and C. Z. Wei. Asymptotic properties of general autoregressive models and strong consistency of least–squares estimates of their parameters. *Journal of Multivariate Analysis*, 13(1):1–23, 1983.

[15] L. Ljung. *System Identification: Theory for the User, Second Edition*. Prentice-Hall, Upper Saddle River, New Jersey, USA, 1999.

[16] H. B. Mann and A. Wald. On the statistical treatment of linear stochastic difference equations. *Econometrica*, 11(3/4):173–220, 1943.

[17] C. Manuelli, S. G. Cheong, E. Mosca, and M. G. Safonov. Stability of unfalsified adaptive control with non SCLI controllers and related performance under different prior knowledge. In *Proc. European Control Conf.*, Kos, Greece, Jul. 2007.

[18] R. McGowan and R. Kuc. A direct relation between a signal time series and its unwrapped phase. *IEEE Transactions on Acoustics, Speech, and Signal processing*, ASSP-30(5):719–726, 1982.

[19] A. S. Morse, D. Q. Mayne, and G. C. Goodwin. Applications of hysteresis switching in parameter adaptive control. *IEEE Trans. Automat. Contr.*, 37(9):1343–1354, Sep. 1992.

[20] T. J. Muench. Consistency of least square estimators of coefficients on explosive stochastic difference equations. Technical Report Accession Number AD0609320, Defense Technical Information Center, 1964.

[21] J. Park. *Controller certification : The generalized stability margin inference for a large number of MIMO controllers*. PhD thesis, University of California, San Diego, 2008.

[22] J. Park and R. R. Bitmead. Controller certification. *Automatica*, 44(1):167–176, 2008.

[23] R. Pintelon and J. Schoukens. *System Identification: A Frequency Domain Approach*. IEEE Press, New York, New York, USA, 2001.

[24] K. Poolla, P. Khargonekar, A. Tikku, J. Krause, and K. Nagpal. A time-domain approach to model validation. *IEEE Transaction on Automatic Control*, 39(5):951–959, 1994.

[25] M. M. Rao. Consistency and limit distributions of estimators of parameters in explosive stochastic difference equations. *Annals of Mathematical Statistics*, 32(1):195–218, 1961.

[26] G. C. Reinsel. *Elements of Multivariate Time Series Analysis*. Springer, New York, New York, USA, 1997.

[27] S. I. Resnick. *A Probability Path*. Birkhäuser, Ithaca, New York, USA, 1998.

[28] M. G. Safonov and T. C. Tsao. The unfalsified control concept and learning. *IEEE Trans. Automat. Contr.*, 42(6):843–847, Jun. 1997.

[29] R. E. Skelton, T. Iwasaki, and K. M. Grigoriadis. *A Unified Algebraic Approach to Linear Control Design*. CRC Press, Bristol, Pennsylvania, USA, 1997.

[30] S. Skogestad and I. Postlethwaite. *Multivariable Feedback Control: Analysis And Design, Second Edition*. John Wiley & Sons Ltd., Chichester, West Sussex, England, 2nd edition, 2005.

[31] M. Stefanovic and M. G. Safonov. Safe adaptive switching control: stability and convergence. *IEEE Trans. Automat. Contr.*, 53(9):2012–2021, Oct. 2008.

[32] K. Steiglitz and B. Dickinson. Phase unwrapping by factorization. *IEEE Transactions on Acoustics, Speech, and Signal processing*, ASSP-30(6):984–991, 1982.

[33] G. W. Stewart. *Matrix Algorithms, Volume II: Eigensystems*. Society for Industrial and Applied Mathematics, Philadelphia, Pennsylvania, USA, 2001.

[34] T. T. Tay, I. M. Y. Mareels, and J. B. Moore. *High Performance Control*. Birkhäuser Boston, Cambridge, Massachusetts, USA, 1998.

[35] G. C. Tiao and R. S. Tsay. Consistency properties of least squares estimates of autoregressive parameters in ARMA models. *Annals of Statistics*, 11(3):856–871, 1983.

[36] J. van Helvoort, B. de Jager, and M. Steinbuch. Direct data-driven recursive controller unfalsification with analytic update. *Automatica*, 43(12):2034–2046, 2007.

[37] G. Vinnicombe. *Uncertainty and Feedback: $\mathcal{H}_\infty$ loop-shaping and the $\nu$-gap metric*. Imperial College Press, Covent Gargen, London, United Kingdom, 2001.

[38] R. Wang, A. Paul, M. Stefanovic, and M. G. Safonov. Cost detectability and stability of adaptive control systems. *Int. J. Robust and Nonlinear Control*, 17(5-6):549–561, 2007.

[39] J. S. White. The limiting distribution of the serial correlation coefficient in the explosive case. *Annals of Mathematical Statistics*, 29(4):1188–1197, 1958.

[40] K. Zhou and J. C. Doyle. *Essentials of Robust Control*. Prentice-Hall, Upper Saddle River, New Jersey, USA, 1998.